

# Protein changes in the neonatal opossum spinal cord during the period when regeneration stops being possible

---

Tomljanović, Ivana

Doctoral thesis / Disertacija

2023

Degree Grantor / Ustanova koja je dodijelila akademski / stručni stupanj: **University of Rijeka / Sveučilište u Rijeci**

Permanent link / Trajna poveznica: <https://um.nsk.hr/um:nbn:hr:193:662153>

Rights / Prava: [In copyright](#) / [Zaštićeno autorskim pravom.](#)

Download date / Datum preuzimanja: **2024-04-20**



image not found or type unknown

Repository / Repozitorij:

[Repository of the University of Rijeka, Faculty of Biotechnology and Drug Development - BIOTECHRI Repository](#)



image not found or type unknown

UNIVERSITY OF RIJEKA  
DEPARTMENT OF BIOTECHNOLOGY

Ivana Tomljanović

**PROTEIN CHANGES IN THE NEONATAL  
OPOSSUM SPINAL CORD DURING THE  
PERIOD WHEN REGENERATION STOPS  
BEING POSSIBLE**

DOCTORAL THESIS

Rijeka, 2022



UNIVERSITY OF RIJEKA  
DEPARTMENT OF BIOTECHNOLOGY

Ivana Tomljanović

**PROTEIN CHANGES IN THE NEONATAL  
OPOSSUM SPINAL CORD DURING THE  
PERIOD WHEN REGENERATION STOPS  
BEING POSSIBLE**

DOCTORAL THESIS

Mentor: Professor Miranda Mladinić Pejatović, PhD

Rijeka, 2022

SVEUČILIŠTE U RIJECI  
ODJEL ZA BIOTEHNOLOGIJU

Ivana Tomljanović

**PROTEINSKE PROMJENE U LEĐNOJ  
MOŽDINI NEONATALNIH OPOSUMA  
TIJEKOM RAZDOBLJA KADA  
REGENERACIJA PRESTAJE BITI MOGUĆA**

DOKTORSKI RAD

Mentor: Prof. dr. sc. Miranda Mladinić Pejatović

Rijeka, 2022.

Mentor: Professor Miranda Mladinić Pejatović, PhD

Doctoral thesis was defended on May 12<sup>th</sup>, 2022 at the University of Rijeka, Department of Biotechnology, in front of the Evaluation Committee:

1. Associate Professor Ivana Ratkaj, PhD
2. Assistant Professor Nicholas Bradshaw, PhD
3. Associate Professor Dubravka Švob Štrac, PhD

## **Zahvale**

Veliko hvala mojoj mentorici, profesorici Mirandi Mladinić Pejatović, što mi je pružila priliku da izradim ovu doktorsku disertaciju u njenom laboratoriju. Draga profesorice, neizmjereno Vam hvala što ste tijekom cijelog vremena imali povjerenje u mene, na svim savjetima, podršci i ohrabrenju kada je to bilo potrebno!

Također, veliko hvala izv. prof. dr. sc. Jeleni Ban, koja mi je svojim znanstvenim i stručnim savjetima pomogla pri izradi ove doktorske disertacije. Draga Jelena, veliko hvala na pomoći, i uvijek na lijepim riječima potpore!

Neizmjereno hvala mojim kolegicama i dragim prijateljicama, Antoneli Petrović, Matei Ivaničić i Marti Pongrac na pomoći uvijek kada je bilo potrebno i na danima punim smijeha i radosti u LMN labu!

Hvala mojim roditeljima na bezuvjetnoj ljubavi, podršci i ohrabrenju. Uvijek ste mi bili najveća životna potpora i radili sve samo da mi olakšate ovaj put.

Hvala mome Josipu na ljubavi, potpori i razumijevanju.

*Mome tati.*

Hvala na beskrajnoj ljubavi i potpori. Uvijek si vjerovao u mene i bio najsretniji za svaki moj uspjeh. Hvala što mi u teškim trenucima uvijek daješ snage. Svoj najveći uspjeh posvećujem tebi, i nadam se da si tamo gore sada ne ponosan, nego preponosan, kako si mi znao reći.

Tvoja Ive



## **Funding**

This experimental work has been conducted on equipment financed by the European Regional Development Fund (ERDF) within the project “Research Infrastructure for Campus-based Laboratories at the University of Rijeka” (RC.2.2.06-0001), the Croatian Science Foundation (Hrvatska Zaklada za Znanost; CSF) grant IP-2016-06-7060, the financial support from the University of Rijeka (18.12.2.1.01, 18-258-6427 and 18-290-1463), and the International Centre for Genetic Engineering and Biotechnology (ICGEB), Grant/Award Number: CRP/CRO14-03.

## Abstract

One of the major challenges of modern neurobiology concerns the inability of the adult mammalian central nervous system (CNS) to regenerate and repair itself after injury. It is poorly understood why regenerative potential is lost with evolution and development and why it becomes very limited in adult mammals. Even though our understanding of molecular and cellular mechanisms that promote or inhibit neuronal regeneration is expanding, it is still unclear what are the key differences between the neuronal systems that can and cannot regenerate, and how they can be manipulated to change the outcome of the injury. Our incomplete understanding of molecular events underlying neuronal development and regeneration is the main reason why neurodegenerative diseases and brain and spinal cord injuries are still mostly incurable today.

A preferred model to study and reveal the cellular and molecular basis of regeneration is the neonatal opossum (*Monodelphis domestica*). Opossums are marsupials that are born very immature with the unique possibility to successfully regenerate spinal cord after injury in the first two weeks of their life. After that, the regenerative capacity is abruptly lost: at 14 days in cervical spinal segments and at 17 days in less mature lumbar spinal segments.

In this thesis, we used neonatal opossums to study molecular and cellular properties of spinal tissue that has and does not have the capacity to regenerate after injury, to pinpoint the key differences. Using a comparative proteomic approach, for the first time, we identified the proteins unique and differentially distributed in the intact opossum spinal tissue with different regenerative capacities. We have identified a total number of 4735 proteins involved in various cellular processes such as cell growth, proliferation, differentiation, transcription, cell signaling, cytoskeleton and extracellular matrix organization, axon guidance molecules, neurotrophic factors and entire intracellular molecular pathways like mTOR and MAPK signaling pathway. We have also identified many myelin associated proteins, known to act as inhibitors of CNS axon regeneration, which was the positive control for our overall experimental procedure. Most interestingly, we have identified a number of proteins related to different neurodegenerative diseases that change in the opossum spinal cord during the period critical for neuroregeneration. The different distribution of the selected proteins detected by comparative proteomics was further confirmed by Western blot, and the changes in the expression of related genes were analyzed by quantitative reverse transcription PCR. Furthermore, we explored the cellular localization of the selected proteins using immunofluorescent microscopy. We showed that during the period of development when

regeneration stops being possible, the substantial number of proteins known to be involved in regeneration and development change their level in the opossum spinal cord. These results upgraded the previous transcriptomic data about the genes differentially expressed in regenerating and non-regenerating opossum spinal cord tissue. Comparison of the data obtained by genomic and proteomic approaches allowed the identification of molecules of interest and narrowed the number of candidates for functional assays.

For the first time, we successfully established primary neuronal spinal cell cultures from neonatal opossums of different ages and different regenerative capacities, which represent a novel mammalian *in vitro* platform, particularly useful to study CNS development and regeneration, and to test the functional role of the candidate molecules, together with the intact neonatal opossum spinal cord preparation. We have also developed the neuroregeneration scratch test to be performed on primary neuronal spinal cell cultures deriving from P5 opossums.

Taken together, the results of this thesis contribute to a better understanding of neuronal regeneration in mammals and identify candidate molecules as future targets to promote neuroregeneration in mammalian CNS.

**Keywords:** *Monodelphis domestica*, spinal cord, regeneration, neurodegenerative diseases, proteomics, primary cell cultures

## Sažetak

Jedan od glavnih izazova suvremene neurobiologije je nemogućnost regeneracije središnjeg živčanog sustava (SŽS) odraslih sisavaca nakon ozljede. Još uvijek nije jasno kako se i zašto sposobnost regeneracije gubi tijekom evolucije i razvoja, te zašto regeneracija kod odraslih sisavaca postaje iznimno ograničena. Iako se naše razumijevanje staničnih i molekularnih mehanizama koji potiču ili inhibiraju regeneraciju zadnjih godina sve više produbljuje, još uvijek je nejasno koje su to ključne razlike između živčanih sustava koji imaju i onih koji nemaju sposobnost regeneracije te kako ih manipulirati sa ciljem da se promjeni ishod ozljede. Naše nepotpuno razumijevanje molekularnih događaja koji su temelj razvoja i regeneracije živčanog tkiva je glavni razlog zašto su neurodegenerativne bolesti, kao i ozljede mozga i leđne moždine danas još uvijek neizlječive.

Prikladan model za proučavanje i otkrivanje stanične i molekularne osnove regeneracije su mladi oposumi (*Monodelphis domestica*). Oposumi su tobolčari koji se rađaju nerazvijeni pa tijekom prva dva tjedna svog života posjeduju jedinstvenu sposobnost potpune regeneracije leđne moždine nakon ozljede. Nakon toga sposobnost regeneracije se naglo gubi: oko 14. dana u vratnom dijelu leđne moždine, te 17. dana u njenom manje razvijenom lumbalnom dijelu.

Mlade oposume koristili smo za istraživanje molekularnih i staničnih svojstava tkiva leđne moždine koje ima sposobnost regeneracije nakon ozljede, te onog koje nema, kako bi se odredile ključne razlike. Uporabom komparativne proteomike, po prvi puta, identificirali smo proteine koji su jedinstveni i različito izraženi u tkivu leđnih moždina oposuma koji mogu i onih koji ne mogu regenerirati. Identificirali smo ukupno 4735 proteina koji sudjeluju u staničnom rastu, proliferaciji, diferencijaciji, transkripciji, staničnoj signalizaciji, organizaciji citoskeleta i izvanstaničnog matriksa, molekule koje usmjeravaju aksone, neurotrofne čimbenike i cijele unutarstanične molekularne puteve kao što su mTOR i MAPK signalni put. Također, identificirali smo niz proteina povezanih s mijelinom za koje se zna da djeluju kao inhibitori regeneracije aksona, što je bila pozitivna kontrola za naš cjelokupni eksperimentalni postupak. Kao najvažniji rezultat, otkrili smo da se mnoštvo proteina povezanih s neurodegenerativnim bolestima mijenja u leđnoj moždini oposuma u vremenu kada regeneracija prestaje biti moguća. Različita distribucija odabranih proteina dodatno je potvrđena Western blotom, a promjene u ekspresiji gena analizirane su metodom kvantitativne reverzne transkripcije lančane reakcije polimeraze. Nadalje, imunofluorescentnom mikroskopijom istražili smo staničnu lokalizaciju odabranih proteina.

Pokazali smo da se tijekom razvoja, u trenutku kada regeneracija prestane biti moguća, znatno mijenja razina proteina za koje se zna da kontroliraju regeneraciju i razvoj leđne moždine oposuma. Dobiveni rezultati su nadogradili prethodna istraživanja vezana za gene različito izražene u tkivu leđne moždine oposuma koje ima i onoga koje nema sposobnost regeneracije. Također, usporedbom rezultata komparativne transkriptomike i proteomike moguće je bilo identificirati molekule od interesa i suziti broj kandidata za funkcionalna istraživanja.

Po prvi puta, uspješno smo uspostavili primarne stanične kulture leđne moždine oposuma različite dobi i različite regenerativne sposobnosti, koje predstavljaju novu *in vitro* platformu, posebno korisnu za proučavanje razvoja i regeneracije SŽS-a, kao i za funkcionalna istraživanja molekula kandidata u neuroregeneraciji, zajedno sa preparatom cjelovite leđne moždine oposuma održavanog u kulturi. Također, uspostavili smo test neuroregeneracije koji uključuje mehaničku ozljedu primarnih staničnih kultura dobivenih iz pet dana starih oposuma.

Zaključno, rezultati ovog istraživanja doprinose boljem razumijevanju regeneracije živčanog tkiva sisavaca, te otkrivaju potencijalne terapijske molekularne mete koje bi mogle biti interesantne za neuroregeneraciju SŽS-a sisavaca.

**Ključne riječi:** *Monodelphis domestica*, leđna moždina, regeneracija, neurodegenerativne bolesti, proteomika, primarne stanične kulture

## Table of content

<b>1. INTRODUCTION.....</b>	<b>1</b>
1.1. Central nervous system regeneration.....	1
1.2. Regeneration and development.....	1
1.3. Regeneration promoting and inhibiting mechanisms.....	2
1.4. Central nervous system injuries.....	4
1.5. Therapeutic interventions for SCI.....	6
1.5.1. Stem cell-based therapies.....	6
1.5.2. Molecular therapies.....	11
1.6. Regenerative biomaterials.....	11
1.7. Animal models of SCI.....	13
1.8. Opossum <i>Monodelphis domestica</i> in neuroregeneration research.....	15
1.9. Proteomics in regeneration studies.....	19
1.10. Neuroregeneration in neurodegenerative disorders.....	20
<b>2. THESIS AIMS AND HYPOTHESES.....</b>	<b>22</b>
<b>3. MATERIALS AND METHODS.....</b>	<b>23</b>
3.1. Materials.....	23
3.2. Methods.....	30
<b>4. RESULTS.....</b>	<b>45</b>
<b>4.1. Protein extraction.....</b>	<b>45</b>
<b>4.2. Establishment of protocols for proteomic analysis of opossum spinal cord tissue and identification of proteins by mass spectrometry.....</b>	<b>45</b>
<b>4.3. LC-MS/MS analysis.....</b>	<b>55</b>
4.3.1. Protein identification and functional classification.....	55
4.3.2. Validation of the selected proteins by Western blot.....	56
4.3.3. Validation of the differentially expressed genes by qRT-PCR.....	57
4.3.4. Immunohistochemical localization of the differentially expressed proteins.....	57
4.3.5. Proteins related to neurodegenerative diseases.....	57

4.3.6. Proteins important for regeneration and neurodegenerative diseases.....	58
4.3.6.1. Proteins related to neurodegenerative diseases.....	58
4.3.6.2. Proteins involved in regeneration and development.....	60
<b>4.4. Functional studies.....</b>	<b>74</b>
4.4.1. Intact opossum spinal cord.....	74
4.4.1.1. HTT marker.....	75
4.4.1.2. Ki67 marker.....	75
4.4.1.3. MAP2 marker.....	76
4.4.1.4. NeuN marker.....	76
4.4.1.5. SMI32 marker.....	76
4.4.1.6. SYN1 marker.....	77
4.4.2. Primary spinal cell cultures.....	88
4.4.2.1. Spinal cord primary cell culture.....	88
4.4.2.2. Neurite outgrowth test.....	88
4.4.2.3. New neuronal regeneration scratch test.....	89
<b>5. DISCUSSION.....</b>	<b>95</b>
5.1. Proteomics.....	95
5.1.1. Inhibitors of CNS axon regeneration: glial scar and myelin associated proteins.....	99
5.1.2. Promoters of regeneration: proteins involved in neurodevelopment.....	101
5.1.3. Proteins related to neurodegenerative diseases.....	104
5.2. Functional assays.....	106
5.2.1. PGL-137 inhibitor.....	108
<b>6. CONCLUSIONS.....</b>	<b>111</b>
<b>7. LITERATURE.....</b>	<b>113</b>
<b>8. LIST OF ABBREVIATIONS.....</b>	<b>128</b>
<b>9. LIST OF FIGURES.....</b>	<b>131</b>
<b>10. LIST OF TABLES.....</b>	<b>133</b>
<b>11. BIOGRAPHY.....</b>	<b>134</b>

# **1. INTRODUCTION**

## **1.1. Central nervous system regeneration**

Many animal species have the ability to regenerate certain parts of the body, which is an extremely interesting phenomenon in biology. A particularly fascinating aspect of regeneration is the possibility of functional nervous system recovery. Unfortunately, the regeneration of the CNS, consisting of the brain and spinal cord, is very limited in higher vertebrates, and thus in humans. While fish, amphibians, reptiles, and invertebrates successfully recover all connections in their CNS after injury, adult birds and mammals have little or no ability for functional regeneration of the CNS (1). Therefore, brain and spinal cord injuries, in addition to neurodegenerative diseases (NDD), cause irreparable damage to neuronal tissue, which consequently leads to incurable neurological losses (2). To overcome the inability of the mammalian CNS to regenerate and recover from injury is one of the biggest challenges of neurobiology. Although our knowledge regarding the molecular and cellular mechanisms that promote or inhibit neuronal regeneration is expanding, it is still unclear what are the key differences among neuronal systems that have and do not have the ability to regenerate, and how they can be manipulated to change the outcome of the injury.

## **1.2. Regeneration and development**

In frogs, fish, and mammals, regeneration depends on the developmental stage of the individual, so these animals show a considerable ability to regenerate the spinal cord, brain, and limbs during larval and embryonic stages of development (3). For example, a salamander can regenerate the tail and entire limbs, but also the heart, brain, jaw, retina, and lens (4–7) making amphibians interesting models for the study of regeneration mechanisms. Frogs (*Xenopus*) also have a long history as model organisms for the investigation of embryonic development (8–10). However, during their maturation, this capacity becomes limited or is completely lost (11). For reasons still unknown, during the maturation, the mammalian CNS loses the ability to regenerate after injury (12,13), just as happens during evolution. Interestingly, in mammals, peripheral nerves retain the ability to fully regenerate throughout life. Although the CNS is more plastic after birth than in adulthood, even then it begins to show a limited ability to regenerate: accurate cellular and molecular mechanisms



associated with this loss are mostly unknown. CNS regeneration in the embryonic stages of development have been demonstrated in mammals such as hamsters (14), rats (15,16), mice (17,18) and opossums (19).

### **1.3. Regeneration promoting and inhibiting mechanisms**

Neuroregeneration is a process that repairs damaged nerve tissue, which involves the formation of new functional neurons that are able to create synapses and integrate into existing neural networks, in order to properly process and transmit information. This process includes axonogenesis which implies axonal regrowth from injured neurons through the site of injury to re-establish synaptic contacts and neurogenesis, that is, the creation of new neuronal cells from precursor cells that develop new axons and establish new synapses with target cells. Usually, animals that have the substantial ability of neurogenesis, also have the ability of axonogenesis (1).

Although the exact molecular mechanisms that lead to the cessation of regeneration during development and evolution have not been elucidated yet, it is thought that differences in regeneration ability are due to several key changes, and not just one. At the cellular level, in animals where regeneration occurs, the regenerative scenario includes the wound healing process and reconstruction of tissue architecture that is necessary for stem cell migration and differentiation, which then form neurons and glia that are integrated into the injured tissue to replace damaged structures. In this process, genetic and epigenetic changes in embryonic transcriptional programs of stem/progenitor cells are important, as well as changes in surrounding cells, such as glial or immune cells. The main difference between regenerative and non-regenerative vertebrates is in the composition of the glial cell population and their response to injury: the regenerative species retain the neurogenic radial glial cells characteristic for early developmental stages (20). Endogenous neural stem cells (eNSC) have the capacity to self-renew and differentiate which can result in the production of new neurons with neurogenesis, or glial cells with gliogenesis (21). Therefore, they are being explored for tissue regeneration. During the embryonic development of vertebrates, neural stem cells are called radial glial cells, which have a characteristic appearance, with radially extending processes. They generate a large number of neurons through the process of neurogenesis. Unlike embryonic stem cells, in adulthood eNSC remain active only within specific niches which are located in the subventricular zone (SVZ), in the forebrain, and in the subgranular zone (SGZ) located in the dentate gyrus (DG) of the

hippocampus (22). The strong correlation between radial glial cells, regeneration, and neurogenesis suggests that certain characteristics of radial glial cells are crucial for their neurogenic capacity. In non-regenerating vertebrates, radial glial cells differentiate into different types of glial cells. The most abundant are GFAP-positive astrocytes, found in white matter, that infiltrate the wound site upon injury and deposit extracellular matrix and proteoglycans, resulting in a glial scar that prevents axonal growth (23). Also, there is reduced production of growth factors in the area of injury, which are very important in the self-repair process of damaged neurons and neural stem cells, as well as the generation of new ones.

Molecules that affect axonogenesis have been intensively investigated, in order to identify extracellular inhibitors of regeneration, such as myelin-associated proteins, tenascins, and proteoglycans, including chondroitin sulfate (24). Disrupting these inhibitory signals, either individually or in combination, has so far failed to induce strong axon regeneration. On the other hand, many extracellular molecules, such as axon guidance molecules [ephrins, semaphorins, Wnt glycoproteins; (25)], growth factors [brain-derived neurotrophic factor (BDNF) and nerve growth factor (NGF); (26,27)] or entire intracellular molecular pathways [PI3K/Akt/mammalian target of rapamycin – mTOR; (28)] that are active during development, have been identified as promoters of regeneration.

Therefore, strategies to promote CNS regeneration in mammals include neutralizing potential growth inhibitory molecules, transplantation of cells or tissues that support axonal elongation, and delivery of axonal growth-promoting factors (29,30). Although these approaches show promising results, they are still insufficient for functional tissue recovery after injury. The full list of the molecules that affect regeneration and the way they interact is still incomplete and insufficient.

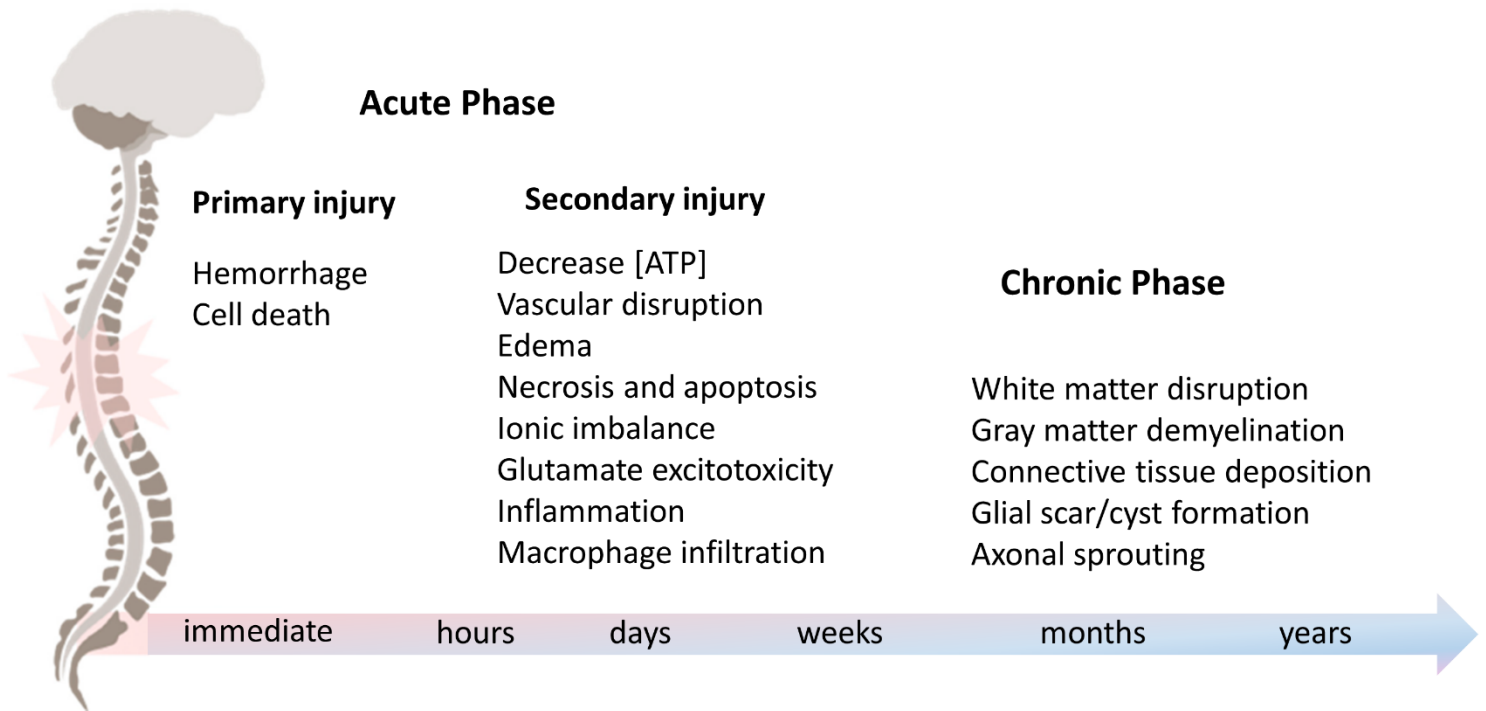
#### 1.4. Central nervous system injuries

Traumatic brain injury (TBI) and spinal cord injury (SCI) are the two most common types of CNS injuries. TBI is defined as disruption of brain activity due to an external force or violent impact to the head (31) while SCI is most commonly caused by direct mechanical force on the spine that fractures or dislocates vertebrae, primarily damaging white matter and axons, and in some cases motor neurons (32).

Traumatic SCI is one of the most severe injuries of the CNS leading to devastating motor, functional, sensory, structural, and social disorders in the lives of affected individuals. There is an urgent clinical need to discover and develop more effective therapeutic strategies for the treatment of SCI (33). The reason for the slower progress in finding effective drugs and therapeutic approaches in the treatment of SCI lies in the heterogeneous and complex pathophysiology of this severe disorder (34).

There are several types of SCI classification, among which spinal cord injury can be described as a two-phase process in which the initial acute phase includes both primary and secondary injury, while the chronic phase includes processes that occur weeks, months, and even years after the acute phase (**Figure 1**). The primary injury refers to the initial physical trauma to the spinal cord which usually occurs with dislocation or fracture of the spine. The initial trauma leads to immediate hemorrhage and cell death. This triggers a pathophysiological cascade where the secondary injury takes place. Secondary SCI occurs within minutes or hours after the primary injury and can last from days to years, and over such a long period causes progressive damage to the spinal cord tissue in the injured area. The mechanism of secondary SCI is accompanied by a series of biochemical, cellular, and molecular processes that contribute to the self-destruction of spinal cord tissue by interfering with the possibility of neuronal regeneration and recovery (35). Secondary injury can be divided into acute, subacute, and chronic phases. The acute phase occurs immediately after the primary injury and the processes characteristic of this phase are vascular disruption, excitotoxicity, ionic imbalance, calcium influx, oxidative stress, lipid peroxidation, neuroinflammation, edema, and cell death by necrosis (36). With injury progression, the subacute phase occurs accompanied by cell apoptosis, retrograde degeneration of the distal end of an axon (Wallerian degeneration), retraction bulb formation, axon demyelination, extracellular matrix remodeling, and glial scar formation around the injured site. Eventually, a chronic phase occurs which involves white matter

disruption, gray matter demyelination, connective tissue deposition, glial scar/cyst formation, and axonal sprouting (35).



**Figure 1. Pathological and physiological changes during acute and chronic phases after spinal cord injury.**

The figure schematically shows initial trauma to the spinal cord that immediately triggers a cascade of events where the secondary injury takes place. Weeks to months, and even years after the acute phase, the chronic phase is established. The illustration was adapted from Pereira et al., 2019.

Ultimately, the brain and spinal cord tend to reorganize their neural circuits and restore their functionality in a process called neural plasticity. In addition to the existing research, additional investigations were made focusing on the discovery of the causes of CNS inability to successfully regenerate damaged neural circuits (35). Therefore, great efforts and financial resources are being invested to develop new therapeutic strategies for the treatment of nerve tissue injuries that would enable clinically significant recovery of SCI patients.

In recent years, the goal of therapeutic recovery strategies has been predominantly aimed at targeting numerous inhibitors of neuronal regeneration following primary or secondary spinal cord injury. Recent strategies include preventing glial scar formation in lesions, supporting neuronal regeneration and re-establishment of the damaged synapses, antagonizing myelin-associated inhibitory signaling, and distributing effective drugs, substrates, and cells to required sites within the injured spinal cord (33).

## **1.5. Therapeutic interventions for SCI**

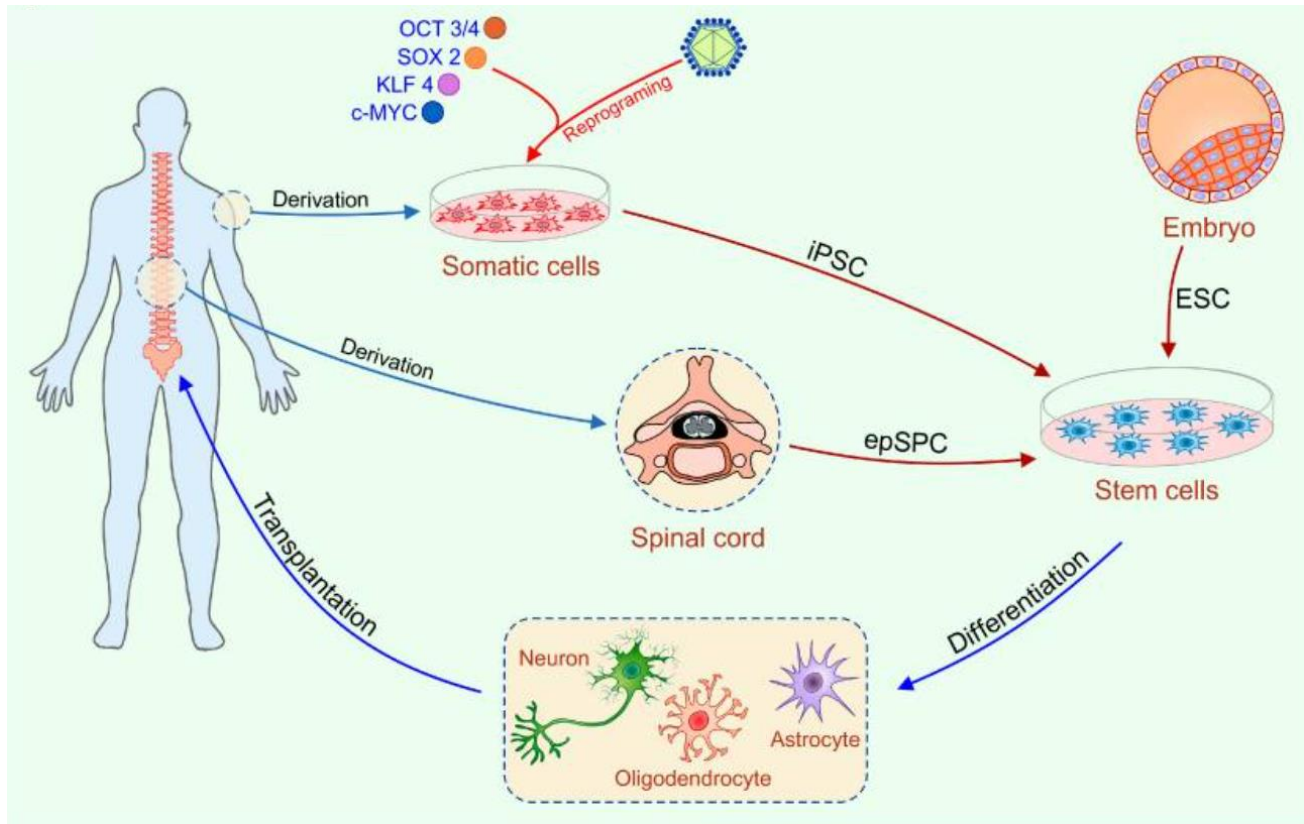
Current therapeutic interventions for SCI are surgical and consist of decompression and pharmacological interventions using corticosteroid methylprednisolone in order to limit the inflammatory response (30). The use of methylprednisolone is currently not recommended because of very serious and frequent side effects, as well as the lack of strong evidence of clinical benefits (30,35), although it has been used in the treatment of SCI for the past 50 years.

### **1.5.1. Stem cell-based therapies**

Over the past few decades, stem cell-based therapies have become a new strategy in the development of therapies for the treatment of CNS injuries (37). The reason for stem cell transplantation lies in their ability to differentiate and replace damaged nerve tissue, but also to modify the microenvironment and regenerate damaged neural circuits. Although there are a number of benefits offered by the use of stem cells transplantation, there are also challenges to be considered, such as the establishment of effective differentiation protocols, selecting a cell source, analyzing and monitoring integration, and survival of transplanted cells (35). Several types of cells are used in cell-based therapies such as mesenchymal stem cells (MSC), oligodendrocyte progenitor cells (OPC), neural stem cells (NSC), induced pluripotent stem cells (iPSC), embryonic stem cells (ESC), and others (38).

ESCs are characterized by the ability to self-renew indefinitely, by the expression of cytoplasmic and nuclear pluripotency-associated stem cell markers, atypical cell cycle regulation, and the ability to differentiate in any of the three embryonic germ layers (ectoderm, mesoderm, and endoderm). These characteristics strongly support the development of ESC-based therapeutic applications (39).

In 2006, a group of scientists showed that stem cells with properties similar to ESCs could be generated from mouse fibroblasts by simultaneously introducing four genes (Oct4, Sox2, Klf4, c-Myc) (40). This breakthrough discovery of methods to generate iPSCs from somatic cells has opened up new therapeutic opportunities for the treatment of SCI and for the development of cell-based therapeutic strategies thanks to their ability to differentiate into neural progenitor cells (NPCs): neurons, oligodendrocytes, astrocytes, neural crest cells and mesenchymal stromal cells that can act to replace lost or dead neurons, induce axonal growth and stimulate synapses formation, reduce inflammation and repair damaged axons (remyelination) (**Figure 2**). All of the benefits of these cells have prompted their application in developmental cell transplantation studies, patient-specific disease studies, and drug screening. Consequently, the development of personalized medicine is accelerating (35,41).

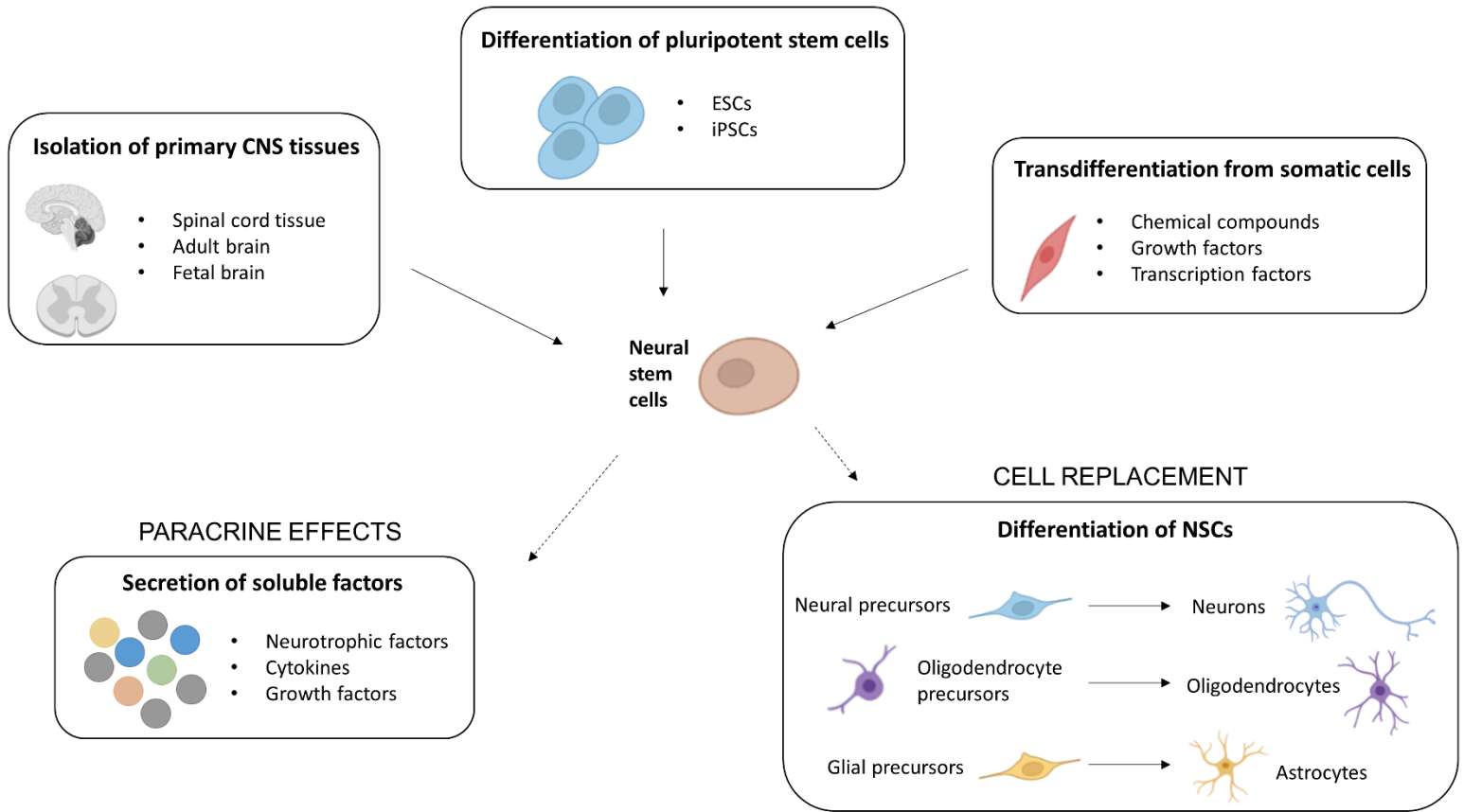


**Figure 2. Human embryonic stem cells (hESC), induced pluripotent stem cells (iPSC) and ependymal stem/progenitor cells (epSPC) as promising tools in the therapy of SCI.** Source: Gazdic et al., 2018.

NSCs are one of the leading recent strategies in the development of therapies for a number of neurodevelopmental, and neurodegenerative diseases and neurotrauma (37). Their potential has been recognized thanks to their ability to differentiate into neurons, oligodendrocytes, and astrocytes, but also to functionally replace and integrate into damaged neuronal circuits (**Figure 3**). This approach also promotes spinal cord regeneration by secretion of neurotrophic factors (37) such as BDNF and NGF, growth factors such as vascular endothelial growth factor (VEGF), transforming growth factor (TGF- $\beta$ ), and epithelial growth factor (EGF) on the injury site, improving axonal growth, preventing inflammation, and protecting damaged cells (2,42). Generally speaking, NSC transplantation has been shown to be beneficial for their effective differentiation and survival, promoting axonal growth, remyelination, CNS regeneration, and glial scar reduction (43). Most cell transplantation studies have transplanted human NSCs into animal

models, imposing the need for the administration of immunosuppressive drugs. Several preclinical and clinical studies have been conducted to develop an effective therapeutic strategy that does not involve immunosuppression. However, after the removal of immunosuppressive agents, the recipient's immune system began to reject the transplanted cells. For this reason, the importance of developing iPSC-based therapies is being promoted, which appears to be the most favorable and safest source of cells for SCI treatment (35).





**Figure 3. Neural stem cell sources and their therapeutic applicability after cell transplantation.**

There are three main sources to generate NSCs: direct isolation from primary CNS tissue, differentiation from pluripotent stem cells and lineage reprogramming of somatic cells. Once on the injury site, NSCs can be differentiated and also secrete paracrine factors that may support neurological repair. The illustration was adapted from Pereira et al., 2019, and created with BioRender.com.

### **1.5.2. Molecular therapies**

Novel pharmacological neuroprotective therapies for the acute phase of SCI, which are currently under clinical trials, are minocycline and riluzole, two drugs whose mechanism of action is focused on targeting secondary events, such as excitotoxicity and inflammation. Besides the two mentioned drugs, additional molecular approaches in the treatment of SCI are cytokines, which use has also proven to be a promising strategy for the treatment of SCI due to their regenerative characteristics that promote functional and morphological recovery of traumatic SCI (35).

Glycoprotein granulocyte colony-stimulating factor (G-CSF) is the most widely studied cytokine for the treatment of SCI but is commonly used to treat neutropenia (44,45). Because of its neuroprotective effects, it has been suggested as a treatment for neuronal injury (46,47). Its outcomes are manifested in reduced expression of inflammatory cytokines (48). Furthermore, interleukin-4 (IL-4) is another promising cytokine as a new therapeutic treatment strategy of SCI (49). Its characteristics are the activation of macrophages to manifest a phenotype associated with the recovery of injured tissue. Both G-CSF and IL-4 have demonstrated safe and effective administration and some degree of recovery (38).

Scientists are intensively probing potential drugs and their synthesis in order to facilitate and speed up the recovery of patients suffering from SCI. Additional pharmacological approaches under investigation include the use of monosialotetrahexosylganglioside (GM-1) (50), magnesium (51), basic fibroblast growth factor (bFGF or FGF-2) (52), and hepatocyte growth factor (53).

### **1.6. Regenerative biomaterials**

Regenerative biomaterials are one of the recent strategies in the development of therapies for the treatment of SCI. At the SCI site, they can deliver drugs, fill cavities, and provide adsorption sites for the host and for transplanted cells. The main purpose behind the idea of developing regenerative biomaterials is their possibility to mimic the physiological extracellular matrix of the spinal cord and reconstruct a suitable regenerative niche for SCI repair (33). As extracellular matrix substitutes for SCI, biomaterial scaffolds must have the following specifications: they need to maintain a balance of mechanical strength and softness in order to avoid crushing of surrounding residual tissues (54), they must possess a certain degree of permeability, convenient porosity, surface topography and good cellular biocompatibility (55). In addition, the scaffold degradation rate

should match with the rate of axon and tissue regeneration (56). While some of the regenerative biomaterials can inhibit apoptosis, inflammation, and glial scar formation, others have shown the ability to promote and support neurogenesis, angiogenesis, and axonal growth. However, there are some limitations and additional problems to be addressed, such as material safety and efficacy as well as standardization of their production, in order that regenerative biomaterial scaffolds become a risk-free therapeutic approach in SCI treatment (33).

Natural, synthetic, and combined materials are used to manufacture biomaterial scaffolds for SCI repair. Natural materials have been widely used to develop regenerative scaffolds for the purpose of repairing SCI because of their advantages, such as low toxicity, biodegradability and biocompatibility, favorable intrinsic cell interaction, and biological functionality (57). Collagen, hyaluronic acid, chitosan, alginate, gelatin, agarose, and fibrin are the most common natural materials applied in SCI repair (33). Collagen, a protein of the extracellular matrix, supports cell adhesion, proliferation, differentiation, and migration, and has a weak immune rejection response after transplantation. For these reasons, collagen has become the most popular choice among natural materials for the production of biomaterial scaffolds in regenerative medicine (58,59). Besides the listed natural regenerative biomaterials, nanomaterials are also used and have an important role in the diagnosis and treatment of numerous neurological diseases (60). Because of their structure and properties, there has been fast-growing interest in using them in a wide range of applications, including drug delivery. They cross the blood-brain barrier and, with better efficacy and safety, deliver specific molecules to target cells (61).

The use of synthetic materials in the field of regenerative medicine has a lot of advantages. Some of these include controlled biodegradability and porosity, low or no levels of toxicity, minimal inflammatory response, and adaptive mechanical and physicochemical properties. Since different kinds of synthetic polymers can be combined with each other, they can be used for the adjuvant treatment of CNS injuries resulting in positive outcomes (62). Poly- $\epsilon$ -caprolactone, polylactic acid, poly (lactic-co-glycolic acid), poly- $\beta$ -hydroxybutyrate, polyethylene glycol, poly (2-hydroxyethyl methacrylate), and polyvinyl alcohol are various polymeric regenerative biomaterials studied in the repair and treatment of SCI (33).

The combination of natural and synthetic regenerative materials seeks to improve the performance of scaffolds in order to advance therapeutic strategies for SCI (33). Although each material has its advantages and disadvantages, it is still unknown which combination of materials is most favorable and what the most appropriate time for cell transplantation is.

### **1.7. Animal models of SCI**

In order to understand the complex biomedical and pathological mechanisms of traumatic SCI and to develop new therapeutic strategies for their treatment, different animal models have been developed (63). Although an ideal animal model for preclinical trials does not exist, several features are required: relevance in mimicking the pathophysiology of human SCI, availability, reproducibility, and animal potential to generate injuries of various types and severity. The most commonly used animal models in SCI studies are small rodents, rats and mice, due to their wide availability, ease of maintenance and use, but also cost-effectiveness compared to primate and larger non-primate animal models (64). Rat models of SCI animals better mimic the morphological, electrophysiological, functional, and pathophysiological features of human SCI compared to mice and non-primates (65). Larger animal models, such as pigs, dogs, cats, and primates, have been used in preclinical models in recent years to successfully translate promising therapeutic treatments from small rodent models to human clinical trials. The benefit of using larger animals, especially non-primates, is the similarity to humans, in terms of their physiology, neuroanatomy, and size, which greatly favors the development of new drugs, advances in bioengineering, rehabilitation, and electrophysiological studies to treat human SCI (66).

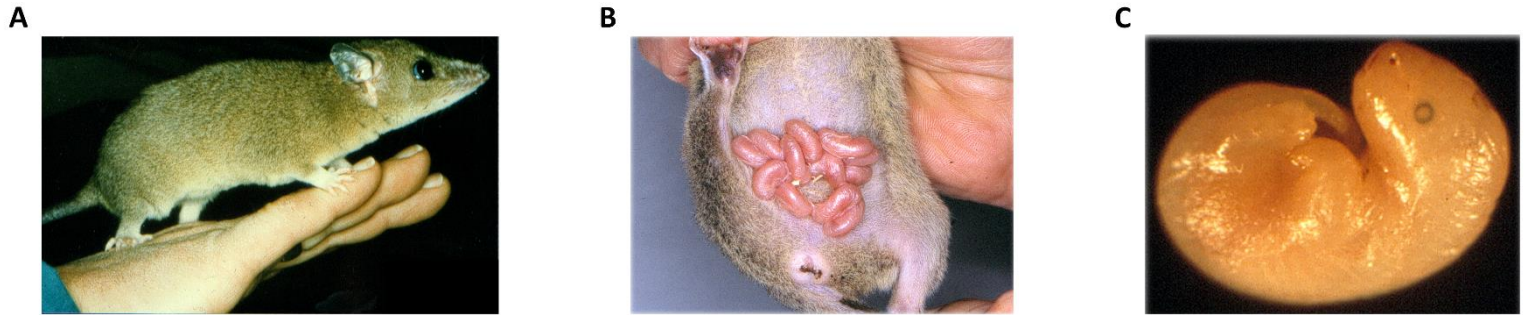
However, there are some limitations to the use of both small and large animal models in preclinical trials. The greatest limitation is the animal ability to predict possible treatment outcomes of human SCI due to the severity, incidence, and location of spinal cord injuries whose degree of variability is higher in humans than in laboratory animals. Larger animals are more relevant for preclinical trials compared to small rodents, but due to their extremely high cost of housing involving specialized facilities and more food, their use is limited in this area. Although numerous research studies are in favor of rats as an animal model of a spinal cord contusion injury, mouse models have been used far more extensively in SCI studies primarily for the availability of mutant and transgenic mice, which is important for the detection of cellular but also molecular mechanisms of traumatic SCI (63).

Besides *in vivo*, there are also *in vitro* animal models that investigate molecular and cellular changes in the pathophysiology of SCI in a more simplified and controlled environment (67). *In vitro* models greatly reduce the number and suffering of animals used in research. In this case, the SCI is not performed on live animals, but the anesthetized animal is sacrificed and its brain or spinal cord tissue is isolated and maintained in culture, where the mechanical or pharmacological experimental injury is induced. *In vitro* models have many other advantages: they simplify the pathophysiology of injury and allow the separation of individual molecular components involved in complex pathophysiological processes of injury. In addition, *in vitro* preparations may be exposed to solutions that contain known and controlled concentrations of ions, neurotransmitters, new potential neuroprotective drugs, and other molecules. At the same time, it is easier to perform experimental genetic modifications. The spinal cord can be maintained *in vitro* for weeks, retaining functionality, developmental course, and regeneration capacity. In this model, experimental mechanical or pharmacological injuries can be induced, in order to study axonal regeneration and growth (68,69). *In vitro* models have been validated and have already been used in research to prove the importance of certain molecules in neuronal regeneration (70,71).

The second preparation is the *in vitro* CNS primary dissociated cell culture, a simpler preparation that allows better resolution and is more suitable for genetic manipulation of candidate molecules and testing of their influence on the properties of selected cells. Both intact spinal cord tissue and dissociated cultures contain a heterogeneous cell population, however, primary CNS cultures can be enriched in neurons when grown in a selective neuronal medium and controlled environment. This allows us to monitor individual cells and to investigate molecular mechanisms specific for different CNS cell types (72–74). Research studies on primary CNS cultures have contributed to many important discoveries regarding development and regeneration, such as neurite outgrowth, axon guidance, synaptogenesis, and neuronal network formation closely mimicking the physiological state of cells *in vivo* (75,76).

### 1.8. Opossum *Monodelphis domestica* in neuroregeneration research








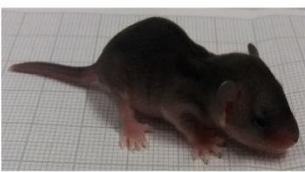
The South American gray short-tailed opossum *Monodelphis domestica* is a small, pouchless nocturnal marsupial (**Figure 4A**) (77). They are native to Brazil and neighboring countries. Some areas of investigation, especially in the field of developmental research, have developed because of the marsupial characteristics of *M. domestica* laboratory animals. For instance, the pups (usually from 1 to 12) are born after a short (14-day) gestation at a highly immature stage of development (13,78–80). Since they are born very immature, as embryos, they have a unique possibility to successfully regenerate CNS after injury postnatally, in the first 2 weeks of their life (**Figure 5**). The ability to fully regenerate abruptly stops around the postnatal day (P) 12 in the cervical part of the spinal cord, while in the less mature lumbar segments regeneration continues until postnatal day 17 (81–83). Opossum neonates are easily accessible since opossums lack pouches (**Figures 4B and 4C**). Because of that, the opossum represents a unique opportunity to study mammalian CNS that has the ability to regenerate, without the need for killing or invasive operations on pregnant females, as is the case with mice or rats. Also, the other advantage is that the tiny neonatal opossum CNS can be maintained in culture and is similar to the intact animal for its ability to regenerate. The use of neonates instead of embryos reduces the total number of animals used and their suffering, which is in line with 3R (reduction, refinement, and replacement).



**Figure 4. Opossum *Monodelphis domestica*:** A. adult animal; B. mother with pups attached to her mammary glands; C. neonatal opossum. Source: <https://genome.cshlp.org> (The opossum genome) and Saunders et al., 2002.

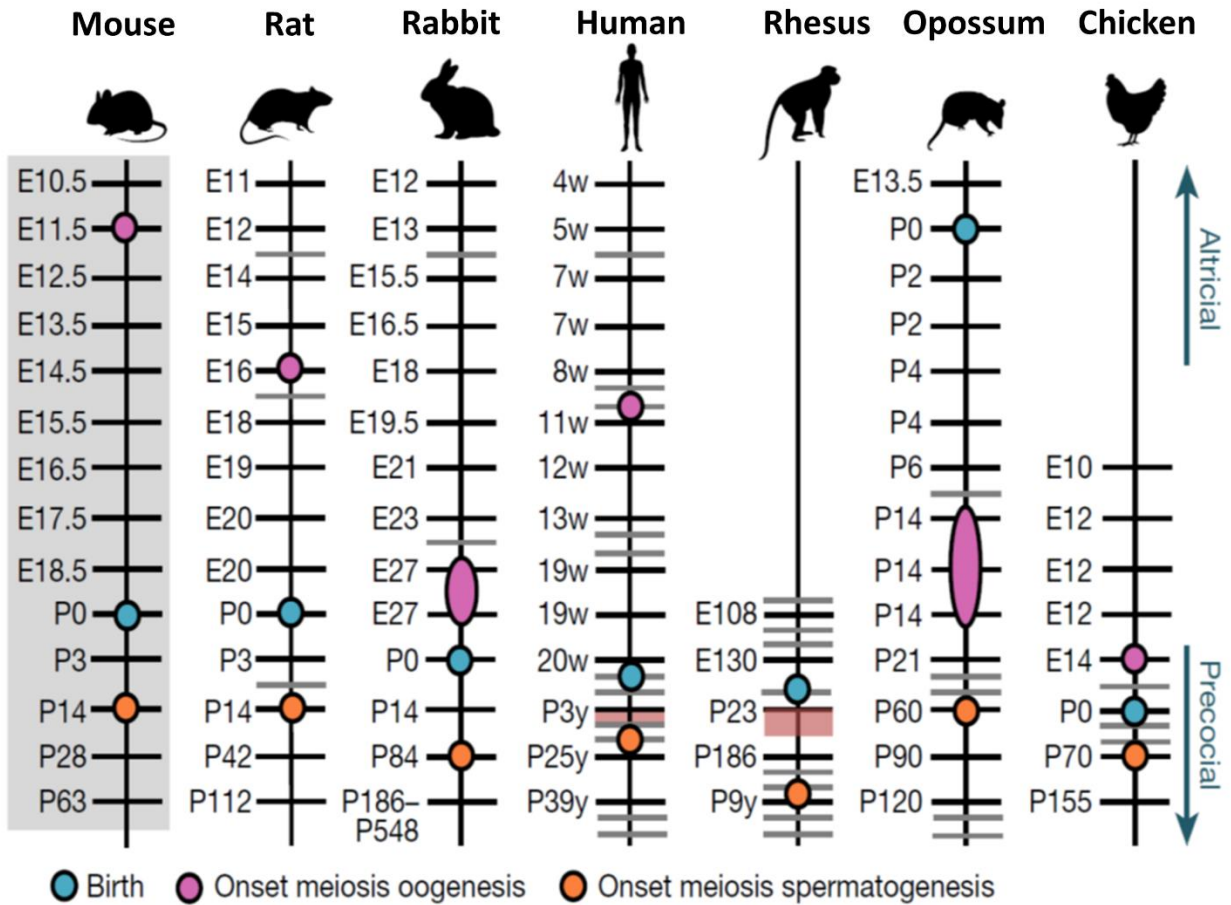
*In vivo* studies were done on opossums, confirming the regenerative capacity (12,79,84,85). After the axons were completely severed in the spinal cord of neonatal opossums, which were attached to the mother but anesthetized during surgery, they grow again and form functional connections. These are precise enough for the animal to walk, climb up, and swim in a coordinated manner like uninjured animals. Therefore, functional regeneration of connections does occur successfully in the opossum spinal cord, provided that the animal is young enough. Apart from successful *in vivo* regeneration, previous studies of CNS regeneration of neonatal opossums have demonstrated successful regeneration after *in vitro* injury of an intact spinal cord maintained in culture (68,86–88).

According to recent transcriptome analysis, in line with previous studies (89,90), P0 opossum corresponds to embryonic day 12 (E12) rat or E11.5 mice embryo and 40 day old human embryo (79). P14 opossums are comparable to P0 mouse or rat, and P21 opossum corresponds to P3 mouse or rat (**Figure 6**). However, opossums differ from embryos by their possibility to breathe and suckle with effective neuronal circuits (80).

	<b>P3</b>	<b>P4</b>	<b>P5</b>	<b>P6</b>
				
<b>size (mm)</b>	<b>9.14</b>	<b>11.5</b>	<b>12.6</b>	<b>13.5</b>
<b>weight (g)</b>	<b>0.14</b>	<b>0.19</b>	<b>0.22</b>	<b>0.25</b>
	<b>P16</b>	<b>P17</b>	<b>P18</b>	<b>P30</b>
				
<b>size (mm)</b>	<b>31.2</b>	<b>33</b>	<b>33.33</b>	<b>45</b>
<b>weight (g)</b>	<b>1.43</b>	<b>1.63</b>	<b>1.71</b>	<b>3</b>

**Figure 5. The age, body weight and size of opossums.** In the upper row *Monodelphis domestica* at postnatal ages P3-6 are shown, which have the ability to successfully regenerate the spinal cord after injury. In the bottom row *Monodelphis domestica* at postnatal ages P16-18 and P30 are shown, without the capacity to regenerate.





**Figure 6. Stage correspondences across species throughout the entire development.** Source: Cardoso-Moreira et al., 2019.

Because of *M. domestica* species-specific characteristics, besides studies on regeneration, other areas of investigation have developed, providing an additional opportunity for research that other laboratory animals did not provide. Thus, *M. domestica* is used as a model for melanoma caused by ultraviolet radiation, for angiogenesis and corneal cancer. It is also used as a model for dietary-induced hypercholesterolemia rather than other laboratory animals because of its omnivorous characteristics (77). Because of their less developed immune system (91), neonatal opossums are valuable models for studying immune system development in mammals, as well as for cell transplantation and grafting studies (92).

Marsupials (Metatheria) diverged from placental mammals (Eutheria) between 170 and 190 M years ago (93–95), making them excellent models for comparative evolutionary studies (96). Based on the studies done in 2007 (94,97) there is a high degree of protein sequence homology between *M. domestica* and other mammalian species, especially with human proteins (~96.7%). These findings should encourage scientists for future investigations on opossums.

### **1.9. Proteomics in regeneration studies**

There are very few research studies that have used comparative proteomic analysis to detect differences between regenerating and non-regenerating systems: for example, between peripheral sensory and motor nerves in rats (98), after rat spinal cord injury (99), and following complete transection of opossum neonatal spinal cord (100–102). In the studies done on the opossum, spinal tissue that can or cannot regenerate was compared after traumatic injury revealing increased activity of proteins associated with the inflammatory response. The main goal of these studies was to reveal the cellular response to traumatic SCI, however, our study was the first attempt to compare the proteomes of intact, non-injured mammalian CNS tissue with different regeneration capacities. The spinal cord is an excellent model for studying the development and regeneration of the CNS, from its origin to the creation of complex neural networks (11). This approach revealed the basic properties of neuronal tissue related to regeneration.

### **1.10. Neuroregeneration in neurodegenerative disorders**

Neurodegenerative diseases are incurable conditions that are characterized by the progressive loss of the structure and function of the central or peripheral nervous system (PNS), resulting in degeneration and death of nerve cells.

Huntington's disease (HD) is an autosomal dominant neurodegenerative disorder that is caused by excessive expansion of CAG repeats in the first exon of the Huntingtin gene (HTT), which causes an increase in the cytoplasmic HTT protein chain near the N terminus in the polyglutamine-rich region. The wild-type huntingtin has a positive effect on the transcription of BDNF, a factor necessary for the survival of neurons in the brain. However, this useful activity of huntingtin is lost in the mutated form of the protein, resulting in reduced expression of BDNF observed in HD patients. This causes a lack of neurotrophic support, due to which newly formed neurons fail to go through the process of maturation or fit into the existing neural network, which could be one of the reasons why neuroregeneration is unsuccessful (103). Since wild-type huntingtin plays a role in brain development and neuronal survival (104) it is suggested that restoring its activity and increasing BDNF production could be one of the therapeutic approaches for treating HD (103).

Alzheimer's disease (AD) is a neurological disorder that leads to progressive loss of cognitive functions. It is characterized by extracellular deposits of  $\beta$ -amyloid ( $A\beta$ ) peptides leading to the formation of senile plaques and intracellular neurofibrillary tangles. The two major isoforms of  $A\beta$  are the 42-residue  $A\beta_{42}$  and the 40-residue  $A\beta_{40}$ .  $A\beta_{42}$ , which is mostly generated in the last stage of the disease, is believed to be crucial in suppressing neuroregeneration and reducing the viability of progenitor cells.  $A\beta_{42}$  acts on the microenvironment by reducing the levels of several neurotrophic factors, such as BDNF $\alpha$ , and increasing the levels of fibroblast growth factor 2 (FGF2). Therefore, it is hypothesized that a strong mitogen such as FGF-2 could prevent neuronal differentiation and maturation in the absence of neurotrophic factors, leading to developmental malfunction of newly generated neurons (105). Another potential target for treating AD is the inhibition of JNK3, which is a part of c-Jun N-terminal kinases (JNKs) that, among other things, play an important role in neuronal plasticity and regeneration. In addition to memory and learning (106,107), JNK3 is an enzyme important in brain development (108), neurite formation, and plasticity (109,110). Under pathological conditions, JNK3 enhances  $A\beta$  production and acts as a degenerative signal transducer which leads to pathogenesis and neuronal death in AD (111).

Parkinson's disease (PD) is a complex progressive neurodegenerative disease characterized by a movement disorder, and the second most common neurodegenerative disease, after AD. Symptoms such as tremor, bradykinesia, rigidity, and postural instability are the result of decreased dopamine secretion in the part of the brain that plays an important role in controlling voluntary movements (112). One study reported a reduced number of proliferative cells in the SVZ of PD patients compared to the control group (113). In addition, fewer proliferating cells [epidermal growth factor receptor (EGFR)-positive cells] in the SVZ of human PD patients compared with age-matched controls were also reported in a different study. The EGF receptor is necessary for increased precursor cell proliferation. Such results suggest that adult neuroregeneration in PD is indeed impaired (114). Dopamine depletion is thought to be one of the causes of impaired adult neuroregeneration because it impairs precursor cell proliferation in Parkinson's disease (113).

A common characteristic in neurodegenerative diseases, including Parkinson's, Alzheimer's, and Huntington's disease are alterations in adult neurogenesis. This is interesting because proteins that are responsible for different pathological diseases trigger the loss of different neural populations (112). Proteins that are involved in neurodegeneration, are also involved in plastic processes, when in physiological conditions. For example, in AD, because of extracellular aggregation of amyloid-precursor protein (APP),  $\beta$ -amyloid plaques and intracellular neurofibrillary tangles are formed (115,116). However, both APP and  $\beta$ -amyloid play key roles in normal functioning, endogenous  $\beta$ -amyloid is even necessary for hippocampal synaptic plasticity and memory (117).

For these reasons, understanding the mechanisms of neurogenesis regulation is essential for the development of new therapeutic approaches for currently incurable neurodegenerative diseases. Future clinical studies should be based on strategies aiming to stimulate neuronal plasticity (112), especially proper stimulation or supply of growth factors because there is more and more evidence that they restore some of the cognitive loss (118).

## 2. THESIS AIMS AND HYPOTHESES

One of the major challenge of modern biology concerns the inability of the adult mammalian CNS to regenerate and repair itself after injury. Even though our understanding of molecular and cellular mechanisms that promote or inhibit neuronal regeneration is expanding, it is still unclear what are the key differences between the neuronal systems that can and cannot regenerate. Therefore, this study aims to detect proteins differentially distributed in the spinal cord tissue of young opossums that can or cannot regenerate to pinpoint the candidates that could revert regenerative potential and to develop new, experimental, mammalian *in vitro* platforms to study CNS development and neuroregeneration.

### **HYPOTHESES:**

- I. During the period of development when regeneration stops being possible, the level of proteins that control neuroregeneration changes in the opossum spinal cord.
- II. By comparing the results of comparative transcriptomics and proteomics it is possible to identify molecules of interest and narrow down the number of candidates for functional tests.
- III. Proteins associated with neurodegenerative diseases have an important function during CNS development and are possibly important for neuroregeneration as well.
- IV. The postnatal opossum *Monodelphis domestica* has many advantages for setting up the new spinal cord cell culture preparation, providing the possibility to study development, regeneration and test the functional role of the candidate molecules in neuroregeneration.

### **3. MATERIALS AND METHODS**

#### **3.1. Materials**

##### **3.1.1. Reagents for protein precipitation**

Acetone (VWR International, USA), 20 mM dithiothreitol (DTT; Sigma Aldrich, Germany), chloroform (Carl Roth, Germany), methanol (Sigma Aldrich, Germany), trichloroacetic acid (TCA; Sigma Aldrich, Germany)

##### **3.1.2. Buffers for cell lysis, 1D and 2D SDS-polyacrylamide gel electrophoresis (PAGE) and western blot (WB)**

RIPA lysis buffer: 50 mM Tris-HCl, pH 8.0 (Sigma Aldrich, Germany), 150 mM NaCl (Sigma Aldrich, Germany), 0.5% (w/v) sodium deoxycholate (Sigma Aldrich, Germany), 0.1% (w/v) sodium dodecyl sulphate (SDS), 1% (v/v) NP-40 (Abcam, UK)

Quantification buffer #2: 0.5 M Tris-HCl pH 6.8, 10% (w/v) SDS, glycerol (Sigma Aldrich, Germany), dH<sub>2</sub>O

4x Laemmli sample buffer: 0.5 M Tris-HCl pH 6.8, glycerol, 8% (w/v) SDS, 2 M DTT, bromophenol blue (dash; Bio-Rad, USA), dH<sub>2</sub>O

Stacking gel: 0.5 M Tris-HCl pH 6.8, 30% (v/v) acrylamide (stock is 30% acrylamide/bis-solution with ratio 29:1; Carl Roth, Germany), 1% (w/v) SDS, 1% (w/v) ammonium persulfate (APS; Sigma Aldrich, Germany), 0.1% (v/v) N,N,N',N'-Tetramethylethylenediamine (TEMED, Sigma Aldrich, Germany), dH<sub>2</sub>O

Resolving gel: 1.5 M Tris-HCl pH 8.8, 30% (v/v) acrylamide (stock is 30% acrylamide/bis-solution with ratio 29:1), 1% (w/v) SDS, 1% (w/v) ammonium persulfate, 0.05% (v/v) TEMED, dH<sub>2</sub>O

10x SDS running buffer: 250 mM Tris, 1.92 M glycine (Sigma Aldrich, Germany), 1% (w/v) SDS; for 1x SDS running buffer mix 1 part of 10x SDS running buffer with 9 parts of dH<sub>2</sub>O

1x Transfer buffer: 25 mM Tris, 192 mM glycine, 20% (v/v) methanol, dH<sub>2</sub>O

Tris buffered saline (TBS)-Tween: 198 mM Tris, 1.5 M NaCl; 0.1% (v/v) Tween<sup>®</sup> 20 (Carl Roth, Germany), dH<sub>2</sub>O

Blocking buffer: 5% (w/v) bovine serum album (BSA; Carl Roth, Germany) or 5% (w/v) powdered milk (Carl Roth, Germany) in TBS-T

Primary antibody solution: 3% (w/v) BSA or 3% (w/v) powdered milk in TBS-T

Secondary antibody solution: 1% (w/v) BSA in TBS-T

Proteins were transferred to nitrocellulose membrane packed with blotting paper, pore size 0.2 µm (GE Healthcare, USA)

Coomassie brilliant blue stain (stock solution): 0.1% (w/v) Coomassie Brilliant Blue G250 (Sigma Aldrich, Germany), 2% (v/v) ortho-phosphoric acid (Thermo Fisher Scientific, USA), 10% (w/v) ammonium sulfate (VWR International, USA), dH<sub>2</sub>O; for working solution 1 part of methanol was mixed with 4 parts of stock solution

Re-hydration buffer: 2 M urea (Sigma Aldrich, Germany), 7 M thiourea (Sigma Aldrich, Germany), 4% (w/v) CHAPS (Sigma Aldrich, Germany); 65 mM DTT was freshly added to the buffer

Equilibration buffer: 1.5 M Tris-HCl pH 8.8, 6 M urea, glycerol, 2% (w/v) SDS, bromophenol blue (dash), dH<sub>2</sub>O

Agarose solution: 0.5% (w/v) agarose (Sigma Aldrich, Germany), bromophenol blue (dash), 1 part of 10x running buffer and 4 parts of ultrapure water

Fixation solution: 30% (v/v) ethanol (Gram-Mol, Croatia), 10% (v/v) acetic acid (Sigma Aldrich), dH<sub>2</sub>O

### **3.1.3. Reagents for mass spectrometry (MS)**

100 mM sodium thiosulfate (Sigma Aldrich, Germany), 30 mM potassium hexacyanoferrate (Sigma Aldrich, Germany), acetonitrile (ACN; Sigma Aldrich, Germany), 100 mM ammonium bicarbonate (Sigma Aldrich, Germany), recombinant trypsin (Sigma Aldrich, Germany), acetone, formic acid (Thermo Fisher Scientific, USA), trifluoroacetic acid (TFA; Thermo Fisher Scientific, USA);

Digestion buffer: 95% (v/v) 100 mM ammonium bicarbonate and 5% (v/v) acetonitrile

Matrix composition: 2.5 g of  $\alpha$ -cyano-4-hydroxycinnamic acid powder (Sigma Aldrich, Germany) dissolved in a solution containing 0.5 mL of acetonitrile and 0.5 mL of 0.1% trifluoroacetic acid

Urea buffer, pH 8.5: 8 M urea, 100 mM Tris, dH<sub>2</sub>O

Ammonium bicarbonate buffer: 50 mM ammonium bicarbonate, dH<sub>2</sub>O

#### **3.1.4. Reagents for RNA extraction and integrity**

Nuclease-free water (New England Biolabs (NEB), USA)

70% (v/v) ethanol (Honeywell, USA) in nuclease-free water

DEPC H<sub>2</sub>O: 0.1 % (v/v) diethyl pyrocarbonate (DEPC; Sigma Aldrich, Germany) in dH<sub>2</sub>O

Tris-acetate-EDTA buffer (TAE), 50x: 50 mM ethylenediaminetetraacetic acid (EDTA) disodium salt (Sigma Aldrich, Germany), 2 M Tris, 1 M glacial acetic acid (Sigma Aldrich, Germany)

Agarose gel: 1x TAE buffer, agarose, SYBR<sup>®</sup> Safe DNA Gel Stain (Thermo Fisher Scientific, USA), MassRuler DNA Loading Dye, 6x (#R0621, Thermo Fisher Scientific, USA)

#### **3.1.5. Reagents for immunofluorescence on tissue**

Fixation buffer: 4% paraformaldehyde (PFA; Sigma Aldrich, Germany), pH 6.9

10x phosphate-buffered saline (PBS): 1.37 M NaCl, 27 mM KCl (Sigma Aldrich, Germany), 100 mM Na<sub>2</sub>HPO<sub>4</sub> (Sigma Aldrich, Germany), 18 mM KH<sub>2</sub>PO<sub>4</sub> (Sigma Aldrich, Germany), dH<sub>2</sub>O

Tissue storage solution: 30% (w/v) sucrose (Sigma Aldrich, Germany) in 1x PBS

Washing buffer PBS-T: 0.1% (v/v) Tween<sup>®</sup> 20 in 1x PBS

Blocking solution: 3% (v/v) normal goat serum (NGS; PAN-Biotech, Germany), 3% (v/v) 10% BSA, 0.3% (v/v) 10% Triton X-100 (Bio-Rad, USA), 10x PBS, dH<sub>2</sub>O

Antibody solution: 1% (v/v) NGS, 1% (v/v) 10% BSA, 0.1% (v/v) 10% Tween<sup>®</sup> 20, 10x PBS, dH<sub>2</sub>O



### **3.1.6. Reagents for primary neuronal culture from opossum CNS**

10x Krebs solution, pH 7.5: 113 mM NaCl, 4.5 mM KCl, 1 mM MgCl<sub>2</sub> x 6H<sub>2</sub>O, 25 mM NaHCO<sub>3</sub>, 1 mM NaH<sub>2</sub>PO<sub>4</sub>, 1 mM CaCl<sub>2</sub>x2H<sub>2</sub>O, 11 mM glucose, 0.5% (v/v) Penicillin / Streptomycin / Amphotericin B Solution (all from Sigma Aldrich, Germany), dH<sub>2</sub>O

Hanks' Balanced Salt Solution (HBSS), pH 7.5: HBSS, 10 mM HEPES (PAN-Biotech, Germany), 3.5 g/L glucose, 0.3 g/L BSA, 1% (v/v) Penicillin-Streptomycin (PAN-Biotech, Germany)

Enzyme solutions: 0.5% (v/v) and 2.5% (v/v) Trypsin-EDTA solution in HBSS (Santa Cruz Biotechnology (SCBT), USA), collagenase type I (Sigma Aldrich, Germany)

Triturating solution: 10 µg/mL Deoxyribonuclease I from bovine pancreas Type IV (DNase I; Sigma Aldrich, Germany), 1 mg/mL trypsin inhibitor (SCBT, USA), 1% (w/v) BSA, HBSS

BSA cushion: 5% (w/v) BSA in HBSS

Substrates that promote cell adhesion: poly-L-lysine, poly-D-lysine, poly-L-ornithine hydrobromide, Laminin from Engelbreth-Holm-Swarm murine sarcoma (all from Sigma Aldrich, Germany)

Plating medium: Dulbecco's minimum essential medium with stable glutamine (DMEM; PAN-Biotech, Germany) supplemented with 10% (v/v) of fetal bovine serum (FBS; PAN-Biotech, Germany) and 1% (v/v) Penicillin-Streptomycin

Neuronal medium: Neurobasal™ Medium (Thermo Fisher Scientific, USA), B-27™ Supplement (50X), serum free (Thermo Fisher Scientific, USA), 1 mM stable glutamine (PAN-Biotech, Germany), 1% (v/v) Penicillin-Streptomycin

### **3.1.7. Reagents for intact opossum spinal cord kept *in vitro***

Enriched Basal Medium Eagle (BME medium): BME medium (PAN-Biotech, Germany) enriched with 0.2% FBS, 10 µg/mL insulin (Sigma Aldrich, Germany), 250 ng/mL amphotericin B (Sigma Aldrich, Germany), 100 µg/mL gentamycin (Sigma Aldrich, Germany), 30 ng/mL nerve growth factor-7S (NGF-7S; Sigma Aldrich, Germany)

### 3.1.8. Primary antibodies

**Table 1. List of primary antibodies**

<b>Antigen</b>	<b>Host</b>	<b>Catalog no.</b>	<b>Supplier</b>	<b>Dilution</b>
Akt	Rabbit	9272	Cell Signaling	WB 1:1000
p-Akt	Rabbit	4058	Cell Signaling	WB 1:1000
APBB1	Mouse	sc-398389	Santa Cruz	WB 1:100
BACE1	Rabbit	ab183612	Abcam	WB 1:1000
BLBP	Rabbit	ab32423	Abcam	WB 1:1000 IHC 1:1000
c-Jun	Mouse	sc-74543	Santa Cruz	WB 1:100
Erk 1/2	Rabbit	9102	Cell Signaling	WB 1:1000
p-Erk 1/2	Rabbit	4370	Cell Signaling	WB 1:1000
Flotillin-1	Mouse	sc-74566	Santa Cruz	WB 1:100
GAP43	Rabbit	ab75810	Abcam	WB 1:20000
GAPDH	Mouse	HRP-60004	Proteintech	WB 1:10000
GFAP	Mouse	G3893	Sigma Aldrich	WB 1:1000
HIP1	Mouse	sc-47754	Santa Cruz	WB 1:100
HTT	Rabbit	ab109115	Abcam	WB 1:5000 IHC 1:100
Ki67	Rabbit	ab15580	Abcam	IHC 1:400
Map2	Mouse	M1406	Sigma Aldrich	IHC 1:500
MAPK9	Mouse	sc-271133	Santa Cruz	WB 1:100
MAPK10	Rabbit	2305	Cell Signaling	WB 1:1000
MAPKAPK-2	Rabbit	12155	Cell Signaling	WB 1:1000
MBP	Goat	sc-13912	Santa Cruz	WB 1:100
MEK 1/2	Rabbit	8727	Cell Signaling	WB 1:1000
NDEL1	Mouse	sc-365094	Santa Cruz	WB 1:100
NeuN	Mouse	MAB377	Merck Millipore	IHC 1:400
NRG1	Mouse	sc-393006	Santa Cruz	WB 1:100
p38	Rabbit	8690	Cell Signaling	WB 1:1000
p-p38	Rabbit	4511	Cell Signaling	WB 1:1000

PAX2	Rabbit	ab79389	Abcam	WB 1:1000 IHC 1:200
PAX6	Rabbit	ab5790	Abcam	WB 1:1000
Rab7	Rabbit	9367	Cell Signaling	WB 1:1000
p-SAPK/JNK	Mouse	9255	Cell Signaling	WB 1:1000
SMI-32	Mouse	NE1023	Calbiochem	IHC 1:500
Synapsin	Rabbit	AB1543	Sigma Aldrich	IHC 1:500

### 3.1.9. Secondary antibodies

**Table 2. List of secondary antibodies**

Antibody	Host	Catalog no.	Supplier	Dilution
Anti-goat	HRP	sc-2354	Santa Cruz	WB 1:2000
Anti-mouse	HRP	7076	Cell Signaling	WB 1:2000
Anti-rabbit	HRP	7074	Cell Signaling	WB 1:2000
Anti-mouse	Alexa Fluor 555	A21137	Invitrogen	IHC 1:500
Anti-rabbit	Alexa Fluor 488	A11070	Invitrogen	IHC 1:500

### 3.1.10. Primers

**Table 3. Primers used for qRT-PCR analysis**

Gene	Forward primer	Reverse primer
APPBP1	GCTGCTGCTGTGGGTAATCA	TGGACTCTGGTGCCTGACCTA
BACE1	AGTGTGGGAATACAGGGTGG	AGAAACTACCTGGCACCTCC
BLBP	CAGGTGGGGAATGTGACTAA	TGCAGTTCCTATCATCTGGA
cJUN	CAAGTGCCGGAAAAGGAAGC	CGCTGTTCACGTGGTTCATG
DCC	CCCCAGAATCCAGATGAAGA	GCATTCAAAACGTGATGGTG
GAP43	GTCCTAAAGCAGAAGAGGCC	CGGAGAGTTGTCAGTGGAAG
GAPDH	ATGCCCCAATGTTCGTGATG	GTCATGAGTCCTTCCACAATGC
GFAP	AACAAAACAAGGTCCTGGCA	GTGGTCAGATCTTCAGCCAG
HIP1	GCAAGGCTGAAAGTTTGGAG	CAAACCCCAAAATCCAAATG

HTT	AATCCCGGAATTTTGTAGGG	AACAGGAAGGGTCATTGCAC
MAPK9	CTCTTTTCCTGTGGCCAACC	CTCTTTGGGCTTTGGACACC
MAPK10	ACTAGGAACACCATGCCCAG	AATCCGGAAGAGCTTGGGG
MAPK14	GAGGCCTAAGTTCTACCGGC	gcagcaCATACGGACCCATA
MBP	AGCCAGGGTGTGGATATGGA	CCTTGTATCCCTTGTGAGCTGAT
NDEL1	TGCCAGGCTCTATGCTAGGT	ACAGTCCAGCCAAAATGTCC
NEDD4L	ATTGTGTTCCAGAGGGCAAC	TCCAATGCAGTGTGTTGGTT
NUDCD2	CCTTTGCCACATCAACTTT	GTTGCAAGGATAGGGGATGA
NUP43	TCCAGCCCTACCACATCTTC	ACTTGTATTCCGGGGAGCTT
PARK7	CAAAGGCCTCATAGCTGCTG	TTGCCATCCTTTTCCACACG
PAX2	TACTACGAAACGGGCAGCAT	ATAGAAGAGACGCTGGGCA
PAX6	AATCGAAGGGCAAAGTGGAG	GTTGTGGGATTGGCTGGTAG
PSEN1	TCTCTACCTGCACCCTCTCT	TCTGCAGGGAAAGAAGGAGG
RAB7A	GCCATGCACTGTGCTAAAGA	GGAAGGGGCTCAGAATTAGG
RAB8A	AGTCTCTGAGGGTGGTTTGG	GTACAGTGGATGCATGGGGA
RAB8B	CGCTTTCAACACCACCTTCA	AATTCCCATGGCTCCTCTGT
RELN	TGTTTCTCTGCCTCCCTCTG	AGCCAGAGAACAGCAGTCAT
SEMA4A	ACTCCTCCCATTGACCCAG	CCCAGGAGAAAGGACCATGT
UCHL1	CCGATGGAGATTAACCCCGA	CAGTGAGGGGAAAGAGCAGA

## **3.2. Methods**

### **3.2.1. Animals**

In this study, South American grey short-tailed opossum (*Monodelphis domestica*) pups of both sexes at postnatal day 5, 18 and 30 were used. The *M. domestica* colony was maintained at the animal house facility of the University of Trieste, in accordance with the guidelines of the Italian Animal Welfare Act, and their use was approved by the Local Veterinary Service, the Ethics Committee board and the National Ministry of Health (Permit Number: 1FF80.N.9Q3), in accordance with the European Union guidelines for animal care (d.l.116/92; 86/609/C.E.). The animals are housed in standard laboratory cages in a temperature and humidity controlled environment (27-28°C; 50-60% humidity) with a 12/12 h light/dark cycle and *ad libitum* access to food and water.

### **3.2.2. Spinal cord extraction and preparation**

An optimized protocol has been developed for protein isolation from the spinal cord tissue of young opossums, which is quantitatively very limited (about 10 mg per animal), and the optimal results of 0.2 µg protein/mg tissue were obtained. In this research, spinal cords from neonatal opossums P5 and P18, with different regenerative capacities were used. P30 spinal cords were used as an additional control for analysis of protein and gene expression, since, at that age spinal cord regeneration does not occur in opossums.

All efforts were made to minimize suffering and to reduce the number of animals used. Animals were sacrificed by decapitation, all the organs were removed, the body was washed in ice cold oxygenated dissection solution and attached to the dissecting pad. Small incisions were made on both sides of the cervical spine. The tip of the spine was held with forceps (Dumont®, Carl Roth, Germany), while vertebrae were cut on both sides with spring scissors (Fine Science Tools, Germany). In the end, the whole spinal cord up to the sacral part was uncovered. Afterwards, all nerves on the side of the spinal cord were excised with fine scissors (World Precision Instruments, UK) making the spinal cord accessible for extraction. The whole spinal cord tissue was lysed with RIPA lysis buffer supplemented with protease and phosphatase inhibitors (Roche Applied Science, CH) and incubated on ice for 10 minutes. Tissue was then homogenized with an electric homogenizer (Tissue Master 125, Omni International, USA) and sonicated (Sonopuls Mini20, Bandelin, Germany) 3 x 5 seconds on the ice at an amplitude of 20-50%, depending on the

postnatal day of the tissue. After that, the suspension was centrifuged (5424 R centrifuge, Eppendorf, Germany) for 30 minutes at 14000 rpm at 4°C. Supernatants of whole cell lysate were used for further analysis or stored at -80°C.

### **3.2.3. Protein precipitation**

Sample preparation is an important step in proteomic methodologies, and the quality of the results depends on the nature of the sample and the properties of the proteins. Therefore, we tested various pre-treatment methods that included six different precipitation procedures: acetone, acetone containing 20 mM DTT, a mixture of chloroform and methanol, 20% TCA, a mixture of 20% TCA and acetone and 100% TCA.

### **3.2.4. Protein concentration**

Protein concentration in samples was determined using a Qubit™ protein kit (Thermo Fisher Scientific, USA) according to the manufacturer's instructions. Briefly, a Qubit™ working solution was prepared by diluting Qubit™ protein reagent 1:200 in Qubit™ protein buffer. 199 µL of Qubit™ working solution and 1 µL of the sample were then mixed in each tube. The concentration was measured on a Qubit™ fluorometer (Thermo Fisher Scientific, USA).

### **3.2.5. Two-dimensional gel electrophoresis (2D SDS-PAGE)**

Prior to electrophoresis, 800 µg of protein was precipitated with cold acetone. Four volumes of acetone were added to one volume of protein sample. The mixture was vortexed and incubated at -20°C overnight. This was followed by centrifugation at 14000 rpm for 15 min at 4°C. The supernatant was discarded and the pellet was air dried. Proteins were re-suspended in the re-hydration buffer before the first step of 2-DE. Spinal cord samples containing 800 µg of total protein were applied to an immobilized pH 3-10 nonlinear gradient with 17 cm strips (Bio-Rad, USA) in a focusing tray for active re-hydration. The IPG strip was covered with mineral oil (Bio-Rad, USA) and placed in a system for isoelectric focusing (IEF; PROTEAN i12 IEF Cell, Bio-Rad, USA) and the process of active re-hydration started (16h, 20°C, 50V). IEF was conducted at 20°C with a current limit of 50 µA per strip. An IEF program was applied that involved pre-focusing, followed by four steps with an initial rapid step of 250V to 1000V with an increase to a total of 43 000 volt hours (Vh). During pre-focusing, the electrode wicks were used to improve the disposal of excess water, salts and proteins with pI values outside the pH range of the IPG strips.

Small electrode wicks immersed in miliQ-H<sub>2</sub>O were placed at the anode and cathode ends of the IPG strips just beneath the electrodes. Prior to conducting SDS-PAGE in the second dimension, the IPG strips were equilibrated on a rotating platform (Cleaver Scientific, UK) for 10 minutes using 1% DTT and 2.5% IAA dissolved in equilibration buffer. After the first dimension separation, the proteins were separated on Protean II XL (Bio-Rad, USA) using 12% polyacrylamide gels. The IPG strips were placed on the top of the polymerized gel with 5 µL of Precision Plus Protein Dual Xtra Standards (Bio-Rad, USA) on the end. The IPG strip was fixed with agarose solution. Electrophoresis was conducted under conditions of 15 mA during the first 30 minutes and 30 mA to the end of electrophoresis. The gels were stained using two different protocols: Coomassie Brilliant Blue G-250 (Bio-Rad, USA) stain for electrophoresis and Pierce<sup>®</sup> Silver stain (Thermo Fisher Scientific, USA) according to the manufacturer's instructions. Gels were fixed in a mixture of 30% (v/v) ethanol in water with 10% (v/v) acetic acid. The 2D analysis of protein pellets was performed in triplicate. For gel imaging, ChemiDoc MP Imaging System (Bio-Rad, USA) was used. The gels were analyzed using ImageMaster 2D Platinum 7 software (GE Healthcare, USA) to see if there were any differences in the spinal cord tissue with different regenerative capacities.

### **3.2.6. Establishment of protocols for mass spectrometry**

#### **3.2.6.1. In gel protein digestion – MALDI-TOF MS**

Protein spots stained with Pierce<sup>®</sup> Silver Stain were cut from gels and washed with a 1:1 solution of 100 mM sodium thiosulfate and 30 mM potassium hexacyanoferrate. After all the liquid was removed, acetonitrile was added for dehydration, covering the gel particles which have shrunk. Acetonitrile was removed and the gel pieces were rehydrated in 100 mM ammonium bicarbonate for 5 minutes. An equal volume of acetonitrile was then added and incubated for 15 minutes. When all the liquid was removed, gel particles were dried in a vacuum centrifuge (Savant SPD 2010 SpeedVac Concentrator, Thermo Scientific, USA). Gel particles were rehydrated by adding 5 µL of trypsin solution (10 ng/µL) dissolved in digestion buffer and incubated in the thermomixer (ThermoMixer C, Eppendorf, Germany) for 45 minutes at 37°C. After that, the remaining enzyme supernatant was removed and replaced with 10 µL of the digestion buffer (without enzyme) and digested overnight in the thermomixer at 37°C.

Protein spots stained with Coomassie Brilliant Blue G-250 stain were washed with a 1:1 solution of ultrapure water and acetone three times for 15 minutes. Acetonitrile was added for dehydration of gel pieces, which were then rehydrated with a solution of 100 mM ammonium bicarbonate. The samples were then incubated for 15 minutes in acetonitrile. Protein digestion took place overnight with 15 µl trypsin (10 ng / µl) at 37°C.

The next day, the same procedure was followed in both protocols. After overnight digestion sufficient volume of 50 mM ammonium bicarbonate was added and incubated for 15 minutes. The same was done with acetonitrile and the supernatant was recovered. The extraction was repeated two times with 1% formic acid and acetonitrile in an equal volume. The extracts were pooled out and the samples were dried in a vacuum centrifuge. Peptides were re-dissolved in 10 µL of 0.1% formic acid and sonicated briefly. Pipette tips with C-18 filler (Merck Millipore, USA) were used for purification and concentration of the samples before application to the MALDI plate (MTP Anchorchip ground steel 384, Bruker, USA). C18 tips are ready-to-use pipette-tip columns of C18 resin that enable fast and efficient capture, concentration, desalting and elution of peptides for MALDI mass spectrometry and other methods. The sample was mixed with the matrix in equal volume. Mass spectra were recorded with the help of the mass spectrometer MALDI-TOF MS (UltrafleXtreme, Bruker, USA) in a reflectron positive mode ranging from 700 to 3500 Da. Calibration was performed with the standard mixture of peptides with a small mass (Sigma Aldrich, Germany). The spectra were analyzed in the program FlexAnalysis (Bruker Daltonics, version 3.0) and the identification of peptide mass fingerprinting of the samples was conducted with the MASCOT algorithm (Matrix Science Co., UK). Searching parameters: 50 ppm precursor tolerance, maximum of 1 missed cleavage, carbamidomethylation of cysteine and methionine oxidation as variable modifications.

#### **3.2.6.2. Filter aided sample preparation (FASP)**

Part of the methods was done with rat spinal cord tissue (collaboration with prof. Andrea Nistri, SISSA, Trieste), which was also an additional value and served as a control. The opossum spinal cord tissue is hard to work with due to its small size (about 10-20 mg). Moreover, it was attempted to minimize the number of animals sacrificed. Rat spinal cord tissue is very similar in composition to opossum spinal cord tissue and the lysis was done as described in section 3.2.2.



FASP combines both purification and digestion of proteins. Ultrafiltration spin columns (Abcam, UK) were used to retain the protein sample while removing impurities, as well as for alkylation and subsequent digestion. 10 kDa cut-off spin filters were used. Urea buffer was used for washing the filters. The pH of this buffer was adjusted to pH 8.5 using HCl. DTT, which was dissolved in urea buffer to a final concentration of 8 mM, was used to reduce the proteins and IAA (final concentration of 50 mM also dissolved in urea buffer) for alkylation of proteins. Ammonium bicarbonate buffer was used for buffering solutions to slightly alkaline pH during chemical purification. Between every step centrifugation was performed, each time for 10 minutes at 20000 g. For overnight digestion at 37°C, 1 µL of trypsin stock solution was added to 99 µL of ammonium bicarbonate buffer resulting in a final trypsin concentration of 0.01 µg/µL. This working solution was intended for digesting 50 µg of protein. After overnight digestion, the filter was centrifuged for 10 minutes at 20000 g. Another 40 µL of ammonium bicarbonate was added to the filter and again centrifuged for 10 minutes at 20000 g. The flow-through was collected and acidified with 10% TFA to a final concentration of 0.2% TFA. Eluted peptides were further analyzed by nano-liquid chromatography tandem mass spectrometry (LC-MS/MS) using ACQUITY UPLC M-Class system coupled on-line to a Synapt G2-Si via the NanoLockSpray dual electrospray ion source (Waters™, USA). Mobile phase A was 0.1% formic acid in water and mobile phase B was 0.1% formic acid in acetonitrile. Peptides were first trapped onto the Symmetry C18 2G-V/M 5µm, 180 µm x 20 mm reversed phase trapping column (Waters™, USA) using 0.5% (v/v) mobile phase B and 5 µL/min flowrate for 3 min. Secondly, peptides were eluted onto the HSS T3 1.8 µm, 75 µm x 150 mm analytical column (Waters™, USA) that was heated to 40°C, with a gradient of 3-40% (v/v) mobile phase B at a 300 nL/min flowrate over 100 min. Leucine Enkephaline (Waters™, USA) was used as a lock mass and sampled every 60 s into the mass spectrometer via the reference sprayer of the NanoLockSpray source. MS analysis of eluting peptides was performed in LCMSe continuum, positive mode, with the following parameters: m/z 50-2000 mass range (MS and MS/MS), 0.5 scan time, 5-100 min acquisition time and 174 m/s transfer wave velocity. In the low energy mode, data was collected at a constant collision energy of 4 eV and for high energy mode ramp from 19-45 eV was used. The analysis of each sample (rat spinal cord fresh fixed and one day in culture) was done in three technical replicates to test the variability in the testing protocol itself, and then each technical replicate was tested to see if there is a systemic variation that affects the experimental process which causes samples to be biased. An example of systemic variation, in

this case, can be equipment that is out of calibration and causes a bias. Also, during the mass spectrometry analysis, quality control and total ion chromatogram were being checked to see if the standard was going correctly. Protein sequences for identification purposes were downloaded from SwisProt - Uniprot database with a total of 8117 sequences of *Rattus norvegicus* proteins.

### **3.2.6.3. In gel protein digestion – HPLC-MS/MS**

In collaboration with prof. Boris Maček from the Proteome Center in Tübingen, Nano-HPLC-MS/MS was used to analyze the protein gel bands. Opossum spinal cord tissue lysis was done as described in section 3.2.2. Excised protein bands were digested in-gel using trypsin. LC-MS/MS analysis was done on an Easy-nLC 1200 (Thermo Fisher Scientific, USA) coupled to a QExactive HF mass spectrometer (Thermo Fisher Scientific, USA). Peptide mixtures were injected onto the column in HPLC solvent A (0.5% acetic acid) at a flow rate of 500 nl/min and subsequently eluted with a 130 min gradient of 5 - 33% HPLC solvent B (80% ACN in 0.5% acetic acid) at a flow rate of 200 nl/min. The 7 most intense precursor ions were sequentially fragmented in each scan cycle using HCD fragmentation. MS data were processed using the MaxQuant software suite (v.1.5.2.28). Database search was performed using the Andromeda search engine. Spectra were searched against a Uniprot *Monodelphis domestica* database, as well as a database containing 248 commonly observed contaminants. In database search, semi-specificity was required for trypsin and up to two missed cleavages were allowed. Carbamidomethylation of cysteine was set as fixed modification, protein N-terminal acetylation, and oxidation of methionine were set as variable modifications. False Discovery Rate (FDR) was set to 1% at protein as well as peptide level. A minimum of two unmodified peptide counts were required for the respective protein quantification. The label-free algorithm was enabled, as was the “match between runs” option.

### **3.2.7. Functional categorization of proteins**

To obtain an overview of the biological significance the proteins were categorized according to their main biological functions collected from the UniProt<sup>1</sup> protein knowledge database and PubMed<sup>2</sup>. Functional categorization was done using the PANTHER<sup>3</sup> classification system.

### **3.2.8. SDS-PAGE and Western blot**

#### **3.2.8.1. Spinal cord tissue**

For tissue samples, precipitation was performed with ice-cold acetone at -20°C overnight (4 volumes of acetone in 1 volume of sample were added). The next day the samples were centrifuged at 14000 rpm for 15 minutes at 4°C, the supernatant was discarded, and the pellet was air-dried. The protein pellets were re-suspended in Laemmli sample buffer 2x or 4x, depending on the measured concentration, vortexed and put in the ultrasonic water bath (Elmasonic EASY, Carl Roth, Germany) for 15 minutes at 60°C. Samples were heated in the thermoblock (Clever Scientific, UK) at 95°C for 5 minutes.

#### **3.2.8.2. Spinal cord cell culture**

Upon the end of the treatment or at a certain developmental stage, cells were washed twice with 1 mL of ice-cold 1X PBS. After washing, cells were detached with 0.5% trypsin for cell cultures obtained from P5 opossums and 2.5% trypsin for cell cultures obtained from P18 opossums, for 5 minutes at 32°C and then harvested with DMEM medium containing FBS. Cells were centrifuged at 100 g for 5 minutes at 4°C, the supernatant was discarded and Laemmli sample buffer was added to the pellet. Lysates were sonicated for 15 seconds. Samples were heated at 95°C for 5 minutes.

The samples were separated in 1X SDS running buffer using Mini-PROTEAN Tetra Vertical Electrophoresis Cell (Bio-Rad, USA). For protein size identification pre-stained protein marker (Cat# 26619, Thermo Fisher Scientific, USA) was used. The stacking gel was run at 90V for 15 minutes, while the separating gel was run at 150V until the loading dye reached the end of the gel. After protein separation in polyacrylamide gel, proteins were transferred to nitrocellulose membrane (0.2 µm pore size). During the preparation of the gel-membrane (transfer) sandwich,

---

<sup>1</sup> <http://www.uniprot.org>

<sup>2</sup> <http://www.ncbi.nlm.nih.gov>

<sup>3</sup> <http://pantherdb.org/>

all the components were soaked in 1X Transfer Buffer. The transfer sandwich was tightly closed into a gel holder cassette and placed into the Mini Trans-Blot Electrophoretic Transfer Cell (Bio-Rad, USA). The transfer was run at 100V for 90-120 minutes depending on the protein size. After transfer, the membrane was blocked with a blocking solution for 1 hour at room temperature (RT) to reduce unspecific antibody binding. After blocking, the membrane was incubated with primary antibody overnight at 4°C. All primary antibodies were diluted in blocking solution. The next day, the membranes were washed 3 times with TBS-Tween for 10 minutes and probed with suitable secondary antibody conjugated with HRP for 1 hour at RT. After washing 3 x 10 minutes, membranes were incubated with LiteAblot turbo chemiluminescent substrate (Euro-Clone, Italy) for 1 minute and developed using ChemiDoc™ MP Imaging System (Bio-Rad, USA).

### **3.2.9. Western blot bands quantification**

Band density was measured by ImageJ software (National Institute of Health, USA). Obtained values were normalized to GAPDH loading control.

### **3.2.10. RNA isolation and quantification**

Total RNA was isolated using a Monarch Total RNA Miniprep kit (NEB, USA) according to the manufacturer's instructions. Proteinase K (NEB, USA) was added to digest many contaminating proteins and protect nucleic acids. DNase I (NEB, USA) was added to the RNA isolation column to eliminate genomic DNA. RNA was eluted with 50 µL nuclease free water. The concentration and purity of the eluted RNA were analyzed on a Biodrop Duo spectrophotometer (Harvard Bioscience, Holliston, MA, USA), and the quality was then analyzed on a 2% agarose gel. To assess the purity of the samples, the absorbance ratio values at 260 nm and 280 nm ( $A_{260}/A_{280}$ ) and at 260 nm and 230 nm ( $A_{260}/A_{230}$ ) were considered.  $A_{260}/A_{280}$  was about 2.0, while  $A_{260}/A_{230}$  ranged from 2.0 to 2.2 indicating the high purity of RNA.

### **3.2.11. Complementary DNA (cDNA) synthesis by reverse transcription**

The QuantiTect Reverse Transcription Kit (Qiagen, Germany) was used to transcribe RNA into cDNA following the manufacturer's protocol. 1 µg of total RNA was transcribed into cDNA in a 20 µL reaction buffer. Reverse transcription was performed in a thermocycler (Mastercycler Nexus Thermal Cycler, Eppendorf, Germany). The entire reaction took place at 42°C and was then inactivated at 95°C.

### 3.2.12. Quantitative real-time polymerase chain reaction (RT-qPCR) and gene expression analysis

For a single RT-qPCR reaction, 5 µL of cDNA (diluted 10x in dH<sub>2</sub>O) was used as a starting material. The RT-qPCR reaction was performed with Luna Universal qPCR Master Mix (NEB, USA) based on SYBR Green I dye using LightCycler 480 (Roche Holding AG, Basel, Switzerland). The RT-qPCR program consisted of preincubation for 10 minutes at 95°C, 50 cycles of DNA amplification with the following steps: 10 s at 95°C, 10 s at 55°C and 20 s at 72°C, and final melting and cooling. Glyceraldehyde-3-phosphate dehydrogenase (GAPDH) was used as a reference gene. The cycle threshold (Ct) of the GAPDH gene ranged from 16 to 18 cycles. The cut-off value for Ct was 35. Non template controls were performed for each primer pair used in the RT-qPCR reaction. The relative mRNA expression levels of all genes of interest (GOI) were normalized to the level of the reference gene (GAPDH) and calculated by the equation  $2^{-(Ct \text{ value for GAPDH} - Ct \text{ value for GOI})}$ . All samples were made in technical duplicate and biological triplicate. The primers for genes of interest were designed using the Primer3Plus<sup>4</sup> web interface and transcripts for the opossum were downloaded from the Ensembl database<sup>5</sup>. The sequence specificity of designed primers was confirmed using the NCBI Nucleotide BLAST tool<sup>6</sup>. The synthesis service of selected primers was performed by Metabion, Germany. The initial PCR amplification products were run on a 2% agarose gel to verify that the primer pairs multiplied a single product of the predicted size. The change in gene expression of interest is expressed as a “fold change” ( $2^{(-\Delta\Delta Ct)}$ ). The mRNA level in the control sample was designated as 1. Primers used in experiments are listed in **Table 3**.

### 3.2.13. Immunofluorescence on frozen tissue sections

Spinal cords were carefully removed and fixed by immersion in 4% PFA for 12-24 hours at 4°C. After fixation, PFA was removed and the tissue was washed 3x with 1x PBS and immersed in 30% sucrose in PBS, which is a common cryoprotectant used to preserve tissue morphology by preventing ice crystal formation in tissues when water freezes and expands. Before frozen sectioning on a cryostat, lumbar spinal cord segments were embedded in optimal cutting

---

<sup>4</sup> <https://primer3plus.com/>

<sup>5</sup> <https://www.ensembl.org/>

<sup>6</sup> <https://blast.ncbi.nlm.nih.gov/Blast.cgi>

temperature (OCT) medium Killik (Bio-Optica, Milano). Tissues were cut in 16  $\mu\text{m}$  thin sections using the sliding cryostat Leica CM1850 (Leica Biosystems, Germany) and mounted on Superfrost Plus microscope slides (Menzel-Glaser; Thermo Fisher Scientific, USA). The slides were firstly trimmed with a hydrophobic pen (Vector Laboratories, Inc), the tissue sections were washed 2x for 5 minutes in 1x PBS-T, following 0.1 M glycine for 10 minutes after which they were treated with blocking solution for 1 hour at RT. After blocking, sections were incubated with primary antibodies in a humid chamber overnight at 4°C. The primary antibodies used are listed in **Table 1**. For every primary antibody used, the protein sequence similarity between opossum and immunogen was compared using the Universal Protein Resource<sup>7</sup> (UniProt). The next day slides were washed 3x with PBS-T for 5 minutes and then incubated with secondary antibodies in a humid chamber for 2 hours at RT. After that, spinal cord sections were incubated in a 1  $\mu\text{g/ml}$  solution of 4,6 -diamidino - 2 -phenylindole (DAPI; Thermo Fisher Scientific, USA) for 20 min to visualize cell nuclei. After incubation, slides were washed 2x for 5 minutes in PBS-T and the final wash was done in dH<sub>2</sub>O. The excess water from slides was dried, three drops of VECTASHIELD<sup>®</sup> mounting medium (Vector Laboratories, USA) per slide were added and the 24x60 mm coverslip (Thermo Fischer Scientific, USA) was put on the slide. The coverslips were sealed with a thin layer of nail polish. Slides were left to dry for half an hour at RT whereupon they were analyzed using a fluorescent microscope, stored short-term at 4°C or long term at -20°C, protected from light.

#### **3.2.14. Fluorescence microscopy**

Fluorescence microscopy was used to visualize the fluorescence of specific cellular components in as native a state and organization as possible. The staining of samples was analyzed using an Olympus IX83 inverted fluorescent microscope (Olympus, Japan) equipped with a Xenon lamp, Hamamatsu Orca R2 CCD camera (Hamamatsu, Japan), DIC, fluorescence optics and Cell Sense software (Olympus, Japan). Objectives used were 10x/0.3 numerical aperture (NA) air and 20x/0.5 NA air. For each immunohistochemistry sample, a minimum of 15 frames were obtained at slice spacing of 2  $\mu\text{m}$  for 10x and 1.27  $\mu\text{m}$  for 20x. Maximum intensity projection was used for each image. Image processing and analysis were performed with CellSens software and ImageJ/FIJI.

---

<sup>7</sup> <https://www.uniprot.org/>

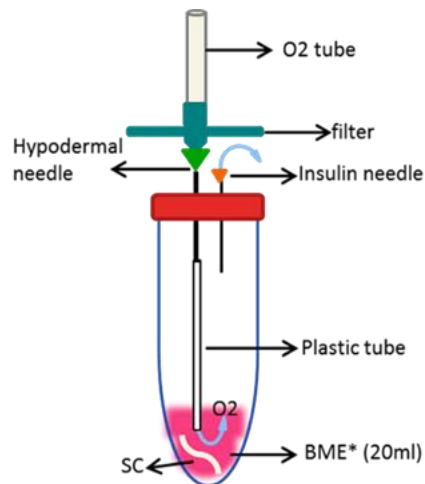
### 3.2.15. Functional studies

#### 3.2.15.1. Pharmacological inhibitor PGL-137

In this research, we used polyglutamine aggregation inhibitor, PGL-137 (sc-204208; SCBT, USA), at a concentration of 50  $\mu\text{M}$ . PGL-137 is a cell-permeable benzothiazole. Benzothiazoles are identified as potential polyglutamine aggregation inhibitors of Huntington's disease.

#### 3.2.15.2. Intact opossum spinal cord kept *in vitro*

The intact opossum spinal cords P5 and P18 were cultured, immediately after extraction, for 24 hours in a continuously oxygenated (95%  $\text{O}_2$ / 5%  $\text{CO}_2$ ) solution containing BME medium. Control samples were cultured in enriched BME medium, while in the treated samples, 50  $\mu\text{M}$  PGL-137 inhibitor was added.



**Figure 7. Schematic representation of the equipment needed for maintaining the spinal cord preparation in culture.**

### **3.2.15.3. Establishment of the primary cortex and spinal cell culture**

Before this study, no scientific literature was available on the primary dissociated spinal cultures derived from opossums. It is important to emphasize that most of the available data in this field of research were obtained using rodents (mice and rats) and that primary cultures derived from brain tissue such as cortex and hippocampus are most commonly used, while there are significantly fewer studies on primary spinal cord cultures. In this study, we successfully established protocols for opossum spinal cord and cortex primary cultures. Successful establishment of opossum-derived primary neuronal cultures consists of several key steps: tissue dissection and dissociation, selection of cellular and growth medium and cell culture conditions. Dissection and isolation of the spinal cord is an extremely sensitive procedure that requires precision and skill. This refers especially to the younger age of the opossum (P5) when the tissues are softer and much smaller, which complicates tissue handling and isolation. On the other hand, opossum tissues of older age (P18) are much more difficult to dissociate due to larger amounts of connective tissue and extracellular matrix. When dissecting nerve tissue, it is important that the tissue is immersed into a solution that allows cells to survive as much as possible during isolation. We tested several different dissection solutions (Krebs solution, Hanks' saline solution and saline with phosphate buffer) with the addition of glucose and antibiotics. The best result was achieved with an oxygenated ice-cold Krebs solution. Dissection is followed by dissociation of isolated tissue consisting of two phases: enzymatic and mechanical. In order to dissociate the tissue into individual cells, it is necessary to degrade the extracellular matrix with enzymes. Trypsin is the most commonly used enzyme in tissue dissociation whose proteolytic activity is sufficient for dissociation of the cortex. Since spinal cord tissue contains more collagen than the cortex, trypsin was used in addition to collagenase to successfully degrade the extracellular matrix of the spinal cord. During the dissociation of the spinal cord and cortical tissue, different concentrations of trypsin and collagenase were tested, as well as different temperature and time of enzymatic incubation. The optimal conditions and composition of the dissociation solution are described below. Cortices and spinal cord tissue were digested with prewarmed trypsin in HBSS by incubating at 32.5°C. The tissue from P5 pups was incubated in 0.5% (v/v) trypsin for 10 min, while that of P18 pups was incubated in 2.5% (v/v) trypsin for 15 min. After trypsin incubation, the spinal cord tissue was washed 3 times in 1x PBS and additionally incubated in 1 mg/mL collagenase type IA dissolved in cell medium, 10 min for tissue from P5 pups, and 15 min for tissue from P18 pups. In enzymatic



tissue dissociation, collagenase type IV (Thermo Fisher Scientific, USA) and commercially available enzyme formulation Accutase<sup>®</sup> (Corning, USA) were tested, however, the dissociation was not efficient. After incubation, enzymes were removed and the tissues were washed 3 times with 1x PBS. Enzymatic dissociation is followed by mechanical tissue dissociation using a 1 mL tip and pipetting up and down 15–20 times in a trituration solution. Furthermore, since the tissue from older pups (P16-18) is much more difficult to dissociate due to higher connective tissue and extracellular matrix, incubation with 5% (w/v) BSA, so-called BSA cushioning, was introduced, which largely removed the remains of dead cells and tissues after dissociation. The supernatant containing dissociated cells was collected and layered on top of the 5% (w/v) BSA cushion in the 5 ml tube to remove the cell debris. The trituration step was repeated two times for P5 and three times for P18 digested cortices and spinal cord tissue. Cells were collected by centrifugation (Megafuge 40R Refrigerated Centrifuge; Thermo Fisher Scientific, USA) for 5 min at 100 g and then resuspended in a plating medium. In order to remove the fibroblasts, a 70 µm cell strainer was placed on the 3 cm Petri dish, the cell suspension was dripped on the top of the strainer and purified by preplating for 5 min at 32°C on the plastic tissue culture dishes. Dissociated cells should be seeded on tissue culture dishes previously treated with substrates that promote cell adhesion. Several types of the most commonly used substrates were tested (poly-L-lysine, poly-D-lysine and poly-L-ornithine), and poly-L-ornithine proved to be the best. In addition to poly-L-ornithine, incubation with laminin (1-2µg/mL, incubation for 3 hours at 32°C) was introduced, which gave very positive results and significantly improved the adhesion and growth of neurons. Cells were counted using the hemocytometer (Bright-Line<sup>™</sup> Hemacytometer; Sigma Aldrich, Germany) and plated in a 6-well or 12-well plate precoated with 50 µg/ml poly-L-ornithine at the density of  $1 \times 10^5$  cells per well.

After establishing a protocol for isolation and dissociation of the cortex and spinal cord tissue, and selection of adequate substrates for cell growth, optimal conditions for the maintenance of primary cultures were determined. We tested several different media used in previous studies on isolated opossum spinal cord: BME, DMEM and Neurobasal medium. DMEM with stable glutamine and the addition of 10% FBS and 1% Penicillin/Streptomycin provided the best cell proliferation and glial and stem cell amplification. FBS contains several growth factors (bFGF, EGF, etc.) that act on the proliferation of glial and stem cells, and also on fibroblasts. Although the full composition of the FBS is not fully known, this medium is a simpler and more economical option compared to

formulations with specifically added growth factors, so we used it as a proliferative medium. For neuronal cultures, the most commonly used was the Neurobasal medium and B27 supplement, which enables neuronal differentiation. 24 hours after plating the cells in the DMEM medium, 2/3 of the medium was changed with the neuronal medium. Subsequent media changes were done once per week changing only a half of the medium with the fresh neuronal medium. The temperature for cell culture is of great importance given that the opossum body temperature is significantly lower (32°C) compared to rodents (37°C). The cortical and spinal cord cultures were maintained in an incubator (Nüve EC 160; Henderson Biomedical, UK) at 32°C, 5% CO<sub>2</sub>, and 95% relative humidity.

#### **3.2.15.4. Neurite outgrowth test**

Neurons were cultured for 24 h until neurite outgrowth, and then PGL-137 inhibitor (50µM) was added to the medium. After 24 hours, the inhibitor was removed, fresh neuronal medium was added, and the neurons were cultured until the 10th day *in vitro* (DIV10) when neuronal networks are generally considered mature (119). With this test, we can investigate the mechanisms that inhibit neurite outgrowth and molecules that enable the pro-regenerative state.

#### **3.2.15.5. New neuronal regeneration scratch test**

After the successful establishment of primary CNS cultures of the opossum, we developed a platform to investigate the regeneration of differentiated (mature) neurons of the postnatal opossum for a better understanding of the molecular mechanisms involved in CNS regeneration. This method is fast and effective and provides us with insight into the injury and regeneration of individual cells in culture. The main goal of our regeneration research is to identify factors that may encourage injured axons to regenerate and re-establish functional connections. The scratch test was performed on primary cultures of neurons isolated from the opossum spinal cord to test their ability to regenerate, but the number and viability of primary spinal cord neurons were extremely small in the cultures derived from older opossum age, so these cultures were not suitable for performing the regeneration test. Spinal cord cultures have been shown to be more demanding and more difficult to maintain than cortical, which was in accordance with *in vivo* observations (12,79,84,85).

### **3.2.16. Statistical analysis**

All experiments were performed at least in duplicate or triplicate and data are represented as mean  $\pm$  standard deviation (SD). Data were analyzed by Student's t-test using Prism software (GraphPad). For MS data, downstream bioinformatics analysis (two-sample t-test) was performed using the Perseus software package (version 1.6.1.3). The accepted level of significance was  $p < 0.05$ .  $p < 0.001$  Very significant \*\*\*, 0.001 to 0.01 Very significant \*\*, 0.01 to 0.05 Significant \*,  $\geq 0.05$  Not significant.

## 4. RESULTS

### 4.1. Protein extraction

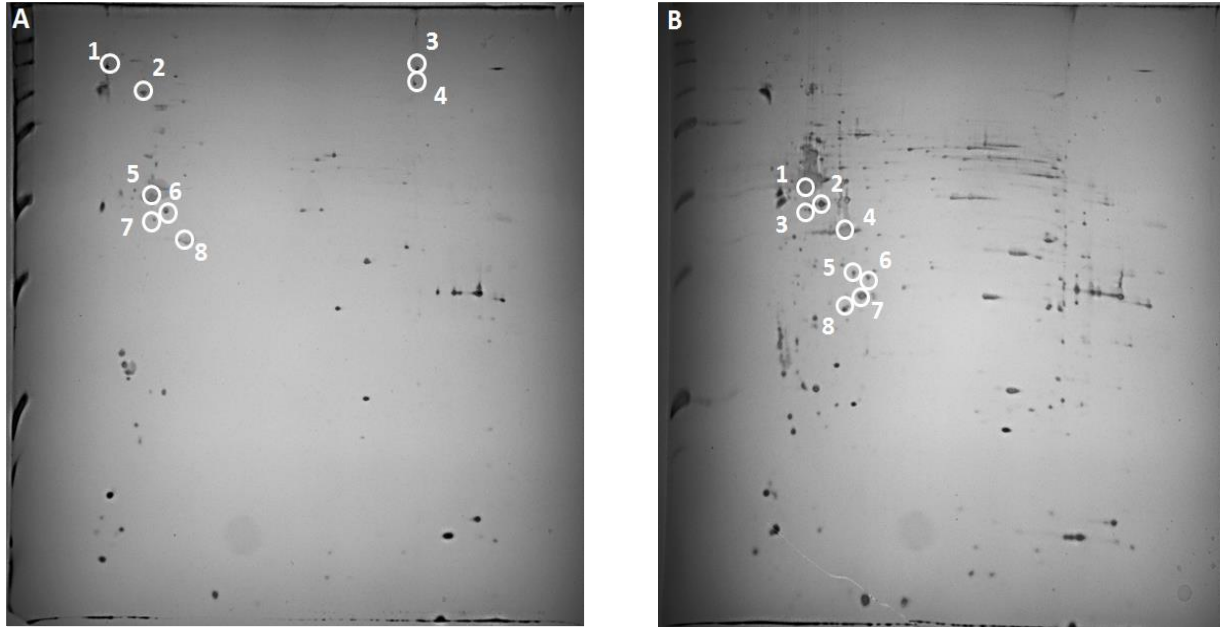
We developed a protocol to optimize protein isolation from opossum spinal cord tissue, which is very limited in quantity (10–20 mg per animal), for optimal results (0.2 µg protein/mg tissue). The protein concentration in the samples was determined using the Qubit® protein kit according to the manufacturer's instructions and then measured on a Qubit® fluorometer. We tested various pre-treatment methods that included six different precipitation procedures: acetone, acetone containing 20 mM DTT, a mixture of chloroform and methanol, 20% TCA, a mixture of 20% TCA and acetone and 100% TCA and chose acetone as the best precipitation method for further experiments.

### 4.2. Establishment of protocols for proteomic analysis of opossum spinal cord tissue and identification of proteins by mass spectrometry

We tested and developed protocols for mass spectrometry analysis of spinal cord samples as well as computer analysis of obtained results. For differential proteomic analysis, protein samples were purified, digested and analyzed by MALDI (in gel digestion), SYNAPT (filter aided sample preparation) and ORBITRAP (in gel digestion) instruments. Part of the methods done on SYNAPT instrument was run-in with rat spinal cord tissue which is very similar in composition to opossum spinal cord tissue and was also an additional value and control.

In gel digestion uses SDS-PAGE which ensures good resolution and using SDS allows the solubility of most proteins. Also, protein spots are cut from the gel to identify unknown proteins, and through electrophoresis, we eliminate contaminated proteins and molecules. Since we were optimizing new protocols we tested two gel staining dyes: Pierce® Silver Stain (**Figure 8**) and Coomassie Brilliant Blue G-250 (**Figure 9**). Silver staining involves multiple steps and reagents, thus making the process relatively long-lasting. Also, the gel requires developing after staining, in order to visualize the proteins, and the length of time required for developing is highly variable between gels, meaning that reproducibility is low. On the other hand, Coomassie staining has many more advantages including increased sensitivity, higher reproducibility and a higher number of protein spots is also obtained compared to silver staining. Due to the increased sensitivity, this method is ideal for experiments involving low molecular weight proteins.

The protocols we used for in gel digestion (2D electrophoresis) and filter aided sample preparation (FASP method), allowed the identification of no more than 200 proteins per sample for the first protocol and 800 for the second. The proteins identified were mainly cellular proteins that are present in large numbers in cells and are involved in cellular processes such as cytoskeleton formation, cellular metabolism, homeostasis maintenance, etc (**Tables 4-9**). Since the number of identified proteins was too small to detect low-molecular and rare cellular proteins which are likely to play an important role in the spinal cord regeneration process, the protocol was modified to allow the identification of a significantly larger number of proteins (at least 1000, but optimally 4000-5000). Nano-HPLC-MS/MS analysis of protein gels done on an ORBITRAP instrument allowed the identification of a significantly higher protein number (section 4.3.).



**Figure 8. Differential protein expression pattern of opossum spinal cord tissue represented in the 2D gel.**

Protein spots in spinal cord P5 (A) and P18 (B) tissue are indicated. 800 µg of total proteins for each age group were subjected to the 2D system with a general isoelectric focusing method (first dimension, IPG strip, pH 3-10 NL, 17 cm; second dimension, 12% SDS-PAGE). Proteins were visualized by silver staining. Circled spots were differentially expressed among these two tissue states, identified and shown in Tables 4 and 5.

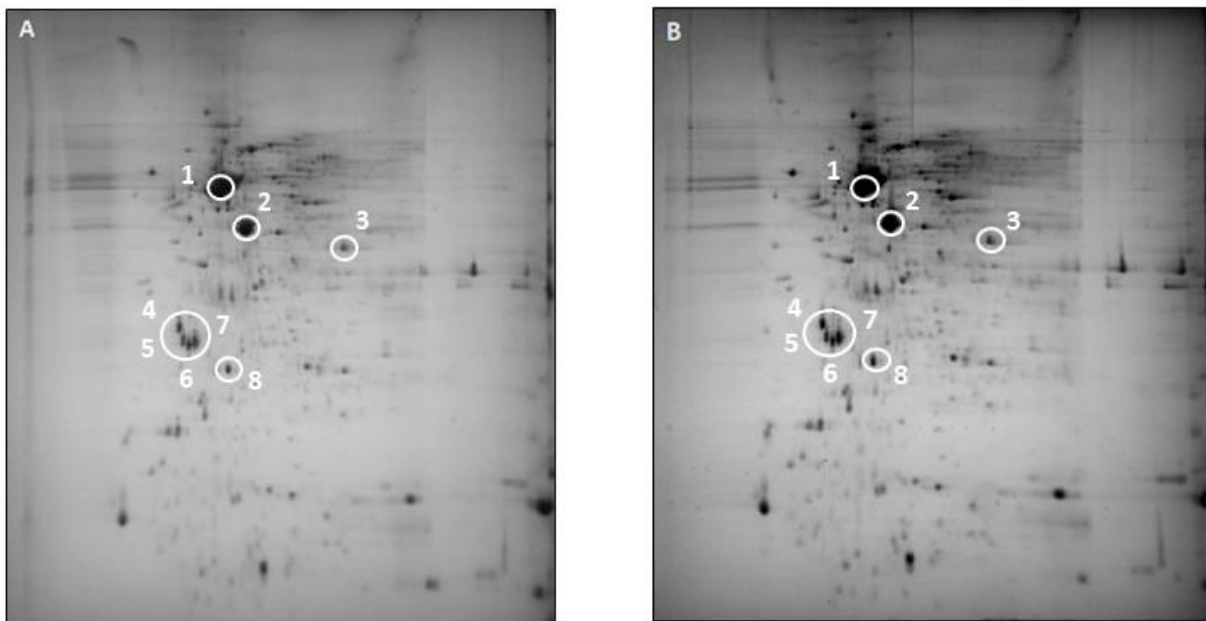
**Table 4. List of proteins identified from opossum spinal cord tissue P5 using 2D electrophoresis in combination with MALDI-TOF/MS.**

<b>Number of spot on the gel</b>	<b>Sequence reference</b>	<b>Protein name</b>	<b>MASCOT SCORE</b>	<b>Sequence coverage (%)</b>	<b>Number of matching peptides</b>	<b>Mw (Da)</b>
<b>1A</b>	TNF10	Tumor necrosis factor ligand	20	6	2	33648
<b>2A</b>	TCPQ	T-complex protein-1 subunit theta	44	11	6	60088
<b>3A</b>	IKBB	NF-kappa-B inhibitor beta	22	10	2	38398
<b>4A</b>	RAB14	Ras-related protein Rab14	40	22	6	24110
<b>5A</b>	TBB5	Tubulin beta-5 chain	115	17	9	50095
<b>6A</b>	HVM16	Ig heavy chain V region	28	41	3	15232
<b>7A</b>	ATG12	Ubiquitin-like protein ATG12	26	12	2	15388
<b>8A</b>	ACTB	Actin, cytoplasmic 1	126	31	9	42052

**Table 5. List of proteins identified from opossum spinal cord tissue P18 using 2D electrophoresis in combination with MALDI-TOF/MS.**

<b>Number of spot on the gel</b>	<b>Sequence reference</b>	<b>Protein name</b>	<b>MASCOT SCORE</b>	<b>Sequence coverage (%)</b>	<b>Number of matching peptides</b>	<b>Mw (Da)</b>
<b>1B</b>	TBB1	Tubulin beta-1 chain	164	40	13	50274
<b>2B</b>	HVM16	Ig heavy chain V region	32	41	3	15232
<b>3B</b>	SUMO3	Small ubiquitin related modifier	43	33	3	12562
<b>4B</b>	ACTB	Actin, cytoplasmic 1	94	20	7	42052
<b>5B</b>	GNAO	Guanine nucleotide-binding protein	53	15	5	40629
<b>6B</b>	VDAC1	Voltage-dependent anion-selective channel protein 1	40	19	3	32502
<b>7B</b>	TBB2A	Tubulin beta-2A chain	37	8	4	50274
<b>8B</b>	ZCHC9	Zinc-finger CCHC domain containing protein	33	8	3	31209





**Figure 9. Differential protein expression pattern of opossum spinal cord tissue represented in 2D gel.**

Protein spots in spinal cord P5 (A) and P18 (B) tissue are indicated. 800  $\mu$ g of total proteins for each age group were subjected to the 2D system with a general isoelectric focusing method (first dimension, IPG strip, pH 3-10 NL, 17 cm; second dimension, 12% SDS-PAGE). Proteins were visualized by Coomassie Brilliant Blue G-250 stain. Circled spots were differentially expressed among these two tissue states, identified and shown in Tables 6 and 7.

**Table 6. List of proteins identified from opossum spinal cord tissue P5 using 2D electrophoresis in combination with MALDI-TOF/MS.**

<b>Number of spot on the gel</b>	<b>Sequence reference</b>	<b>Protein name</b>	<b>MASCOT SCORE</b>	<b>Sequence coverage (%)</b>	<b>Number of matching peptides</b>	<b>Mw (Da)</b>
<b>1A</b>	TBB2B	Tubulin beta-2B chain	17	40	2	49964
<b>2A</b>	TUBA6	Tubulin alpha-6 chain	24	11	6	49938
<b>3A</b>	ATP5B	ATP synthase, H <sup>+</sup> -transporting, mitochondrial F1 complex, beta unit	26	47	2	56354
<b>4A</b>	ACTB	Actin, cytoplasmic 1	92	28	7	42052
<b>5A</b>	GNB1	Guanine nucleotide-binding protein, beta-1	31	28	9	37387
<b>6A</b>	VDAC1	Voltage dependent anion channel 1	28	31	3	30756
<b>7A</b>	MAPRE1	Microtubule-associated protein RP/EB family member 1	26	12	2	29999
<b>8A</b>	PP2	Alpha isoform of regulatory subunit A, protein phosphatase 2	27	23	3	66100

**Table 7. List of proteins identified from opossum spinal cord tissue P18 using 2D electrophoresis in combination with MALDI-TOF/MS.**

<b>Number of spot on the gel</b>	<b>Sequence reference</b>	<b>Protein name</b>	<b>MASCOT SCORE</b>	<b>Sequence coverage (%)</b>	<b>Number of matching peptides</b>	<b>Mw (Da)</b>
<b>1B</b>	TBB2B	Tubulin beta-2B chain	14	30	3	49938
<b>2B</b>	TUBA6	Similar to tubulin, alpha 6	26	41	3	63064
<b>3B</b>	ATP5B	ATP synthase, H <sup>+</sup> transporting, mitochondrial F1 complex, beta unit	31	54	3	56354
<b>4B</b>	ACTB	Actin, cytoplasmic 1	86	20	4	42052
<b>5B</b>	GNAO	Guanine nucleotide-binding protein	51	17	5	40629
<b>6B</b>	VDAC1	Voltage-dependent anion-selective channel protein 1	38	16	3	32502
<b>7B</b>	MAPRE1	Microtubule-associated protein RP/EB family member 1	31	9	3	28679
<b>8B</b>	PP2	Alpha isoform of regulatory subunit A, protein phosphatase 2	39	43	3	65323

**Table 8. List of proteins specific for rat spinal cord tissue using FASP method in combination with ACQUITY UPLC M-Class system coupled on-line to a Synapt G2-Si.**

40S ribosomal protein S21	GTP-binding protein SAR1b
40S ribosomal protein S27	Guanine nucleotide-binding protein subunit alpha-12
40S ribosomal protein S28	Guanine nucleotide-binding protein subunit alpha-13
40S ribosomal protein S30	Heat shock factor-binding protein 1
40S ribosomal protein S7	Heat shock protein 75 kDa mitochondrial
40S ribosomal protein S9	Heterogeneous nuclear ribonucleoprotein C
60S acidic ribosomal protein P1	Heterogeneous nuclear ribonucleoprotein H2
60S ribosomal protein L23	Heterogeneous nuclear ribonucleoprotein Q
60S ribosomal protein L27a	Histone H1t
60S ribosomal protein L27	Microtubule associated protein RP/EB family member
60S ribosomal protein L5	Microtubule-associated proteins 1A/1B light chain 3A
60S ribosomal protein L9	Microtubule-associated proteins 1A/1B light chain 3B
Astrocytic phosphoprotein PEA-15	Mitochondrial 2-oxoglutarate/malate carrier protein
Calbindin	Myelin protein P0
Calnexin	Myosin regulatory light chain 12B
Calpain-2 catalytic subunit	Neural cell adhesion molecule L1
Calponin-3	Neurochondrin
Calretinin	Neuronal membrane glycoprotein M6-a
CD166 antigen	Neuronal-specific septin-3
Cell division control protein 42 homolog	Neuron specific calcium-binding protein hippocalcin
Cytochrome b-c1 complex subunit 2 mitochondrial	Protein S100-A11
Cytochrome c oxidase subunit 7A2 mitochondrial	Ras-related protein Rap-1A

Cytoplasmic dynein 1 light intermediate chain 1	Ras related protein Rap-1b
Cytoplasmic dynein 1 light intermediate chain 2	Ribonuclease inhibitor
Dynamin-1-like protein	Small nuclear ribonucleoprotein associated protein N
Dynamin-3	Sorting nexin-20
Dynein intermediate chain 1 axonemal	Synapsin-2
Dynein light chain roadblock type 1	Synaptophysin
Eukaryotic translation initiation factor 5	Transcription intermediary factor 1-beta
Gamma-synuclein	Transmembrane protein 33
Glutathione S-transferase Mu 1	Vesicle-associated membrane protein-associated protein B

**Table 9. List of proteins specific for rat spinal cord tissue kept in culture for 24 h using FASP method in combination with ACQUITY UPLC M-Class system coupled on-line to a Synapt G2-Si.**

40S ribosomal protein S10	Myosin-7
40S ribosomal protein S11	Myosin light chain 3
40S ribosomal protein S8	Neurexin-2
A-kinase anchor protein SPHKAP	N-myc proto-oncogene protein
ATP binding cassette sub-family B member 9	Palmdelphin
Band 4.1-like protein 1	Parathymosin
Cathepsin B	Phosphate carrier protein
Cytochrome c oxidase subunit 5B	Proteasome subunit alpha type-4
Cytospin-A	Proteasome subunit beta type-6
DNA lyase	Pyruvate kinase PKLR
Dynein light chain 1	Ras-related protein Rab-10
Dynein light chain 2	Ras-related protein Rab-1B
ELAV-like protein 1	Ras-related protein Rab-26

Eukaryotic translation initiation factor 3 subunit B	Ras-related protein Rab-43
Eukaryotic translation initiation factor 3 subunit C	Ras-related protein Rab-4A
Exocyst complex component 8	Ras-related protein Rab-4B
Fibroblast growth factor receptor 1	Ras-related protein Rab-8A
Focal adhesion kinase 1	Ras-related protein Rab-8B
Furin	Reticulon-3
Glutathione S-transferase omega-1	Septin-8
GTPase Hras	Transgelin-3
GTPase Kras	Transmembrane protein 43
GTPase Nras	Tripeptidyl-peptidase 2
Guanine nucleotide-binding protein subunit alpha	Tropomyosin alpha-1 chain
Hexokinase-3	Tropomyosin beta chain
Kinesin light chain 1	Vesicle transport protein SEC20
Mitochondrial import receptor subunit TOM34	Vigilin

### 4.3. LC-MS/MS analysis

#### 4.3.1. Protein identification and functional classification

Spinal cord tissue samples of the P5 and P18 opossums *Monodelphis domestica* were subjected to LC-MS/MS analysis done on an Easy-nLC 1200 coupled to a QExactive HF mass spectrometer. According to the criteria for protein identification, thousands of proteins were identified in two independent biological samples, each in triplicate. We identified a total number of 4735 proteins for two biological samples, among which 1215 proteins (25.66%) were overlapped between both biological samples, with different intensity. 918 of the identified proteins were unique for P5 spinal cords, while 714 were unique for P18 spinal cords. The detected proteins were categorized using the UniProt protein knowledge database and PubMed, based on their molecular function (**Figure 10A**), biological process (**Figure 10B**), cellular component (**Figure 11A**) and protein class (**Figure 11B**), revealing differences between P5 and P18 opossum spinal cord protein content. The

most informative was the categorization based on the molecular pathways in which the detected proteins play a part, revealing more than 70 involved pathways for each age group (**Table 10**). Among the 1215 identified proteins differentially distributed in P5 and P18 opossum spinal cords, the abundance of the proteins related to NDD was prominent. These results were in accordance with the previously detected genes differentially expressed between the regenerating and non-regenerating opossum spinal cords (82,83). In order to reduce the number of the candidate molecules, downstream bioinformatics analyses were performed using the Perseus software package. We noted 615 proteins that had significantly higher expression in P5 spinal cords than in P18 spinal cords, and 600 proteins that had a significantly higher expression in P18 spinal cords than in P5 spinal cords (**Figure 12A**). Pearson correlation coefficients between spinal cords P5 and P18 were 0.881 ( $p < 0.05$ ), implicating good biological reproducibility of the study. Several candidates were chosen for further analysis based on their biological relevance and overlap with the previous transcriptomic data (82,83).

#### **4.3.2. Validation of the selected proteins by Western blot**

To validate and confirm the results obtained by MS, the distribution of selected proteins in the opossum P5, P18 and P30 spinal cord tissue was analyzed by WB technique. Six proteins, known to be specific cell markers or important in CNS development, were selected to undergo tests for confirmation: Glial Fibrillary Acidic Protein (GFAP; astrocytic marker), Paired box protein Pax-6 (PAX6; CNS development), Paired box protein Pax-2 (PAX2; embryonic development), Growth Associated Protein 43 (GAP43; neurite outgrowth), Myelin basic protein (MBP; oligodendrocyte differentiation and myelination in developing CNS) and Brain lipid-binding protein (BLBP; a marker for radial glia). Western blot data confirmed a distribution pattern detected by MS, demonstrating the higher expression of GFAP, PAX6, GAP43, MBP and BLBP in P18 and P30 spinal cords when compared to P5 and the opposite for the PAX2 (**Figure 12B, C**). P30 spinal cords were used as an additional control for the analysis of protein and gene expression, since at that age neuroregeneration in opossum spinal cord tissue is completely abolished. Our results have shown a match between the MS and WB results for the selected proteins known to be important for CNS development, indicating the comprehensive relevance of the obtained MS results (**Table 11A**).

#### **4.3.3. Validation of the differentially expressed genes by qRT-PCR**

To verify if the changes in protein distribution followed the changes in the expression of the related genes, the qRT-PCR transcription analysis was performed for the selected candidates. The results demonstrate the higher expression of 5 genes, including GFAP, PAX6, GAP43, MBP and BLBP in P18 and P30 spinal cords, and the opposite for PAX2 (**Figure 12D**), revealing the congruence with the proteomic data.

#### **4.3.4. Immunohistochemical localization of the differentially expressed proteins**

The cellular distribution of two selected proteins, PAX2 and BLBP, was analysed in the opossum spinal cord tissue with and without regenerative capacity, using immunofluorescence (**Figure 13A**). The choice of the PAX2 and BLBP proteins was related to the existence of commercially available antibodies complementary to opossum tissue. Furthermore, the PAX2 specific antibody was previously used on opossum primary cortical neuronal cultures (120). The results show the abundance of the PAX2 protein in the gray matter of the opossum P5 spinal cord tissue, with a significant decrease in the P18 tissue, where the remaining signal was mostly present in the dorsal horn. The BLBP positive cells were distributed throughout the spinal cord tissue of both P5 and P18 opossum spinal cords, but with a significant increase in the signal in the dorsal and ventral parts of the P18 spinal cords, as previously observed in the rodent spinal cord (121,122). The BLBP immunosignal that is extending from the central canal through the adjacent gray matter, reaching the outer edge of the white matter, resembles the representation of the nestin positive radial glial cells (123). To quantify the immunofluorescent staining, the average intensity of PAX2 and BLBP immunofluorescent signal (expressed in arbitrary units, AU) was measured in selected regions of interest (ROI; 50x50 pixels; **Figure 13B**). The results obtained are in accordance with proteomic data, further supporting the biological relevance of the detected proteins.

#### **4.3.5. Proteins related to neurodegenerative diseases**

Based on the molecular pathway classification, the differential representation of the proteins related to neurodegenerative diseases in the opossum spinal tissue with different regenerative abilities are very prominent (124). Thus, 3.9% of the proteins found to be upregulated in P5 opossum spinal cords are involved in Alzheimer's disease (amyloid secretase and presenilin pathway), 2.6% in Huntington's disease and 1.3% in Parkinson's disease. On the other hand, 1.9% of the proteins upregulated in the P18 opossum spinal cords are involved in Alzheimer's disease



(amyloid secretase and presenilin pathway), 2.8% in Huntington's disease and 0.5% in Parkinson's disease. Several candidates were chosen for further analysis: Huntingtin (HTT), Huntingtin interacting protein 1 (HIP1), Mitogen-activated protein kinase 10 [MAPK10; related to Alzheimer's disease (125)], Rab-8A, member of the RAS oncogene family [RAB8A; related to Parkinson's disease (126)] and Parkinsonism associated deglycase (PARK7). The qRT-PCR transcription analysis was performed to investigate the correlation of gene changes with the protein distribution detected by MS (**Table 11B**). The same pattern of expression as the one detected with MS was observed for the RAB8A (higher expression in P5 spinal cords than in P18), HTT and HIP1 (both with higher expression in P18 spinal cords than in P5), while for MAPK10 and PARK7 no significant difference was detected (**Figure 14**). The results show the partial overlapping between the pattern of gene expression and protein distribution of the selected candidate molecules related to NDD.

#### **4.3.6. Proteins important for regeneration and neurodegenerative diseases**

In addition to the proteins known to be specific cell markers or important in CNS development, we also investigated other proteins important for regeneration and neurodegenerative diseases from our wide base of identified proteins (> 4000) in order to further validate and confirm the results obtained by MS (**Table 12**) (additional unpublished data).

##### **4.3.6.1. Proteins related to neurodegenerative diseases**

Amyloid beta precursor protein binding family B member 1 (APBB1) is a modulator of the actin cytoskeleton, cell motility, and glial or neural cell development. APBB1 deficiency is associated with abnormalities in the accumulation of amyloid- $\beta$  plaques in Alzheimer's disease (127). Serine/threonine protein kinase (Akt) plays a key role as a modulator of the AKT-mTOR signaling pathway and controls the formation process of new neurons during neurogenesis, including proper neuron positioning, dendritic development, and synapse formation (128). Signals and molecules that activate the Akt phosphorylated form (pAkt) are responsible for myelination in the CNS. In particular, the protein Neuregulin 1 (NRG1) activates Akt and promotes proper axon myelination (129). Beta secretase 1 (BACE1) modulates myelination in the CNS and PNS and is required for normal myelination through the neuregulin and Akt pathway. BACE1 cleaves Neuregulin-1 whereupon the processed Neuregulin-1 regulates myelination by phosphorylating Akt protein in

myelin-producing cells (130). Beta secretase also initiates the production of the toxic amyloid  $\beta$  that plays a crucial early part in AD pathogenesis (131).

c-Jun N-terminal kinases play a central role in stress signaling pathways implicated in gene expression, neuronal plasticity, regeneration, cell death, and regulation of cellular senescence. JNK1 (MAPK8) and JNK2 (MAPK9) have a broad tissue distribution, while JNK3 (MAPK10) is mainly localized in neurons. JNK's, particularly JNK3, not only enhance A $\beta$  production, but they play a key role in the maturation and development of neurofibrillary tangles. Therefore, it is possible that inhibition of JNK3 might be considered as a potential target for treating neurodegenerative mechanisms associated with Alzheimer's disease (111). p38 together with JNK is called stress kinase because it is most often activated as a cell response to stress and in some apoptotic processes. Attention to p38 MAPK, in terms of neurodegeneration, is guided by the fact that these kinases are involved in dopaminergic signaling, a pathway known to be disrupted during Parkinson's disease (132). The death of dopaminergic neurons, or its deficiency in general, causes Parkinson's disease (113).

Certain Rab GTPases (Rabs) like Rab8a and Rab8b are linked to Parkinson's disease through disease-associated mutations or interactions with key Parkinson's disease-related proteins (133,134). Rab7 regulates the trafficking of late endosomes and autophagosomes, therefore it is believed that over-expressing Rab7 might be beneficial in Parkinson's disease (135). Another protein linked with Parkinson's disease and memory is ubiquitin carboxyl-terminal hydrolase isozyme L1 (UCHL1) which is selectively expressed in neurons at high levels (136). Presenilin (PSEN1) is associated with Alzheimer's disease and the presenilin hypothesis proposes that PSEN1 mutations cause a loss of essential presenilin functions in the brain, which in turn triggers neurodegeneration and dementia in AD (137).

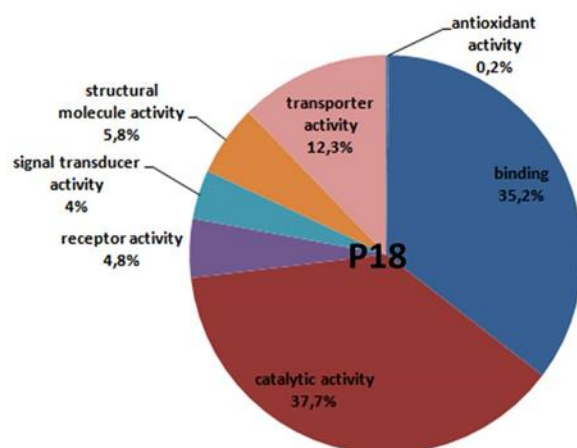
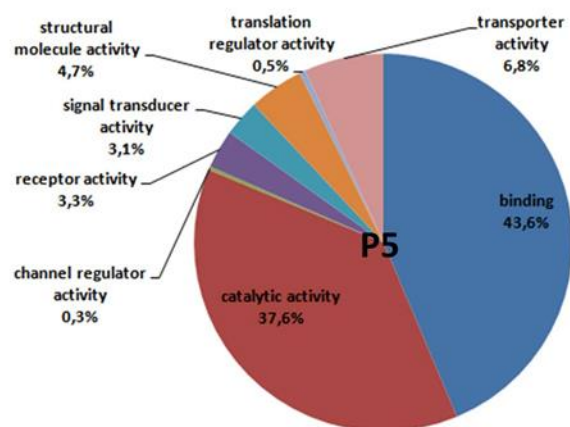
#### 4.3.6.2. Proteins involved in regeneration and development

MEK 1/2 is a member of the MAPK signaling cascade that phosphorylates and activates mitogen-activated protein kinase. MEK1 and MEK2 also phosphorylate ERK kinase. The ERK 1/2 cascade is important for neuron differentiation and regulation of axon regeneration and it is indicated that ERK 1/2 phosphorylation is a key event required for early neuronal differentiation and survival of embryonic stem cells (138,139). Nuclear distribution protein nudeE-like 1 (NDEL1) is a regulator of microtubule organization. As such, it participates in mitosis, neurogenesis, neurite outgrowth, and neural migration (140). Flotillin 1 (FLOT1) has previously been shown to be important for the early stages of neuronal development. It is ubiquitously expressed in all cell types, but its expression is enriched during development, as well as in regenerating axons. Furthermore, FLOT1 promotes hippocampal neuronal differentiation and neurite outgrowth (141).

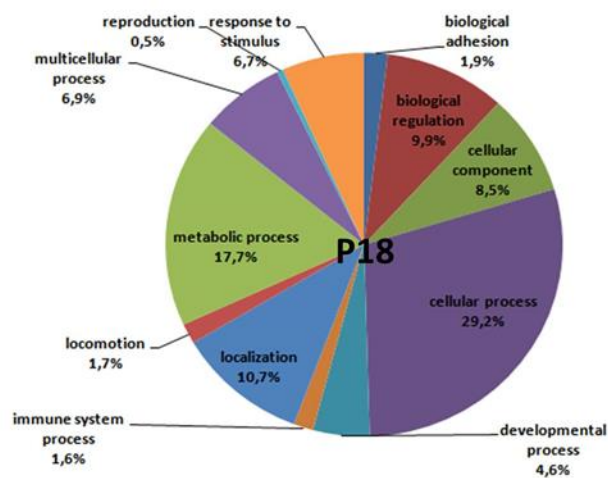
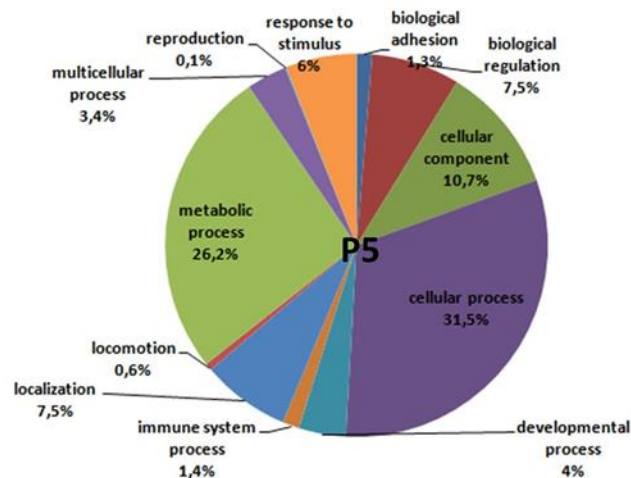
Other proteins related to regeneration and development are neural precursor cell expressed developmentally down-regulated 4-like protein (NEDD4L) important for regulating the cell cycle during stem cell self-renewal and regeneration (142), reelin (RELN) which is an extracellular matrix glycoprotein that regulates the processes of neuronal migration and positioning in the developing brain and during embryonic development and adulthood (143), nucleoporin 43 (NUP43), semaphorin 4A (SEMA4A) which has a critical role in many physiological and pathological processes including neuronal development (144), NudC domain-containing protein 2 (NUDCD2) and DCC netrin 1 receptor (DCC) known by its role in axonal regeneration and synaptic formation (145).

The results have shown high overlapping between the pattern of protein (**Figure 15A, B**) and gene expression (**Figure 16**) with the results obtained by MS (**Table 12**) for the molecules related to regeneration and NDD. We have confirmed 22 out of 32 tested molecules, while for the other 10 molecules (MAPK10, PARK7, APBB1, BACE1, cJun, RELN, NUP43, RAB8B, PSEN1 and UCHL1) the results obtained either on the protein or gene level are not in accordance with results obtained by the MS analysis, indicating the importance of implementing different techniques in confirmatory tests.

**A**

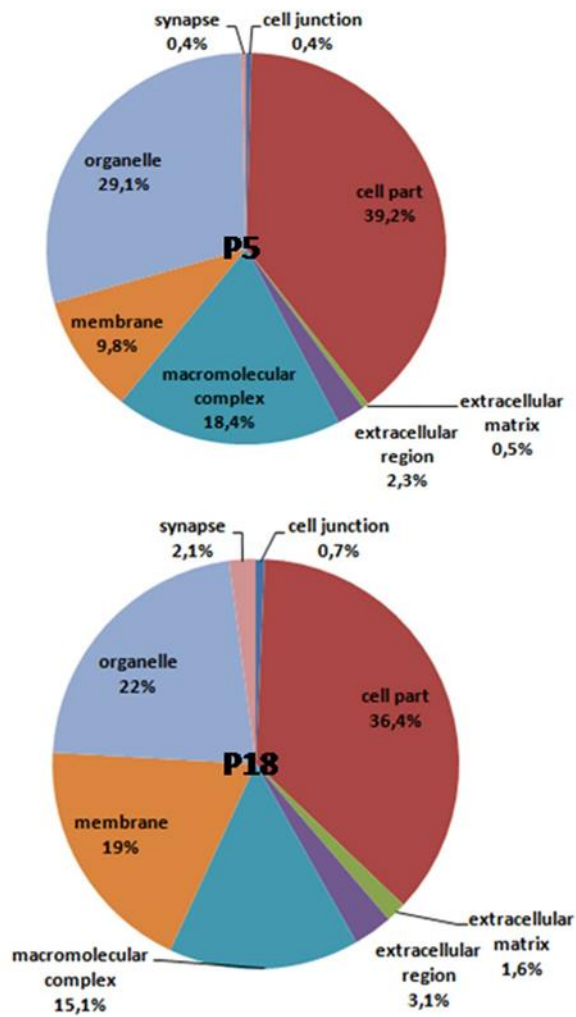


**B**

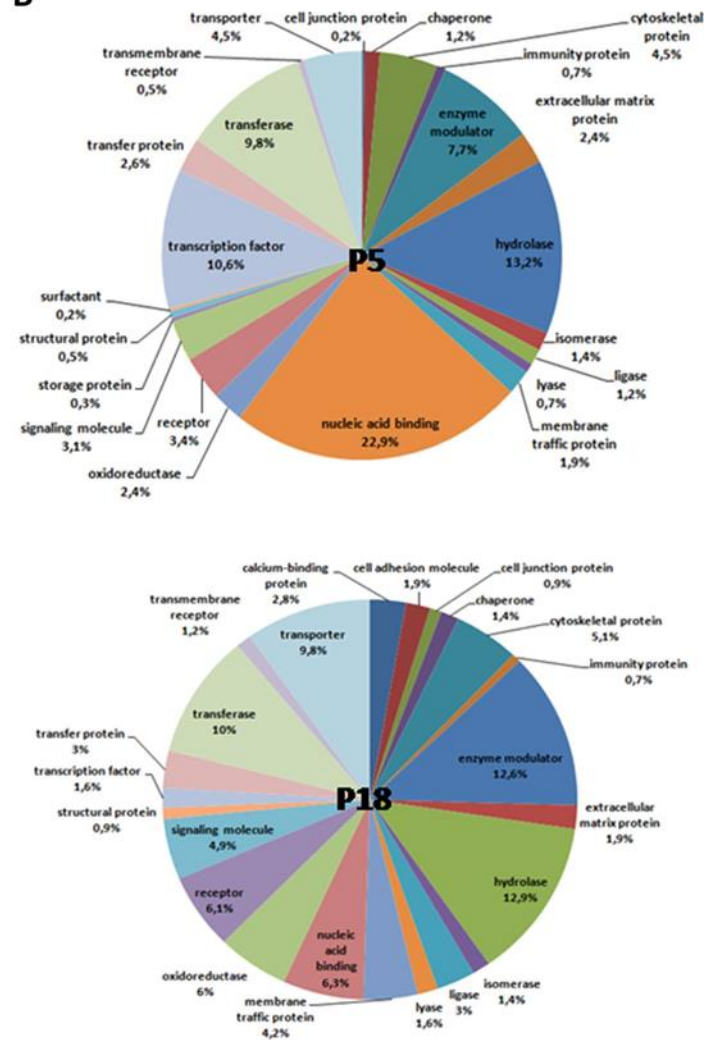


**Figure 10. Functional classification of the proteins identified by MS as differentially distributed in the opossum P5 and P18 spinal cords.** Proteins were classified based on: (A) molecular function and (B) biological process. Source: Tomljanović et al., 2022.

A



B



**Figure 11. Functional classification of the proteins identified by MS as differentially distributed in the opossum P5 and P18 spinal cords.** Proteins were classified based on: (A) cellular component and (B) protein class. Source: Tomljanović et al., 2022.

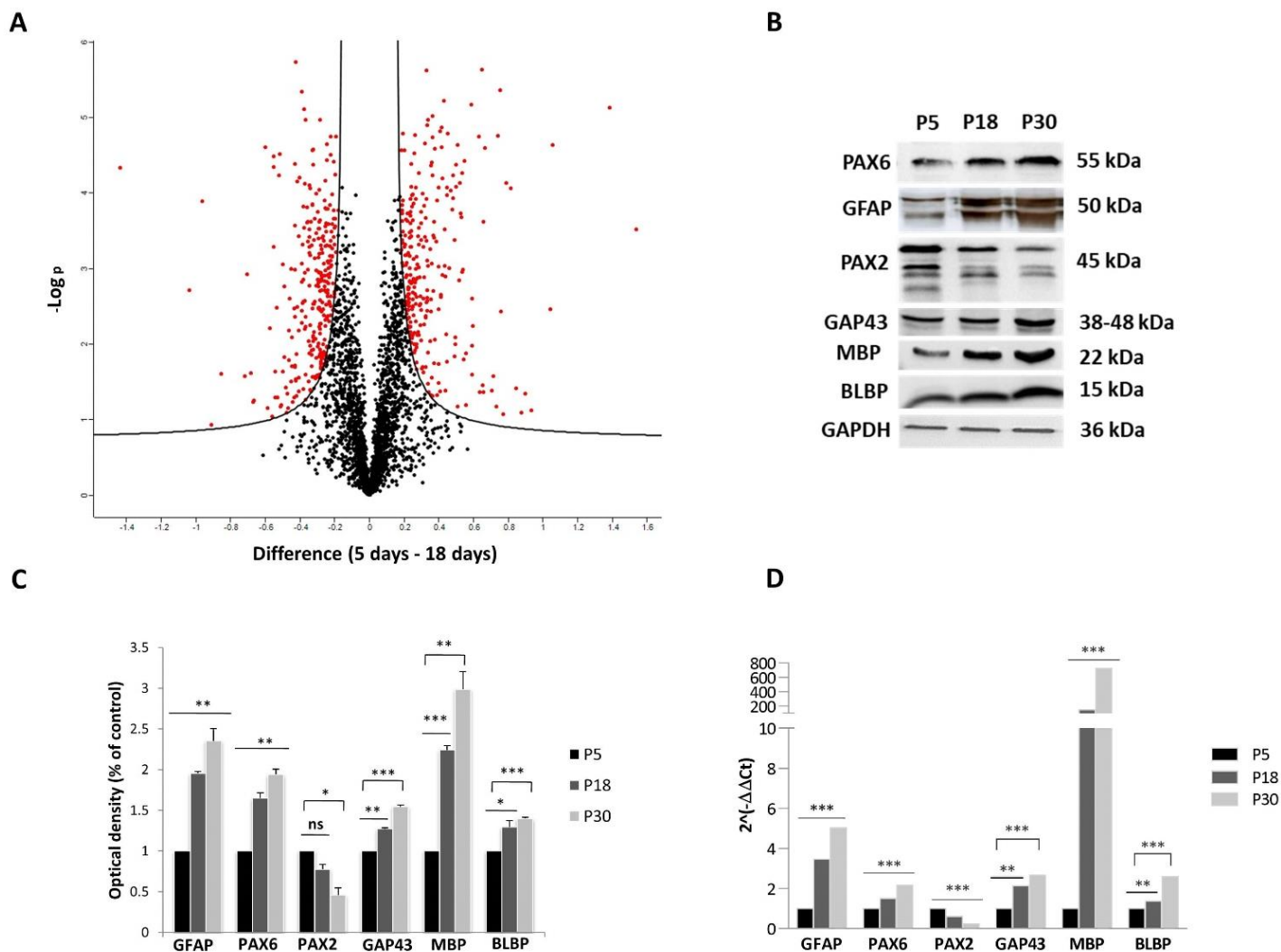
**Table 10. Classification of the proteins identified by MS as differentially distributed in the opossum P5 and P18 spinal cords in divergent molecular pathways with emphasis on functional groups related to neurodegenerative disease.**

<b>P5</b>	<b>P18</b>
5HT2 type receptor mediated signaling pathway (0.9%)	5-Hydroxytryptamine degradation (0.5%)
ATP synthesis (0.4 %)	5HT1 type receptor mediated signaling pathway (1.4%)
<b>Alzheimer disease-amyloid secretase pathway (2.6%)</b>	5HT2 type receptor mediated signaling pathway (2.3%)
<b>Alzheimer disease-presenilin pathway (1.3%)</b>	5HT3 type receptor mediated signaling pathway (0.9%)
Androgen / estrogen / progesterone biosynthesis (0.9%)	5HT4 type receptor mediated signaling pathway (1.4%)
Angiogenesis (3.4%)	Adrenaline and noradrenaline biosynthesis (0.9%)
Apoptosis signaling pathway (3%)	Alpha adrenergic receptor signaling pathway (1.4%)
Axon guidance mediated by Slit/Robo (0.9%)	<b>Alzheimer disease-amyloid secretase pathway (1.4%)</b>
Axon guidance mediated by netrin (0.9%)	<b>Alzheimer disease-presenilin pathway (0.5%)</b>
B cell activation (0.9%)	Anandamide degradation (0.5%)
Beta1 adrenergic receptor signaling pathway (0.4%)	Angiogenesis (2.8%)
Beta2 adrenergic receptor signaling pathway (0.4%)	Angiotensin II-stimulated signaling through G proteins and beta-arrestin (0.5%)
Biotin biosynthesis (0.4%)	Apoptosis signaling pathway (0.9%)
Blood coagulation (0.4%)	B cell activation (0.9%)
CCKR signaling map (2.6%)	Beta1 adrenergic receptor signaling pathway (0.9%)
Cadherin signaling pathway (1.3%)	Beta2 adrenergic receptor signaling pathway (0.9%)
Cell cycle (0.4%)	Beta3 adrenergic receptor signaling pathway (0.9%)
Cholesterol biosynthesis (0.9%)	CCKR signaling map (3.7%)
Cytoskeletal regulation by Rho GTPase (1.7%)	Cadherin signaling pathway (0.9%)
DNA replication (1.7%)	Carnitine metabolism (0.5%)
De novo pyrimidine deoxyribonucleotide biosynthesis (0.4%)	Coenzyme A linked carnitine metabolism (0.5%)
EGF receptor signaling pathway (4.7%)	Corticotropin releasing factor receptor signaling pathway (0.9%)
Endothelin signaling pathway (1.7%)	Cytoskeletal regulation by Rho GTPase (0.9%)

FGF signaling pathway (3.4%)	De novo purine biosynthesis (0.5%)
General transcription by RNA polymerase I (0.9%)	Dopamine receptor mediated signaling pathway (1.4%)
General transcription regulation (2.1%)	EGF receptor signaling pathway (2.3%)
Glycolysis (0.4%)	Endogenous cannabinoid signaling (0.9%)
Gonadotropin-releasing hormone receptor pathway (3%)	Endothelin signaling pathway (3.7%)
Heme biosynthesis (0.4%)	Enkephalin release (0.5%)
Heterotrimeric G-protein signaling pathway-Gq alpha and Go alpha mediated pathway (0.4%)	FGF signaling pathway (1.8%)
Histamine H1 receptor mediated signaling pathway (0.9%)	GABA-B receptor II signaling (1.8%)
<b>Huntington disease (2.6%)</b>	General transcription regulation (0.5%)
Hypoxia response via HIF activation (0.3%)	Gonadotropin-releasing hormone receptor pathway (4.6%)
Inflammation mediated by chemokine and cytokine signaling pathway (5.6%)	Heterotrimeric G-protein signaling pathway-Gi alpha and Gs alpha mediated pathway (3.7%)
Insulin/IGF pathway-mitogen activated protein kinase kinase/MAP kinase cascade (1.7%)	Heterotrimeric G-protein signaling pathway-Gq alpha and Go alpha mediated pathway (4.1%)
Insulin/IGF pathway-protein kinase B signaling cascade (1.7%)	Heterotrimeric G-protein signaling pathway-rod outer segment phototransduction (0.5%)
Integrin signalling pathway (3.4%)	Histamine H1 receptor mediated signaling pathway (1.4%)
Interferon-gamma signaling pathway (0.9%)	Histamine H2 receptor mediated signaling pathway (0.5%)
Interleukin signaling pathway (3.4%)	<b>Huntington disease (2.8)</b>
Ionotropic glutamate receptor pathway (0.4%)	Inflammation mediated by chemokine and cytokine signaling pathway (2.3%)
JAK/STAT signaling pathway (0.9%)	Insulin/IGF pathway-mitogen activated protein kinase kinase/MAP kinase cascade (0.9%)
Methylcitrate cycle (0.4%)	Insulin/IGF pathway-protein kinase B signaling cascade (0.5%)
Muscarinic acetylcholine receptor 1 and 3 signaling pathway (0.4%)	Integrin signalling pathway (3.7%)
N-acetylglucosamine metabolism (0.4%)	Interleukin signaling pathway (0.5%)
Nicotinic acetylcholine receptor signaling pathway (0.4%)	Ionotropic glutamate receptor pathway (2.8%)
Oxidative stress response (0.4%)	Isoleucine biosynthesis (0.5%)
Oxytocin receptor mediated signaling pathway (0.9%)	Metabotropic glutamate receptor group I pathway (0.5%)
PDGF signaling pathway (3.9%)	Metabotropic glutamate receptor group II pathway (1.8%)

PI3 kinase pathway (2.6%)	Metabotropic glutamate receptor group III pathway (4.1%)
<b>Parkinson disease (1.3%)</b>	Methylmalonyl pathway (0.5%)
Proline biosynthesis (0.9%)	Muscarinic acetylcholine receptor 1 and 3 signaling pathway (2.3%)
Ras Pathway (2.1%)	Muscarinic acetylcholine receptor 2 and 4 signaling pathway (0.9%)
T cell activation (1.7%)	Nicotinic acetylcholine receptor signaling pathway (0.5%)
TCA cycle (0.4%)	Opioid prodynorphin pathway (0.9%)
TGF-beta signaling pathway (1.3%)	Opioid proenkephalin pathway (0.9%)
Thiamin metabolism (0.4%)	Opioid proopiomelanocortin pathway (0.9%)
Thyrotropin-releasing hormone receptor signaling pathway (0.9%)	Oxytocin receptor mediated signaling pathway (1.8%)
Toll receptor signaling pathway (0.4%)	PDGF signaling pathway (1.4%)
Transcription regulation by bZIP transcription factor (2.1%)	PI3 kinase pathway (0.9%)
Ubiquitin proteasome pathway (1.3%)	<b>Parkinson disease (0.5%)</b>
VEGF signaling pathway (0.9%)	Purine metabolism (0.5%)
Wnt signaling pathway (5.2%)	Ras Pathway (0.5%)
mRNA splicing (0.4%)	Synaptic vesicle trafficking (0.5%)
p53 pathway by glucose deprivation (0.4%)	T cell activation (0.9%)
p53 pathway feedback loops 2 (1.7%)	TCA cycle (0.5%)
p53 pathway (3.4%)	TGF-beta signaling pathway (1.8%)
	Thyrotropin-releasing hormone receptor signaling pathway (2.8%)
	Transcription regulation by bZIP transcription factor (0.5%)
	VEGF signaling pathway (1.8%)
	Vasopressin synthesis (0.5%)
	Wnt signaling pathway (1.8%)
	p53 pathway by glucose deprivation (1.4%)
	p53 pathway feedback loops 2 (0.5%)
	p53 pathway (0.5%)

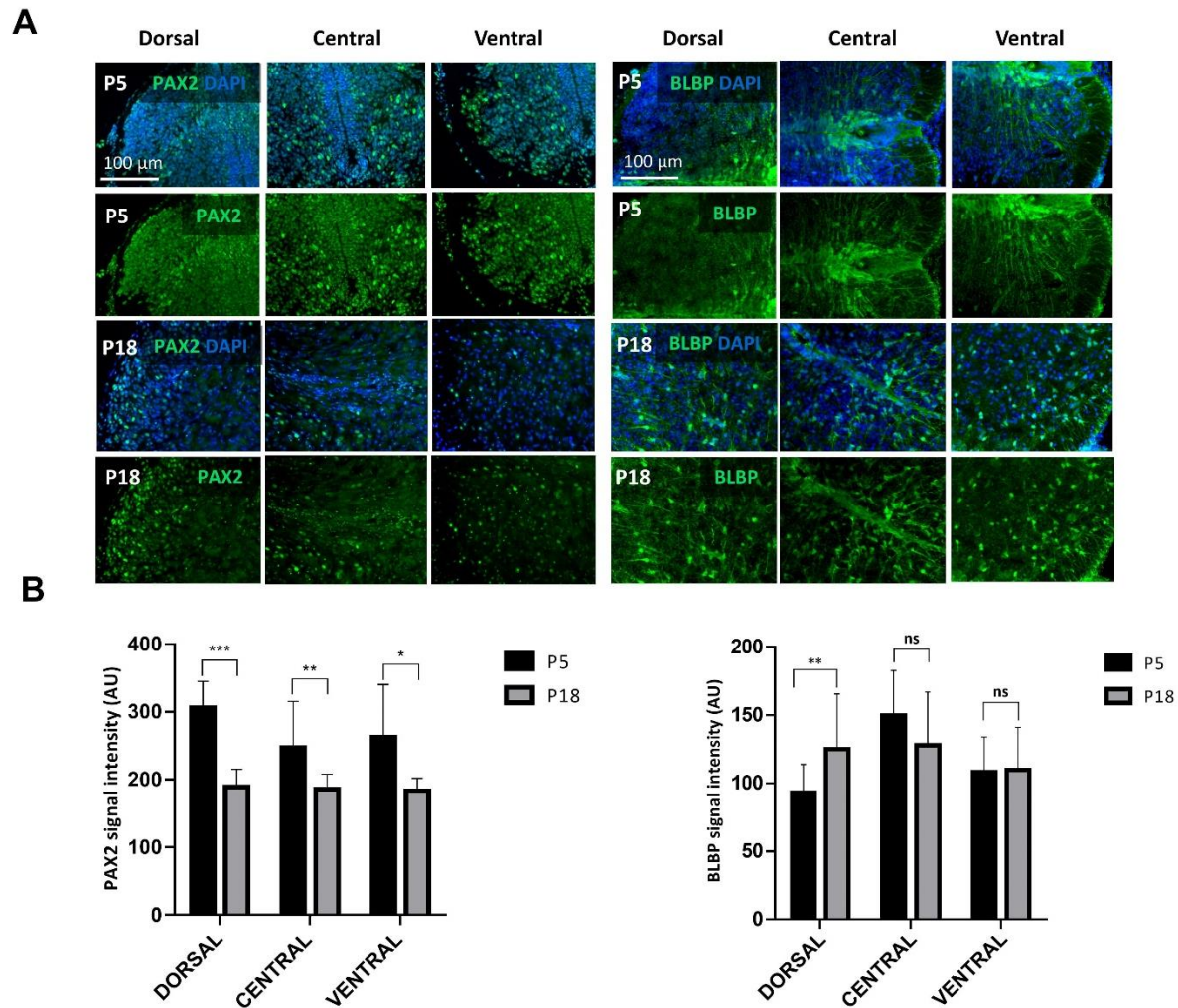




**Figure 12. The MS analysis of the proteins differently distributed in the P5 and P18 opossum spinal cords and the validation of the results by WB and qRT-PCR.**

(A) Plot of the  $-\log p$ -value vs. the  $\log_2$  intensity difference of the P5 and P18 opossum spinal cords. The red dots represent the significantly regulated proteins, showing on the left side of the graph the proteins elevated in P5, and on the right side, the proteins elevated in P18. The proteins without a significant change in distribution between the samples are shown as the black dots on the graph. (B, C) WB analysis of the selected proteins. On (B) the representative image of the detected WB signal is shown, while the quantification of the relative levels of protein expression is shown on the histogram (C). The qRT-PCR data (D) show the relative level of gene expression for the selected candidates in P5, P18 and P30 opossum spinal cords. The obtained values were

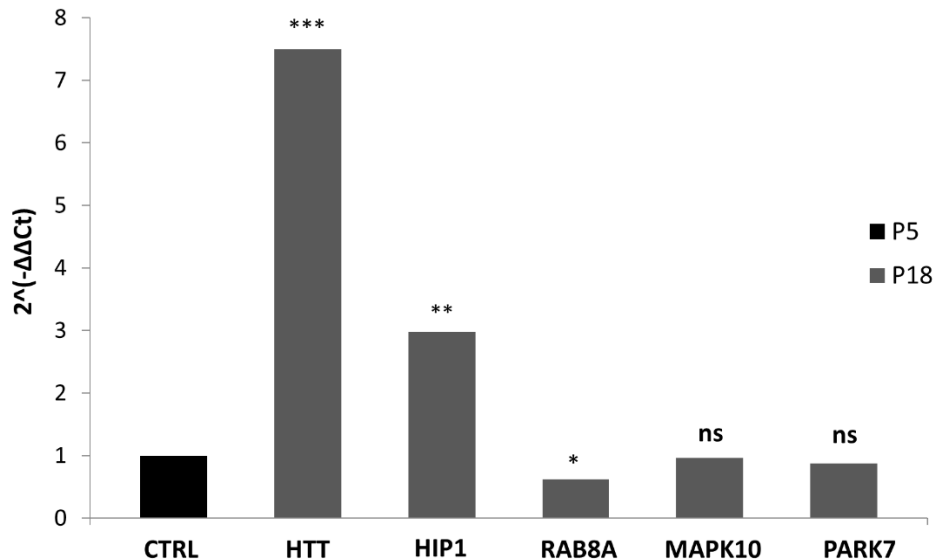
normalized to GAPDH and expressed as fold differences compared to control (P5). Data are presented as means  $\pm$  SD of three independent experiments. Source: Tomljanović et al., 2022.



**Figure 13. Immuno-staining for PAX2 and BLBP, differentially expressed in P5 and P18 opossum spinal cords.**

(A) Spinal cord sections (16  $\mu$ m) were immuno-stained for PAX2 and BLBP (green signal), while the nuclei of all cells were stained with 4',6-diamidino-2-phenylindole (DAPI; blue signal). In the left part of the figure, the representative images of the PAX2 immunostaining are shown, while for the BLBP are shown on the right part. Furthermore, the results for the different parts of the spinal cord (dorsal, central and ventral) are presented. Scale bar, 100  $\mu$ m. (B) Bar graphs represent

the average immunostaining intensity (Arbitrary Units, AU) in dorsal, central and ventral ROIs (50x50 pixels) of P5 and P18 spinal cords. Data are mean  $\pm$  SD from 3 to 5 sections from three different spinal cords for each group. Source: Tomljanović et al., 2022.



**Figure 14. qRT-PCR analysis of the selected proteins related to neurodegenerative diseases in P5 and P18 opossum spinal cord tissue.**

The mRNA levels of the Huntingtin (HTT), Huntingtin interacting protein 1 (HIP1), Mitogen-activated protein kinase 10 (MAPK10), Rab-8A, member of the RAS oncogene family (RAB8A) and Parkinsonism associated deglycase (PARK7) were quantified in the spinal cord tissue of P5 and P18 opossums from at least three independent experiments. The obtained values were normalized to GAPDH and expressed as fold differences compared to control (P5). Source: Tomljanović et al., 2022.

**Table 11. Selected proteins detected by mass spectrometry as differentially distributed in P5 and P18 opossum spinal cords:** (A) specific cellular markers or proteins with the established role in CNS development and (B) proteins related to severe neurodegenerative diseases.

**A**

<b>Proteins unique for P5 spinal cords</b>	<b>ID<sup>1</sup></b>	<b>Gene symbol<sup>1</sup></b>	<b>LFQ intensity</b>
Paired box 2	F6X9M8	PAX2	7x10 <sup>5</sup>
<b>Proteins unique for P18 spinal cords</b>	<b>ID</b>	<b>Gene symbol</b>	<b>LFQ intensity</b>
Myelin basic protein	F7GF44	MBP	1.32x10 <sup>9</sup>
<b>Proteins up-regulated in P18 spinal cords</b>	<b>ID</b>	<b>Gene symbol</b>	<b>Fold change</b>
Paired box 6	F7DII5	PAX6	1.21
Glial fibrillary acidic protein	F6WYV7	GFAP	5.53
Growth associated protein 43	F7BTK7	GAP43	1.68
Fatty acid binding protein	F7ELF5	FABP7 (BLBP)	1.01

**B**

<b>Proteins up-regulated in P5 spinal cords</b>	<b>ID</b>	<b>Gene symbol</b>	<b>Fold change</b>
RAB8A, member RAS oncogene family	F7GGI0	RAB8A	1.07
<b>Proteins up-regulated in P18 spinal cords</b>	<b>ID</b>	<b>Gene symbol</b>	<b>Fold change</b>
Huntingtin	F7C6C4	HTT	1.45
Huntingtin interacting protein 1	F6YXY3	HIP1	1.14
Mitogen-activated protein kinase	F6ZA47	MAPK10	1.01
Parkinsonism associated deglycase	F7A9B9	PARK7	1.23

<sup>1</sup>ID and gene symbol according to UniProt protein knowledge database

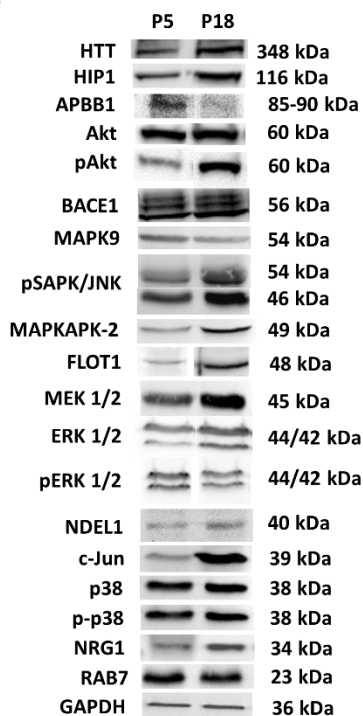
<http://www.uniprot.org>

**Table 12. Proteins important for regeneration and neurodegenerative diseases detected by mass spectrometry in P5 and P18 opossum spinal cords.**

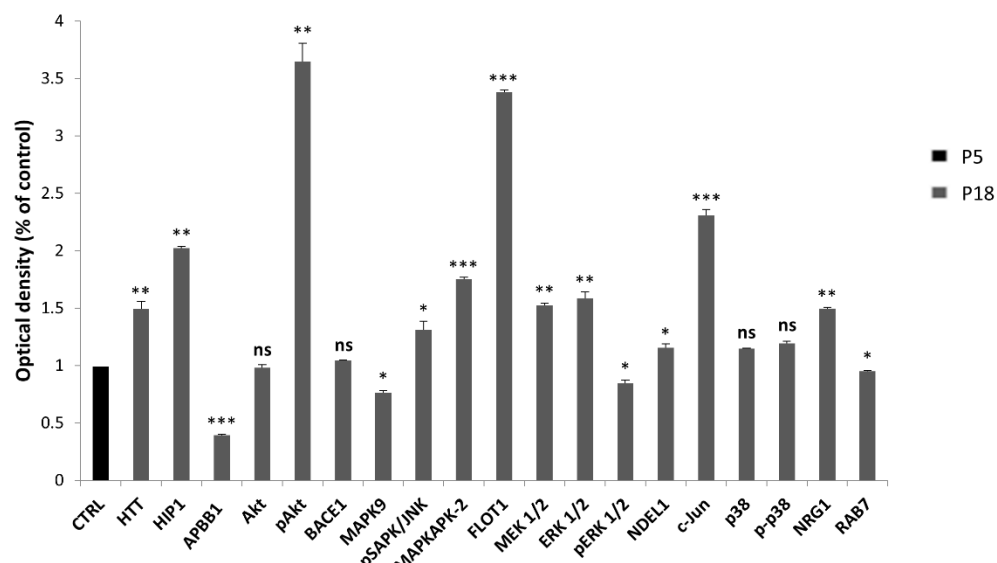
<b>Proteins unique for P5 spinal cords</b>	<b>ID</b>	<b>Gene symbol</b>	<b>LFQ intensity</b>
Amyloid beta precursor protein binding family B member 1	F7FD62	APBB1	1.71x10 <sup>7</sup>
Beta secretase 1	F6QP52	BACE1	1.37x10 <sup>7</sup>
Mitogen-activated protein kinase 9	F6WV79	MAPK9	4.53x10 <sup>7</sup>
Reelin	F6Q6B3	RELN	6.9x10 <sup>7</sup>
Nucleoporin 43	F7FV97	NUP43	2.34x10 <sup>8</sup>
Presenilin	F6PH04	PSEN1	8.35x10 <sup>7</sup>
NudC domain-containing protein 2	F7AYM4	NUDCD2	7.1x10 <sup>7</sup>
DCC netrin 1 receptor	F7F4D5	DCC	6.71x10 <sup>7</sup>
<b>Proteins unique for P18 spinal cords</b>	<b>ID</b>	<b>Gene symbol</b>	<b>LFQ intensity</b>
Nuclear distribution protein nudE-like 1	F7CL14	NDEL1	9.12x10 <sup>7</sup>
Semaphorin 4A	F6VN06	SEMA4A	6.29x10 <sup>7</sup>
<b>Proteins up-regulated in P5 spinal cords</b>	<b>ID</b>	<b>Gene symbol</b>	<b>Fold change</b>
AKT serine/threonine kinase 1	F6QP11	AKT1	1.52
RAB7A, member RAS oncogene family	F7GFV0	RAB7A	1.02
RAB8B, member RAS oncogene family	F7EN14	RAB8B	1.25
<b>Proteins up-regulated in P18 spinal cords</b>	<b>ID</b>	<b>Gene symbol</b>	<b>Fold change</b>
Stress-activated protein kinase JNK	F7GE32	MAPK8	1.09
Flotillin	F7F085	FLOT1	1.64
Mitogen-Activated Protein Kinase Kinase 1	F6XT65	MAPK2K1 (MEK1)	1.08
Mitogen-Activated Protein Kinase Kinase 2	F6S9S9	MAPK2K2 (MEK2)	1.38
Mitogen-activated protein kinase 3	F7EI48	MAPK3 (ERK1)	1.01
Mitogen-activated protein kinase 1	F7FHD1	MAPK1 (ERK2)	1.27
Neural precursor cell expressed developmentally down-regulated 4-like	F7AR59	NEDD4L	1.24

Ubiquitin carboxyl-terminal hydrolase isozyme L1	P50103	UCHL1	1.19
---	--------	-------	------

**A**

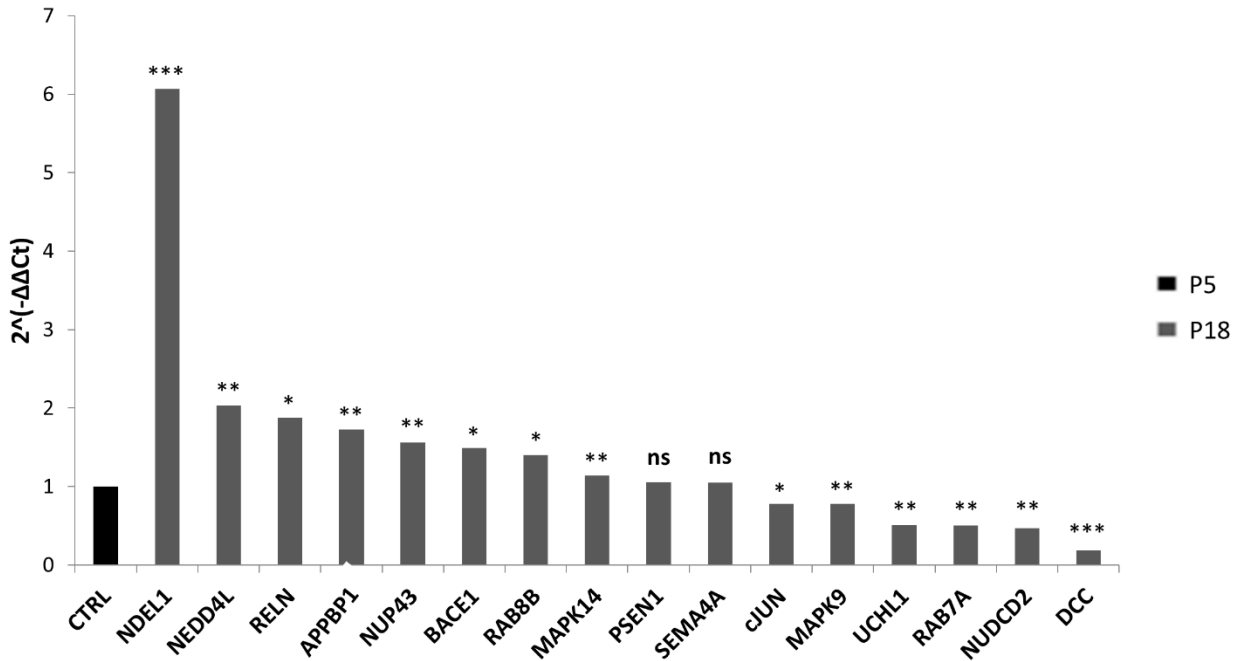


**B**



**Figure 15. WB analysis of proteins related to regeneration and neurodegenerative diseases in P5 and P18 opossum spinal cord tissue.**

(A, B) WB analysis of the selected proteins. On (A) the representative image of the detected WB signal is shown, while the quantification of the relative levels of protein expression is shown on the histogram (B). The obtained values were normalized to GAPDH and expressed as fold differences compared to control (P5). Data are presented as means  $\pm$  SD of three independent experiments.



**Figure 16. qRT-PCR analysis of proteins related to regeneration and neurodegenerative diseases in P5 and P18 opossum spinal cord tissue.**

The mRNA levels of the selected proteins were quantified in the spinal cord tissue of P5 and P18 opossums from at least three independent experiments. The obtained values were normalized to GAPDH and expressed as fold differences compared to control (P5).



#### 4.4. Functional studies

To test the procedure and newly established primary spinal neuronal cultures as a new *in vitro* platform to study development and regeneration and to perform functional assays, we have chosen to test, as the example, the pharmacological polyglutamine aggregation inhibitor, PGL-137. PGL-137 is a benzothiazole compound that crosses the cell membrane and binds within the cell to secondary protein structures known as  $\beta$ -folded plates, which are rich in polyglutamine. Benzothiazoles were identified as potential polyglutamine aggregation inhibitors of Huntington's disease and thus are potentially very promising candidates for future drug development. We wished to check the effect of PGL-137 on our *in vitro* platforms: intact opossum spinal cord and primary spinal cultures.

##### 4.4.1. Intact opossum spinal cord

The intact opossum spinal cords P5 and P18 were cultured for 24 hours as described in section 3.2.15.2. Even though the PGL-137 inhibitor is not supposed to directly inhibit HTT, we checked if it can indirectly, in any way reflect the gene expression or protein level. For that reason, we checked the expression of HTT and HIP1, a protein that interacts with HTT, 24 hours after the PGL-137 treatment. Surprisingly, the treatment with PGL-137 inhibitor resulted in decreased protein (**Figure 17**) and gene (**Figure 18**) expression of HTT and HIP1 in the opossum spinal cords P5 and P18, compared to the control (untreated spinal cords). At the protein level, in treated P5 spinal cords, the relative expression of HTT was further reduced compared to HIP1 (**Figure 17A, B**), while on the gene level, the relative expression of HIP1 was further reduced (**Figure 18A**). In treated P18 spinal cords the relative expression of HTT and HIP1 was almost the same at the protein (**Figure 17A, C**) and gene (**Figure 18B**) level.

The intact opossum spinal cord preparation is biologically more relevant to analyze neuron survival, axonal growth and examine the ability of tissue regeneration. Therefore, we tested the effect of the PGL-137 inhibitor on tissue sections from P5 and P18 spinal cords, compared to the control, by using immunofluorescent microscopy. To quantify the immunofluorescent staining, the average intensity of the immunofluorescent signal of the selected marker (expressed in arbitrary units, AU) was measured in selected regions of interest (ROI; 100x100 pixels). The chosen markers were HTT, marker of proliferation Ki-67 (Ki67), microtubule associated protein 2 (MAP2), neuronal nuclear protein (NeuN), neurofilament H (SMI32) and synapsin 1 (Syn1).

#### 4.4.1.1. HTT marker

Huntingtin, the gene mutated in Huntington's disease, is required for normal synaptic connectivity, regulated gene expression and neuronal survival with aging. Although the exact function of this protein is unknown, it appears to play an important role in nerve cells in the brain and is essential for normal development before birth. In P5 spinal cords, there is a strong expression of HTT, especially in the ventral white matter area and the central canal (**Figure 19A**), followed by a significant decrease in the expression in treated spinal cords (**Figure 19C**), the most noticeable difference is that there is no expression of HTT in the central canal (**Figure 19B**). In P18 samples, HTT exhibits at this stage a more homogeneous distribution across the entire tissue (**Figure 20A**), with a slight decrease in expression in the treated spinal cords (**Figure 20C**), especially in the lateral parts (**Figure 20B**). This was an interesting result because it is still unclear what this protein is doing in the cells under normal conditions in its non-mutated form. Also, a team of scientists recently found that the huntingtin protein plays an important role in repairing damaged nerve cells (146), indicating it has a central role in nerve cell regeneration in their models.

#### 4.4.1.2. Ki67 marker

The marker of proliferation Ki67 is a nuclear protein that is tightly linked to the cell cycle and is expressed in proliferating cells. A recent study provides evidence for Ki67 to be used as a marker of proliferation in the initial phase of adult neurogenesis (147). In the untreated P5 (**Figure 21A**; green signal) and P18 (**Figure 22A**; green signal) spinal cords, Ki67 is mostly expressed in the ventral part. There is a significant decrease in expression of Ki67 in both P5 (**Figure 21B, D**) and P18 (**Figure 22B, D**) spinal cords treated with PGL-137 inhibitor, suggesting that it affected the proliferation.

#### 4.4.1.3. MAP2 marker

Microtubule-associated protein 2 (MAP2) is a dendritically enriched protein and marker of synaptic plasticity. MAP2 is preferentially localized to nerve cells. Within neurons, MAP2 is present in soma and dendrites, implicating a role in determining and stabilizing neuronal morphology during neuron development and differentiation. MAP2 expression in the spinal cord of P5 (**Figure 21A**; red signal) and P18 (**Figure 22A**; red signal) opossums extends through the ventral and dorsal part, with a significant decrease in expression in both P5 (**Figure 21B, C**) and P18 (**Figure 22B, C**) spinal cords treated with PGL-137 inhibitor.

#### 4.4.1.4. NeuN marker

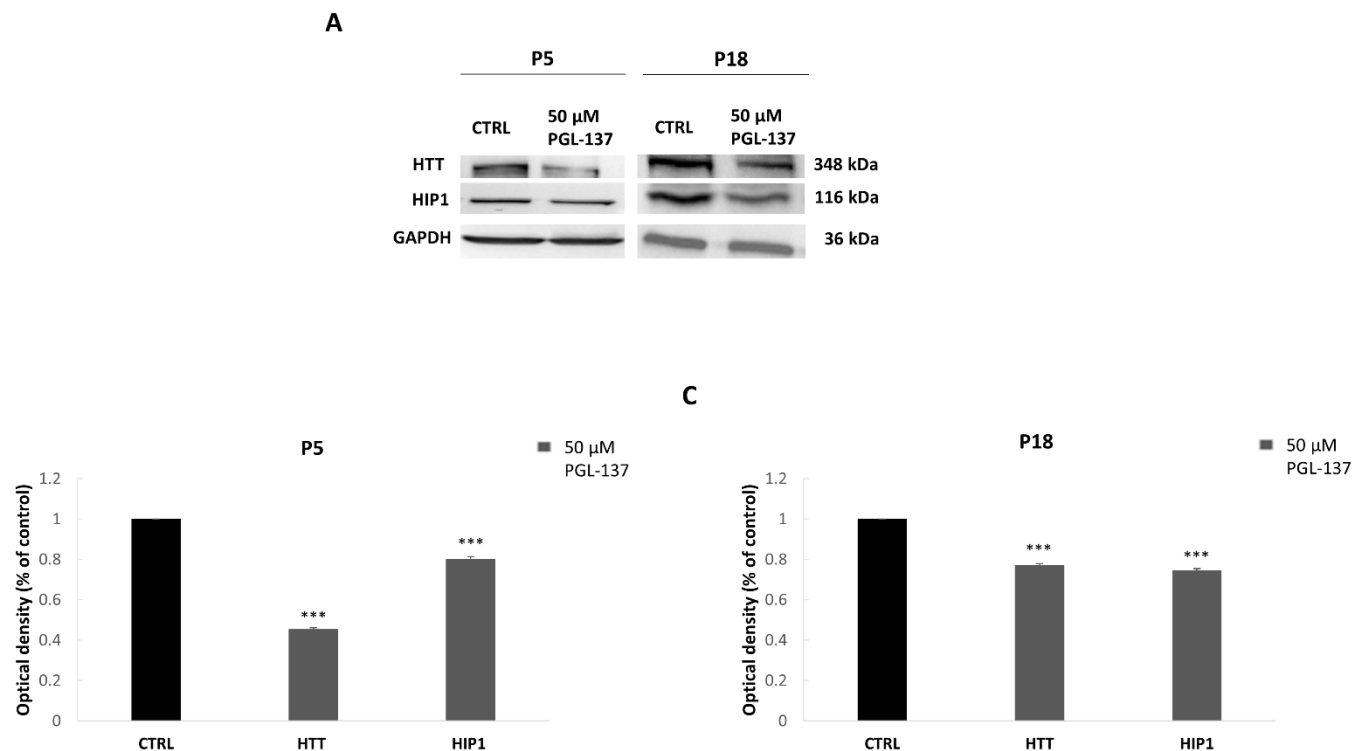
NeuN is a protein specific for neurons. It is located in the nucleus and perinuclear cytoplasm of most neurons of the central nervous system and it is used as a marker of mature neurons. For many years it has been actively used in the immunohistochemical research of neuronal differentiation to assess the functional state of neurons. In the untreated P5 spinal cords (**Figure 23A**), the highest concentration of NeuN positive cells are located in the ventral part and little around the central canal, while in the treated spinal cords (**Figure 23B**) there is a significant decrease in expression of NeuN (**Figure 23C**). In P18 spinal cords (**Figure 24A**) the number of NeuN positive cells increases, suggesting that neurogenesis is in its advanced stage, however, in the treated spinal cords the expression significantly decreases (**Figure 24B, C**).

#### 4.4.1.5. SMI32 marker

SMI32 is a neurofilament protein. Neurofilaments are a major component of the neuronal cytoskeleton, and function primarily to provide structural support for the axons. SMI 32 visualizes neuronal cell bodies, dendrites, and some thick axons in the central and peripheral nervous systems. In the untreated P5 spinal cords (**Figure 25A**; red signal) SMI32 is expressed in the ventral part, whereas a significant decrease in the expression is found in the treated spinal cords (**Figure 25B, D**). In P18 spinal cords (**Figure 26A**; red signal), the expression of SMI32 increases in the dorsal part, with only a slight decrease in the treated ones (**Figure 26B, D**).

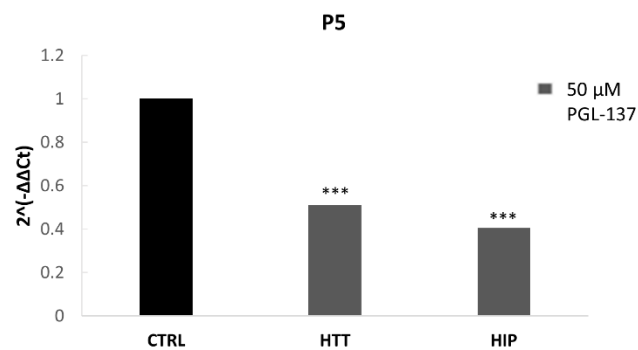
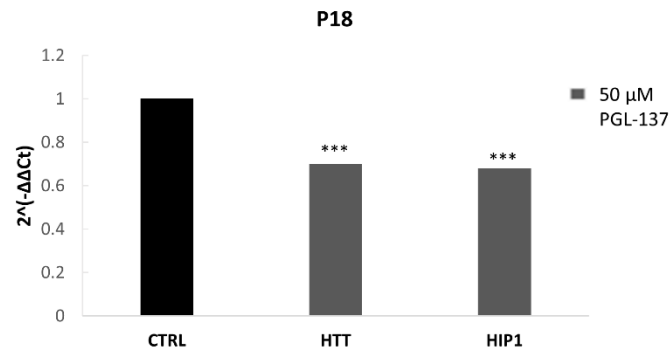
#### 4.4.1.6. SYN1 marker

Synapsin 1 is a member of the synapsin gene family, as a neuronal phosphoprotein, it coats synaptic vesicles, binds to the cytoskeleton, and is believed to function in the regulation of neurotransmitter release. Synapsin 1 plays a role in regulation of axonogenesis and synaptogenesis, regulates neurite outgrowth, and promotes neuronal survival. In the P5 spinal cord (**Figure 25A**; green signal) SYN1 is expressed in the ventral white matter, with a significant decrease in expression in the treated spinal cords (**Figure 25B, C**). As there is progress in development in P18 and well-defined synapses are already present, SYN1 becomes more noticeable, especially in the dorsal area of the spinal cord (**Figure 26A**; green signal). The expression decreases in the treated spinal cords (**Figure 26B, C**), which indicates a down-regulation of SYN1 expression.



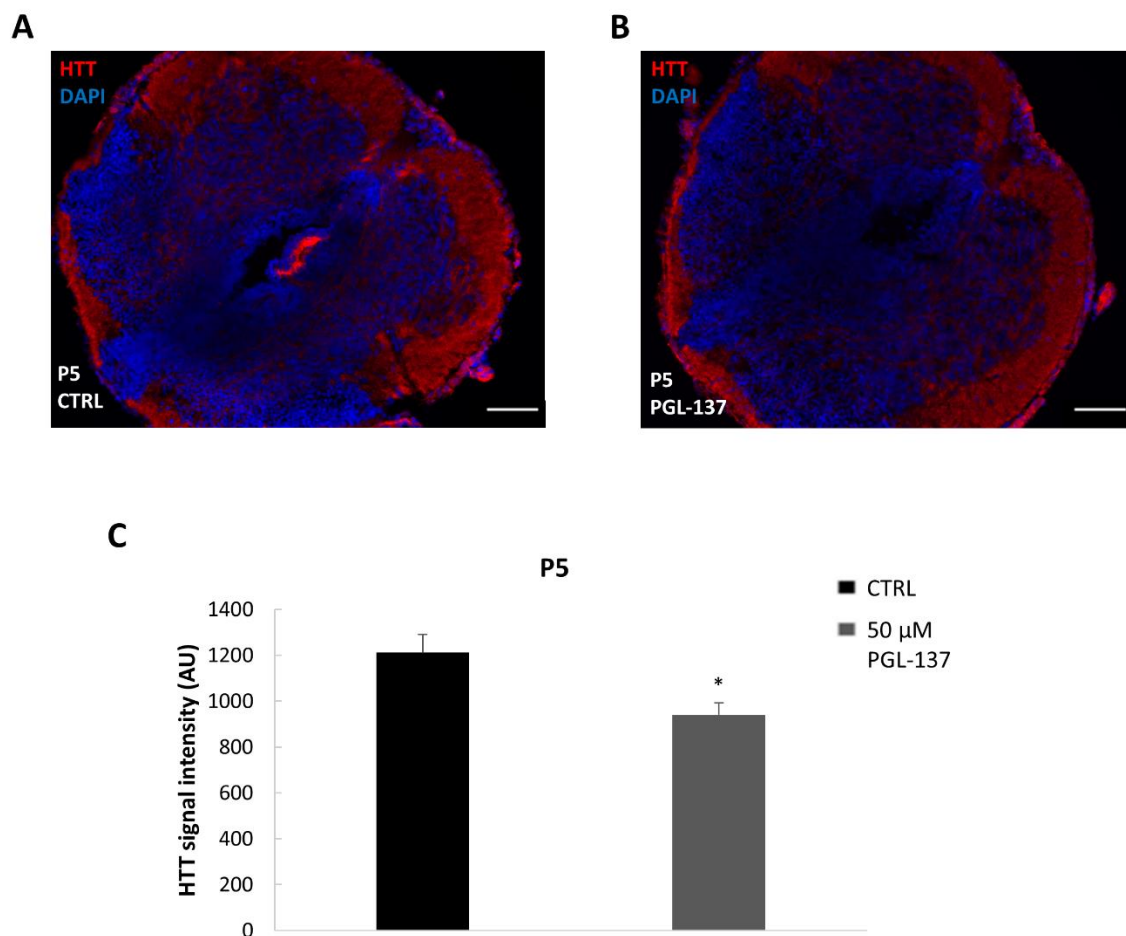
**Figure 17. WB analysis of HTT and HIP1 protein in P5 and P18 opossum spinal cord tissue after treatment with PGL-137 inhibitor.**

WB analysis of the selected proteins. On (A) the representative image of the detected WB signal is shown, while the quantification of the relative level of HTT and HIP1 protein expression is shown on the histogram for P5 (B) and P18 (C) spinal cords. The obtained values were normalized to GAPDH and expressed as fold differences compared to control. Data are presented as means  $\pm$  SD of three independent experiments.

**A****B**

**Figure 18. qRT-PCR analysis of HTT and HIP1 protein in P5 and P18 opossum spinal cord tissue after treatment with PGL-137 inhibitor.**

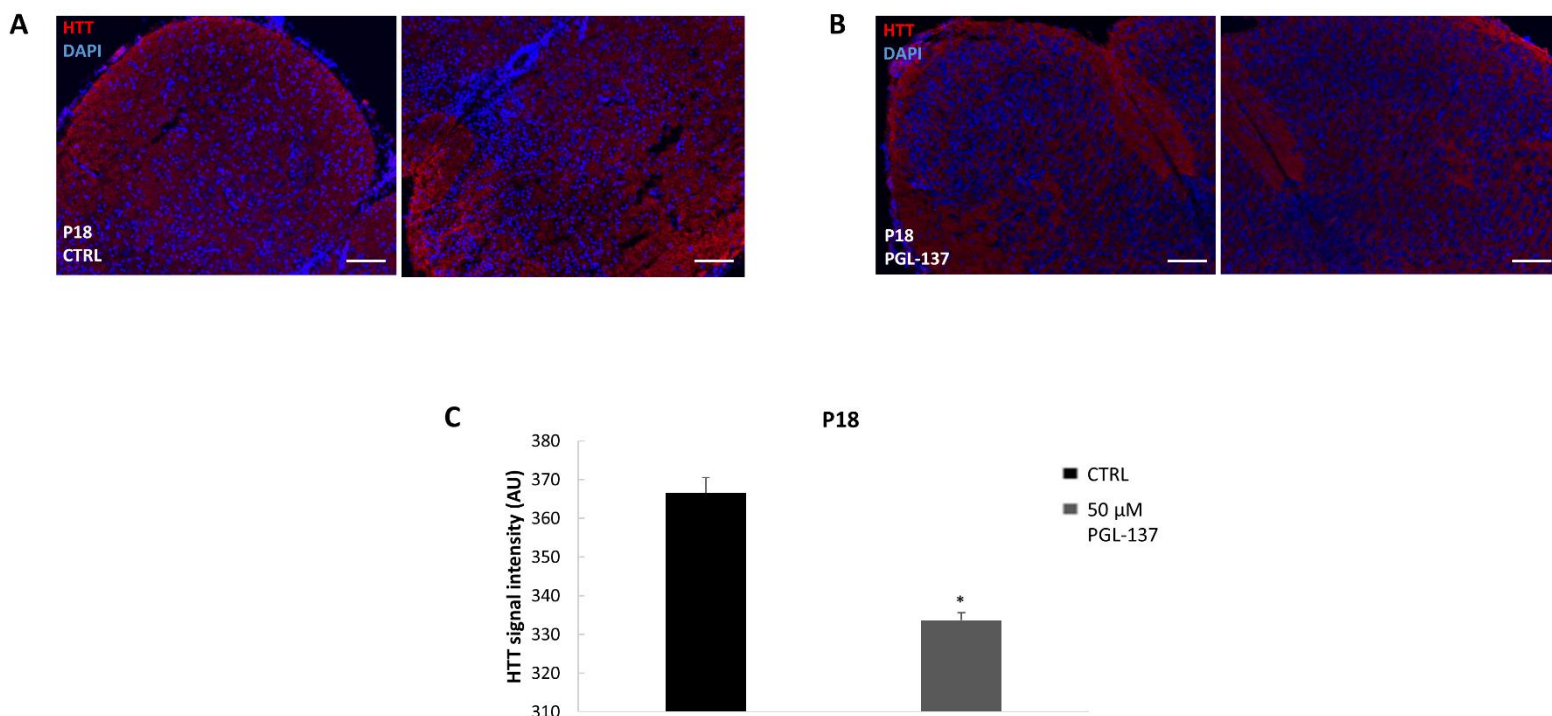
The mRNA levels of HTT and HIP1 were quantified in the spinal cord tissue of P5 (A) and P18 (B) opossums from at least three independent experiments. The obtained values were normalized to GAPDH and expressed as fold differences compared to control.



**Figure 19. Immuno-staining for HTT after treatment with PGL-137 inhibitor in the P5 spinal cord tissue.**

(A, B) Spinal cord sections were immuno-stained for HTT (red signal), while the nuclei of all cells were stained with 4',6-diamidino-2-phenylindole (DAPI; blue signal). On (A) the representative images of the HTT immunostaining are shown in the control spinal cords, while the inhibitor treated are shown on (B). Scale bar, 100 μm.

(C) Bar graphs represent the average immunostaining intensity (Arbitrary Units, AU) in ventral ROIs (100x100 pixels) of P5 control and inhibitor treated spinal cords. Data are mean  $\pm$  SD from 5 to 7 sections from three different spinal cords for each group.



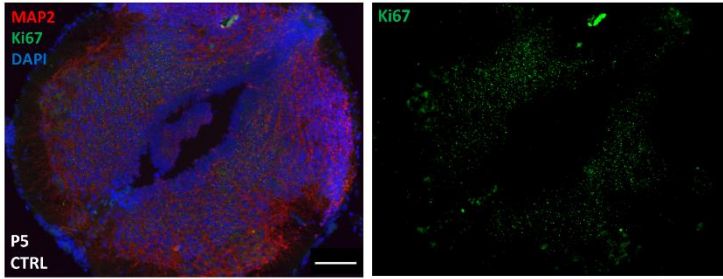
**Figure 20. Immuno-staining for HTT in P18 after treatment with PGL-137 inhibitor in the P18 spinal cord tissue.**

(A, B) Spinal cord sections were immuno-stained for HTT (red signal), while the nuclei of all cells were stained with 4',6-diamidino-2-phenylindole (DAPI; blue signal). On (A) the representative images of the HTT immunostaining are shown in the control spinal cords, while the inhibitor treated are shown on (B). Scale bar, 100  $\mu$ m.

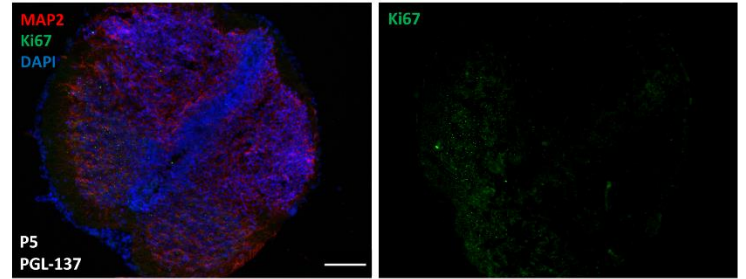
(C) Bar graphs represent the average immunostaining intensity (Arbitrary Units, AU) in ventral ROIs (100x100 pixels) of P18 control and inhibitor treated spinal cords. Data are mean  $\pm$  SD from 5 to 7 sections from three different spinal cords for each group.



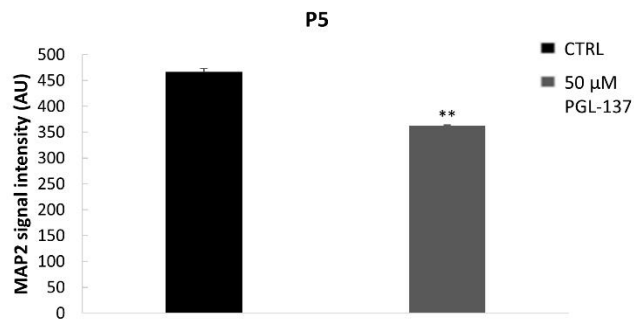
A



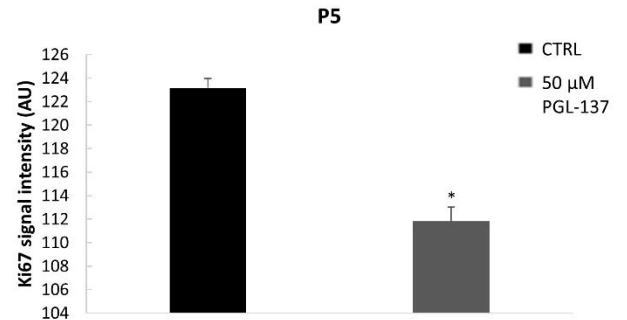
B



C



D

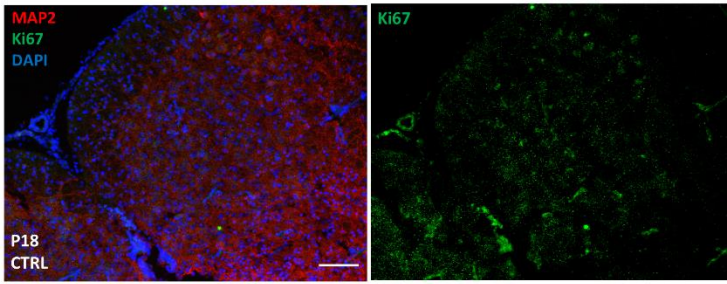


**Figure 21. Immuno-staining for MAP2 and Ki67 after treatment with PGL-137 inhibitor in the P5 spinal cord tissue.**

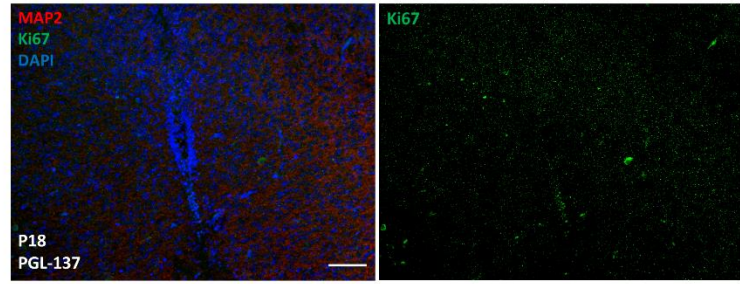
(A, B) Spinal cord sections were immuno-stained for MAP2 (red signal) and Ki67 (green signal), while the nuclei of all cells were stained with 4',6-diamidino-2-phenylindole (DAPI; blue signal). On (A) the representative images of MAP2 and Ki67 immunostainings are shown in the control spinal cords, while the inhibitor treated are shown on (B). Scale bar, 100  $\mu$ m.

(C) Bar graphs represent the average immunostaining intensity (Arbitrary Units, AU) in ventral ROIs (100x100 pixels) of P5 control and inhibitor treated spinal cords for MAP2 (C) and Ki67 (D). Data are mean  $\pm$  SD from 5 to 7 sections from three different spinal cords for each group.

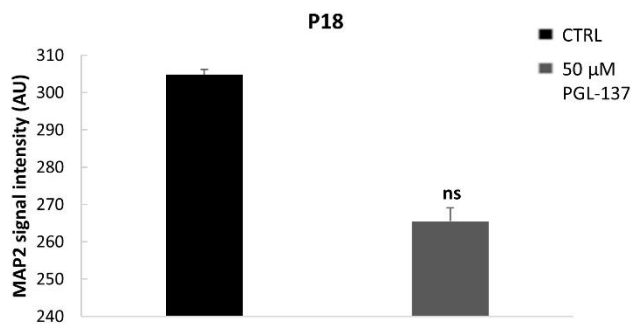
A



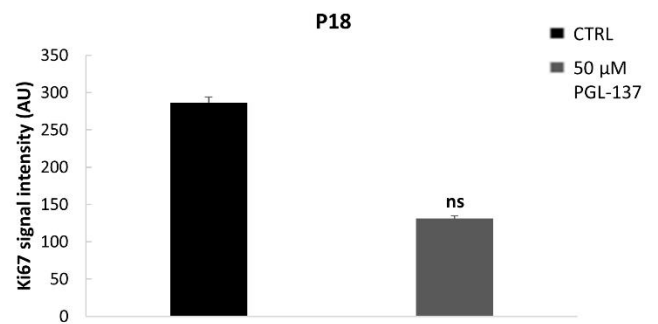
B



C



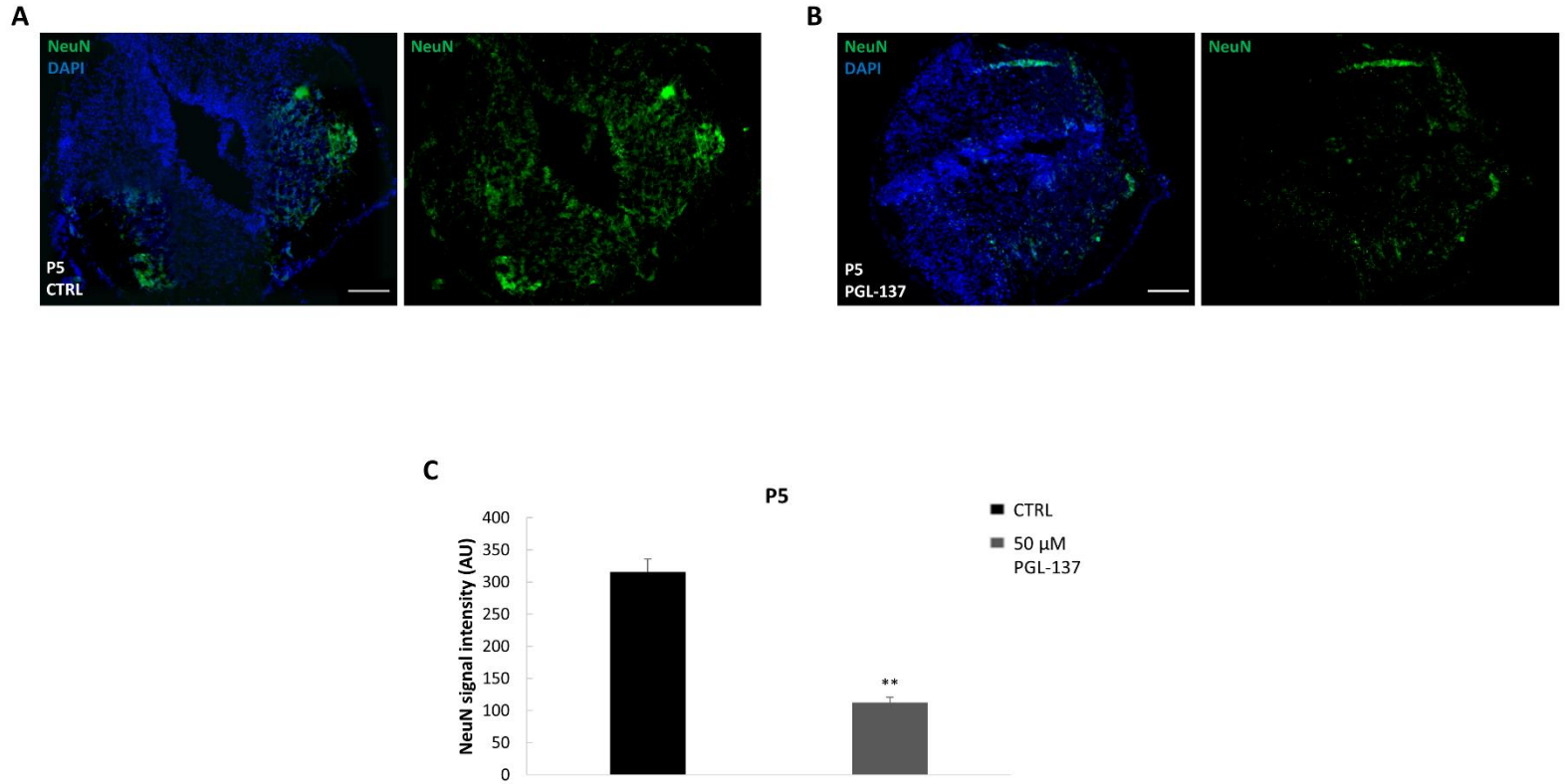
D



**Figure 22. Immuno-staining for MAP2 and Ki67 after treatment with PGL-137 inhibitor in the P18 spinal cord tissue.**

(A, B) Spinal cord sections were immuno-stained for MAP2 (red signal) and Ki67 (green signal), while the nuclei of all cells were stained with 4',6-diamidino-2-phenylindole (DAPI; blue signal). On (A) the representative images of MAP2 and Ki67 immunostainings are shown in the control spinal cords, while the inhibitor treated are shown on (B). Scale bar, 100  $\mu$ m.

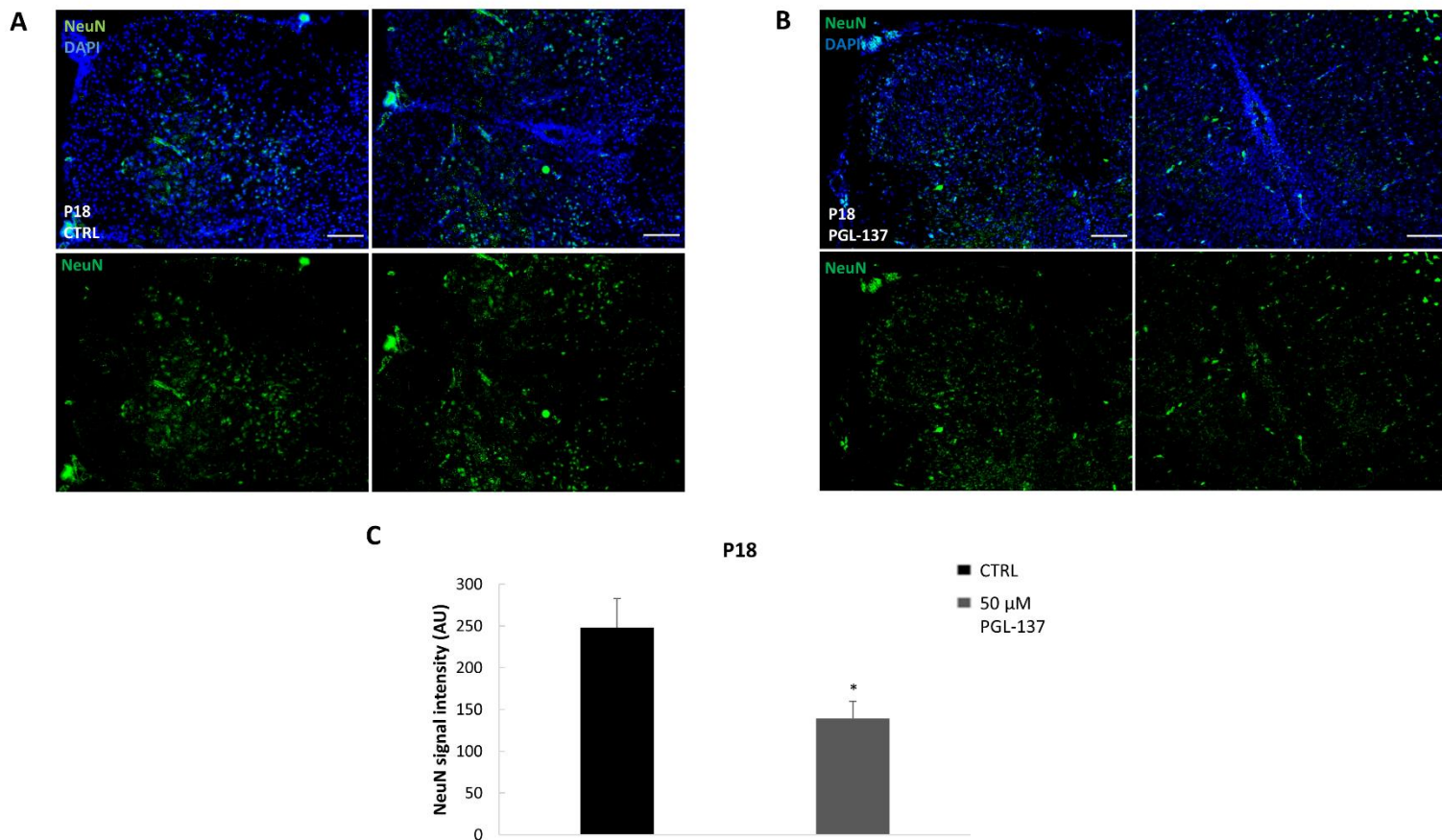
(C) Bar graphs represent the average immunostaining intensity (Arbitrary Units, AU) in ventral ROIs (100x100 pixels) of P18 control and inhibitor treated spinal cords for MAP2 (C) and Ki67 (D). Data are mean  $\pm$  SD from 5 to 7 sections from three different spinal cords for each group.



**Figure 23. Immuno-staining for NeuN after treatment with PGL-137 inhibitor in the P5 spinal cord tissue.**

(A, B) Spinal cord sections were immuno-stained for NeuN (green signal), while the nuclei of all cells were stained with 4',6-diamidino-2-phenylindole (DAPI; blue signal). On (A) the representative images of the NeuN immunostaining are shown in the control spinal cords, while the inhibitor treated are shown on (B). Scale bar, 100  $\mu$ m.

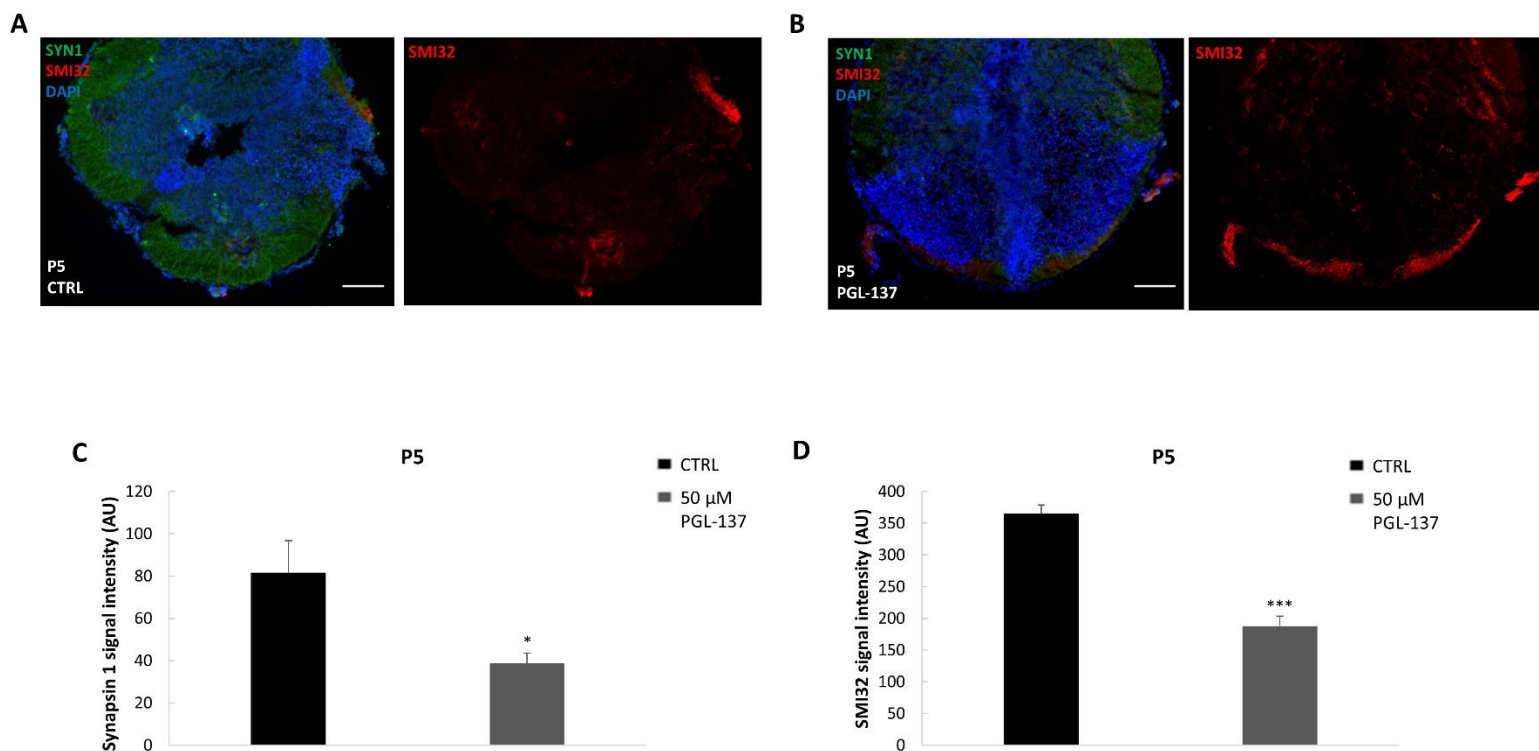
(C) Bar graphs represent the average immunostaining intensity (Arbitrary Units, AU) in ventral ROIs (100x100 pixels) of P5 control and inhibitor treated spinal cords. Data are mean  $\pm$  SD from 5 to 7 sections from three different spinal cords for each group.



**Figure 24. Immuno-staining for NeuN after treatment with PGL-137 inhibitor in the P18 spinal cord tissue.**

(A, B) Spinal cord sections were immuno-stained for NeuN (green signal), while the nuclei of all cells were stained with 4',6-diamidino-2-phenylindole (DAPI; blue signal). On (A) the representative images of the NeuN immunostaining are shown in the control spinal cords, while the inhibitor treated are shown on (B). Scale bar, 100  $\mu$ m.

(C) Bar graphs represent the average immunostaining intensity (Arbitrary Units, AU) in ventral ROIs (100x100 pixels) of P18 control and inhibitor treated spinal cords. Data are mean  $\pm$  SD from 5 to 7 sections from three different spinal cords for each group.

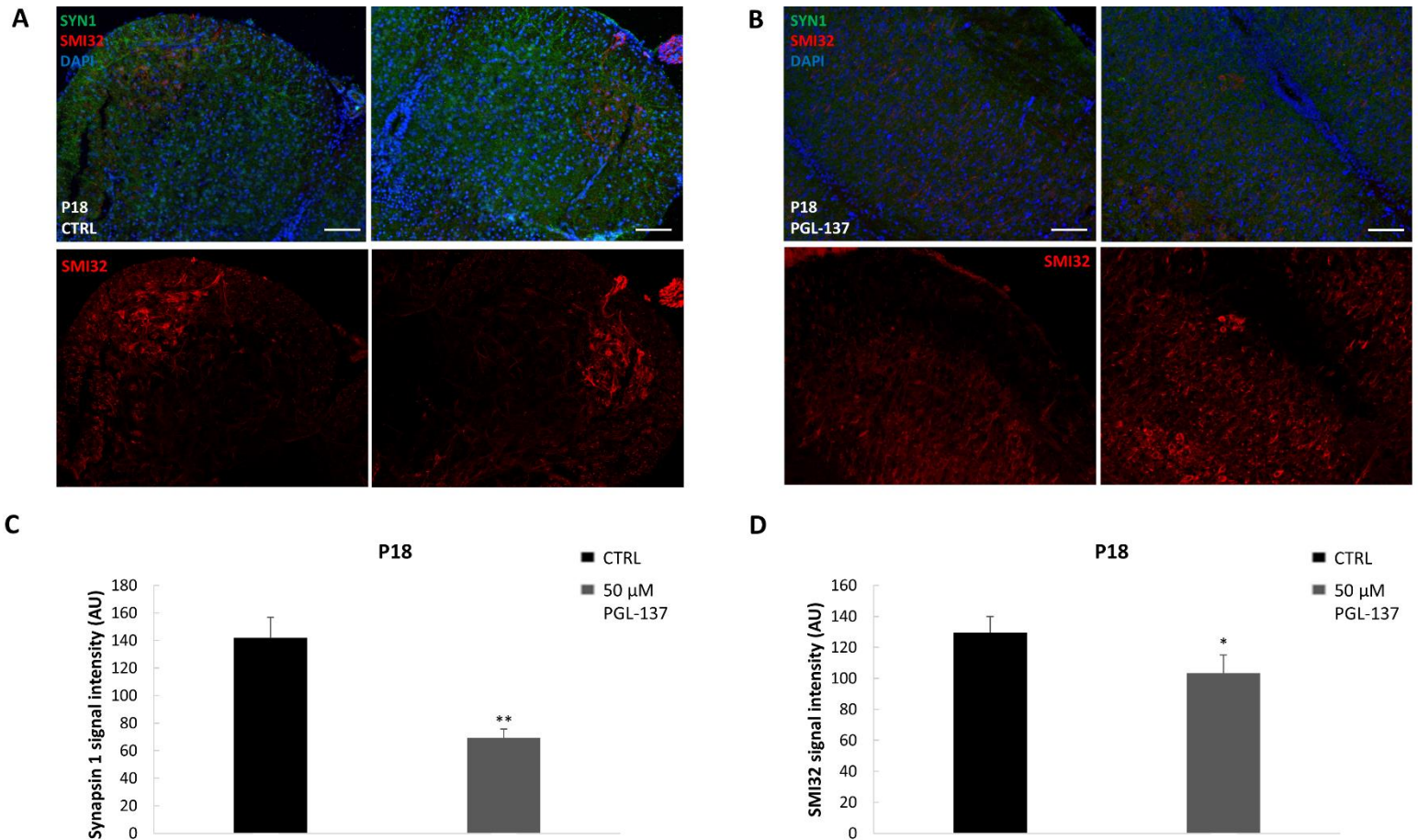


**Figure 25. Immuno-staining for SYN1 and SMI32 after treatment with PGL-137 inhibitor in the P5 spinal cord tissue.**

(A, B) Spinal cord sections were immuno-stained for SYN1 (green signal) and SMI32 (red signal), while the nuclei of all cells were stained with 4',6-diamidino-2-phenylindole (DAPI; blue signal). On (A) the representative images of SYN1 and SMI32 immunostainings are shown in the control spinal cords, while the inhibitor treated are shown on (B). Scale bar, 100  $\mu$ m.

(C) Bar graphs represent the average immunostaining intensity (Arbitrary Units, AU) in ventral ROIs (100x100 pixels) of P5 control and inhibitor treated spinal cords for SYN1 (C) and SMI32 (D). Data are mean  $\pm$  SD from 5 to 7 sections from three different spinal cords for each group.





**Figure 26. Immuno-staining for SYN1 and SMI32 after treatment with PGL-137 inhibitor in the P18 spinal cord tissue.**

(A, B) Spinal cord sections were immuno-stained for SYN1 (green signal) and SMI32 (red signal), while the nuclei of all cells were stained with 4',6-diamidino-2-phenylindole (DAPI; blue signal). On (A) the representative images of SYN1 and SMI32 immunostainings are shown in the control spinal cords, while the inhibitor treated are shown on (B). Scale bar, 100 μm.

(C) Bar graphs represent the average immunostaining intensity (Arbitrary Units, AU) in dorsal ROIs (100x100 pixels) of P18 control and inhibitor treated spinal cords for SYN1 (C) and SMI32 (D). Data are mean ± SD from 5 to 7 sections from three different spinal cords.

#### 4.4.2. Primary spinal cell cultures

##### 4.4.2.1. Spinal cord primary cell culture

We successfully established protocols for primary spinal cell cultures from P5 and P18 opossums. Spinal cord cultures were plated in a proliferative medium, which was replaced the next day with fresh neuronal medium containing B27 supplement and maintained in the incubator for 10 days *in vitro*. At DIV1, using the light microscope, we observed cell survival and neurite outgrowth. Cells were round, well separated and bright (**Figure 27, DIV1**). The cultures deriving from P5 have a higher yield of cells in comparison with cultures from P18 (**Figure 27, bottom row**). At DIV10 we observed neurons, with developed axons and dendrites, indicating neuronal density increased and neuronal differentiation occurred *in vitro* (**Figure 27, DIV10**). Besides neurons, there is also presence of non-neuronal cells in the cultures, such as fibroblasts, that are more abundant in P18 cultures. In comparison with cortical primary cell cultures (120), these cultures have a smaller yield of neurons. This may be for two reasons: firstly because of the stronger enzymatic and mechanical treatment which is required for effective dissociation of the spinal cord, or secondly, spinal cord neurons could have a lower survival rate in culture compared to cortical neurons. All in all, spinal cord cultures are more demanding and more difficult to maintain than cortical, especially the spinal cultures derived from older opossum age (P16-P18), but that is in accordance with *in vivo* observations (12,79,84,85).

##### 4.4.2.2. Neurite outgrowth test

Neurons were cultured for 24 h, the time necessary to observe the neurite outgrowth. To test the relevance of the primary spinal cultures as the platform to be used in the neuroregeneration studies, we applied 50  $\mu$ M PGL-137, to check its possible effect on neurite outgrowth and neuronal network formation. After 24 hours, the inhibitor was removed, fresh neuronal medium was added, and the neurons were cultured to DIV10, as described in section 3.2.15.4. Due to our previous results, we also wished to check the expression of HTT and HIP1 at the protein and mRNA level, in spinal primary cultures after the treatment with PGL-137. In primary cell cultures obtained from P5 spinal cords, the treatment with PGL-137 inhibitor resulted in almost completely diminished protein (**Figure 28A, B**) and gene expression (**Figure 29A**) of HTT and HIP1 compared to the control. In primary cell cultures obtained from P18 spinal cords, the relative expression of HTT

and HIP1 was also very reduced at the protein (**Figure 28A, C**) and gene level (**Figure 29B**). In both cases, relative expression of HTT was further reduced on the protein and gene level, compared to HIP1.

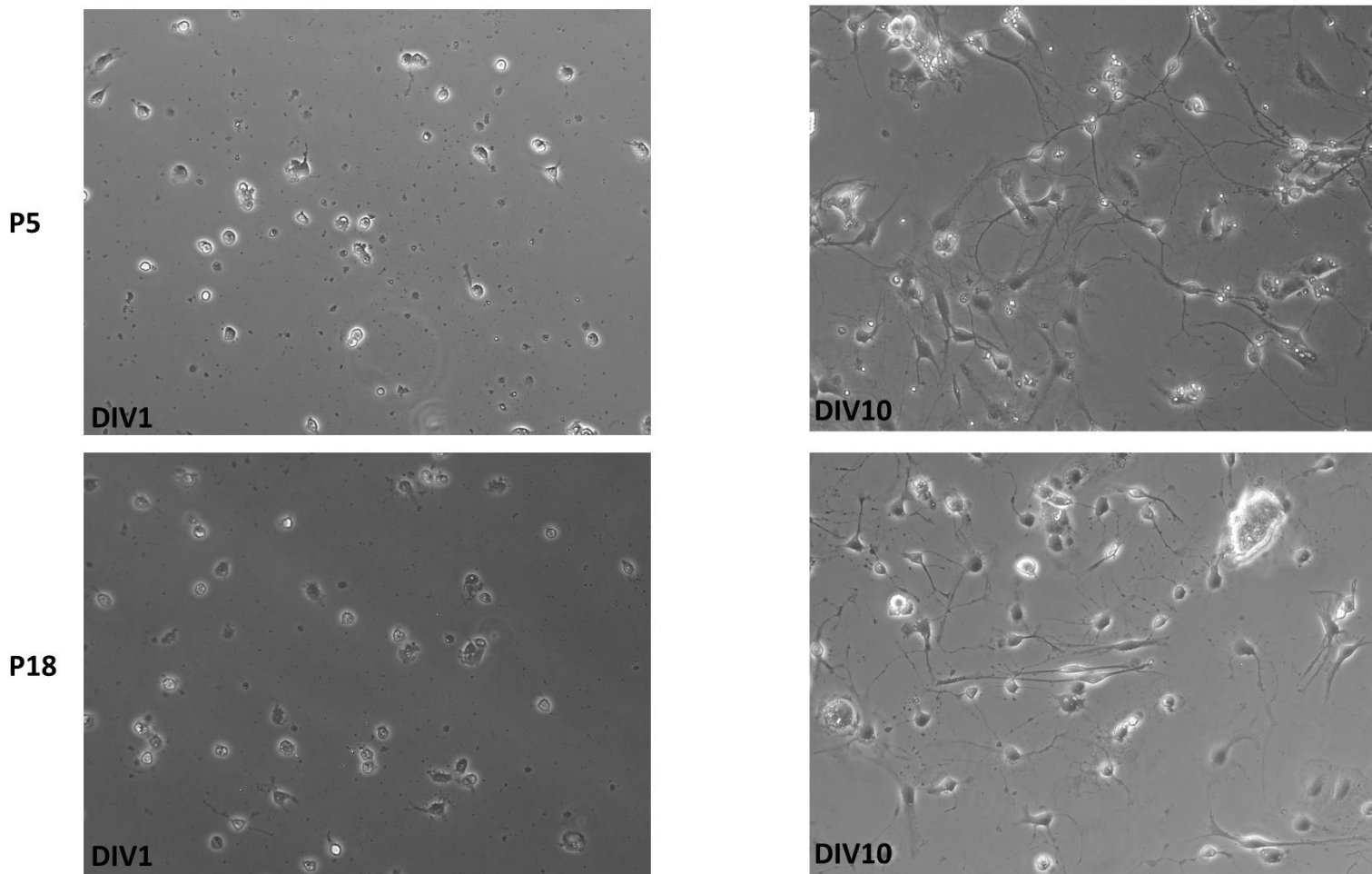
Unlike the intact spinal cord tissue, primary cell cultures are more suitable for pharmacological manipulation of candidate molecules and testing of their influence on the properties of selected cells. In both P5 and P18 neuronal cultures, the PGL-137 inhibitor applied at DIV1, prevented the growth of full-length neurites and neuronal network formation (**Figure 30A**). As a result, significantly shorter neurites were present in both P5 (**Figure 30B, upper row**) and P18 neuronal cultures (**Figure 30B, bottom row**). The average neurite length shortened from 160  $\mu\text{m}$  under control conditions to only 38  $\mu\text{m}$  after administration of PGL-137 inhibitor in P5 spinal cell cultures. In P18 spinal cell cultures, the average neurite length in control conditions was 175  $\mu\text{m}$ , which shortened to only about 44  $\mu\text{m}$  after administration of the inhibitor. The use of the PGL-137 inhibitor on both P5 and P18 primary spinal cell cultures led to a significant decrease in the number of neurons and resulted in impaired neuronal survival, proliferation and neurite outgrowth.

Taken together, the results obtained on the intact spinal cord and primary spinal cell culture suggest a possible role of the PGL-137 inhibitor on various processes relating to neuroregeneration, such as cell viability, proliferation and neuronal network formation, however, future studies are needed in order to confirm this observation.

#### **4.4.2.3. New neuronal regeneration scratch assay**

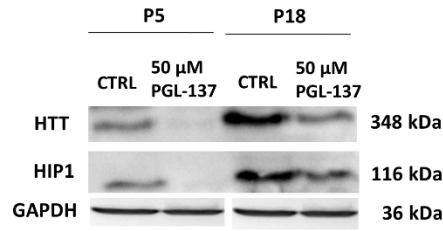
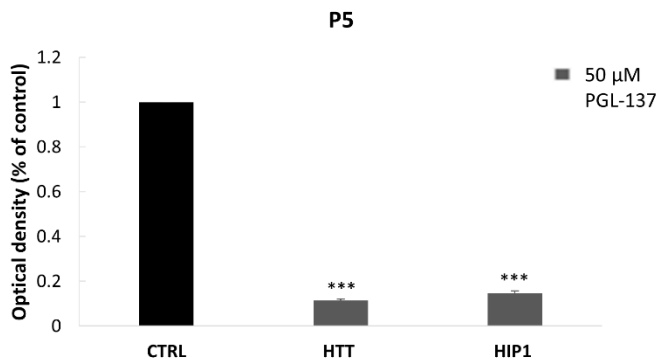
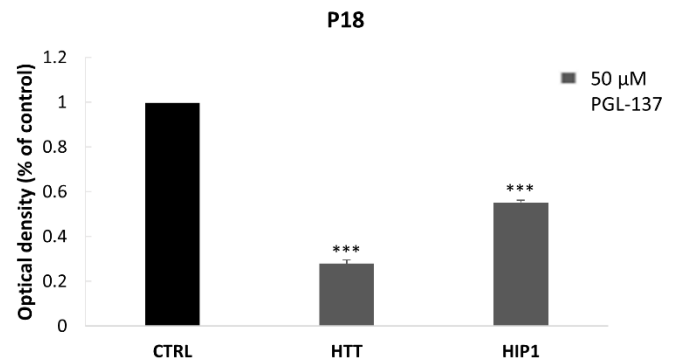
The scratch assay is a fast and effective method and provides us with insight into the injury and regeneration of individual cells in culture. The scratch was performed on primary cultures of neurons isolated from the opossum P5 and P18 spinal cords to test their ability to regenerate. The first incision attempts were made with 200 and 20  $\mu\text{L}$  pipette tips, but the width of the cut was too large and inadequate. An injury was then made with tweezers with a tip thickness of 0.1 mm resulting in an incision about 150  $\mu\text{m}$  wide. However, the number and viability of primary spinal cord neurons were extremely small in the cultures derived from older opossum age (**Figure 31, bottom row**), compared to the cultures deriving from P5 (**Figure 31, upper row**), so they were not suitable for performing the regeneration test. Spinal cord cultures have been shown to be more demanding and more difficult to maintain than cortical, which was in accordance with *in vivo* observations.





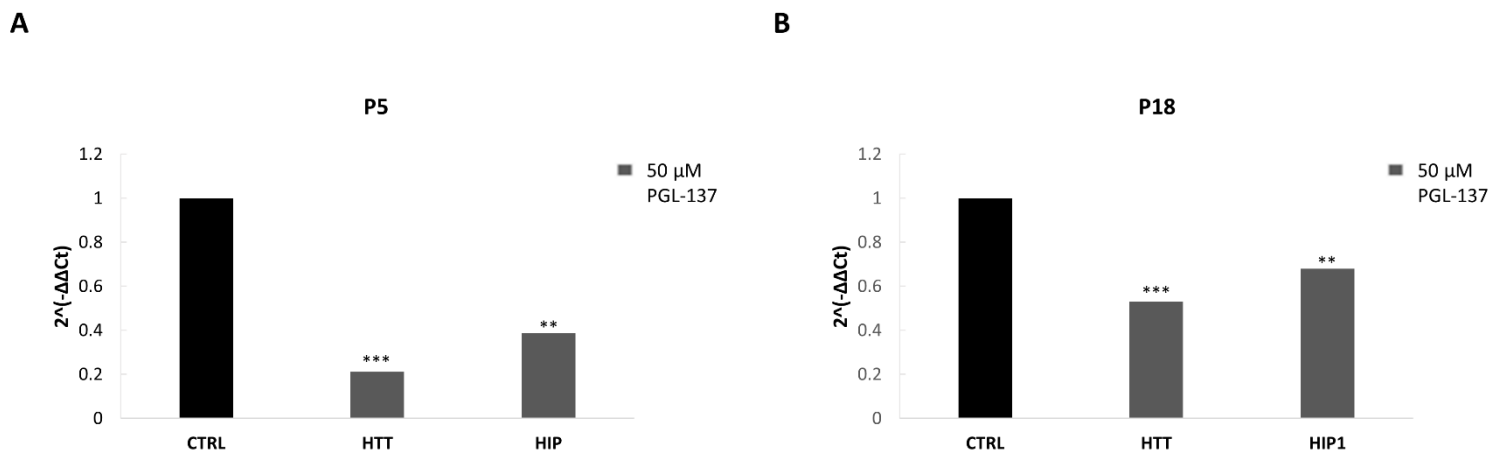
**Figure 27. Brightfield images of spinal cord primary cell cultures from P5 and P18 opossums at two different stages during culture, DIV1 and DIV10.**

The spinal cord primary cells from P5 and P18 opossums were plated in a 12-well plate pretreated with poly-L-ornithine. The cells were cultivated in neuronal medium with B27 supplement. Cultures were maintained in an incubator at 32°C in 5% CO<sub>2</sub> and 95% relative humidity. Images of the cultures were taken at DIV1 and DIV10 with a camera connected to the light microscope at magnification 20x.

**A****B****C**

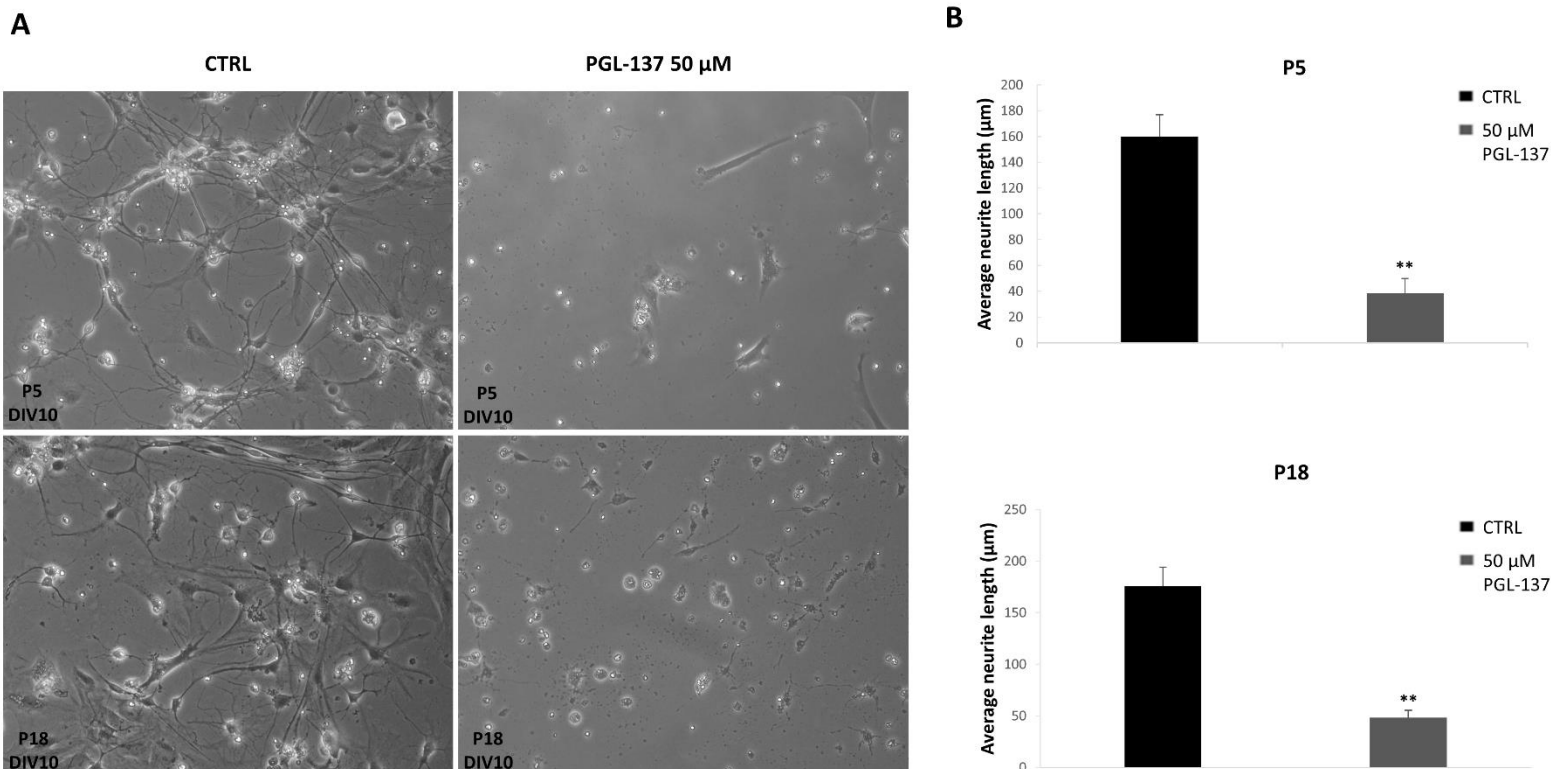
**Figure 28. WB analysis of HTT and HIP1 protein in P5 and P18 primary spinal cell cultures after treatment with PGL-137 inhibitor.**

WB analysis of the selected proteins. Cells were harvested at DIV10. On (A) the representative image of the detected WB signal is shown, while the quantification of the relative level of HTT and HIP1 protein expression is shown on the histogram for P5 (B) and P18 (C) primary spinal cell cultures. The obtained values were normalized to GAPDH and expressed as fold differences compared to control. Data are presented as means  $\pm$  SD of three independent experiments.



**Figure 29. qRT-PCR analysis of HTT and HIP1 protein in P5 and P18 primary spinal cell cultures after treatment with PGL-137 inhibitor.**

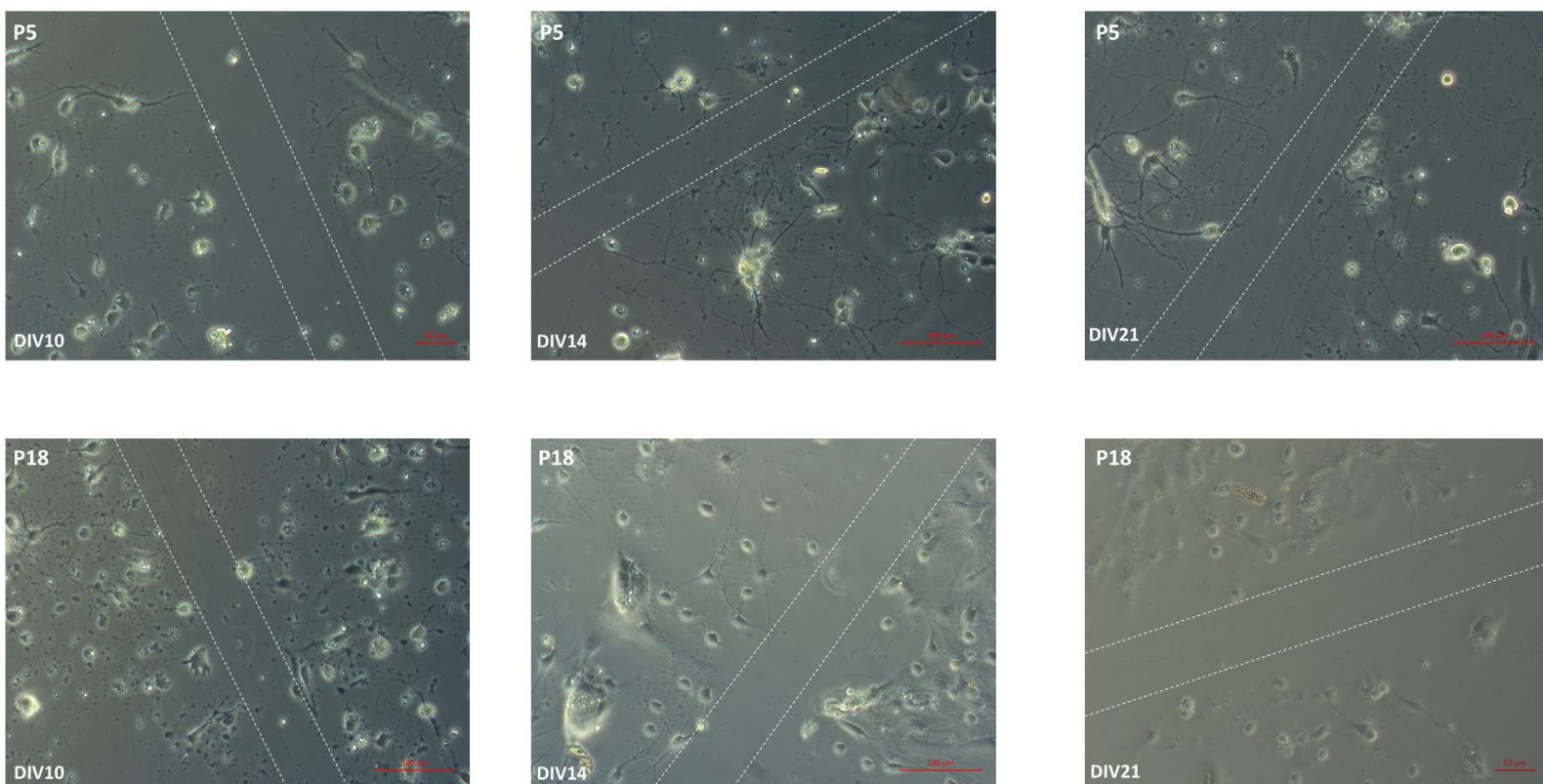
The mRNA levels of HTT and HIP1 were quantified in P5 (A) and P18 (B) primary spinal cell cultures from at least three independent experiments. The obtained values were normalized to GAPDH and expressed as fold differences compared to control.



**Figure 30. Primary neuronal cultures.**

Brightfield images (A) of primary neuronal cultures derived from the P5 and P18 spinal cords of *M. domestica*. Cells were treated at DIV1 with PGL-137 inhibitor for 24h. Images of the cultures were taken at DIV10 with a camera connected to the light microscope at magnification 20x.

The bar graph shows the average neurite length for P5 (B; upper row) and P18 (B; bottom row) spinal neurons for the experimental conditions in the left part of the figure. Data are presented as means  $\pm$  SD of two independent experiments. ImageJ SNT plugin was used to measure the average neurite length. The total number of neurites analyzed: P5 CTRL 84; PGL-137 62. The total number of neurites analyzed: P18 71; PGL-137 56.



**Figure 31. Brightfield images of the scratch test performed on primary spinal neuronal cultures from P5 and P18 opossums at different stages during culture, DIV10, DIV14 and DIV21.**

Primary neuronal cultures derived from the P5 and P18 spinal cords of *M. domestica*. The scratch was made with tweezers with a tip thickness of 0.1 mm resulting in an incision about 150  $\mu\text{m}$  wide, at different stages during cultures. Images of the cultures were taken at DIV10, DIV14 and DIV21 with a camera connected to the light microscope at magnification 20x.

## 5. DISCUSSION

### 5.1. Proteomics

In this study, we determined the protein profile of the opossum *Monodelphis domestica* intact spinal cords with different regenerative capacities.

When establishing protocols for mass spectrometry analysis of spinal cord samples we tested different methods including two-dimensional polyacrylamide gel electrophoresis (2-DE), a technique used for the separation of complex protein mixtures from tissues, cells, or other biological samples (148). The next method we tested was filter aided sample preparation (FASP), which is used for the on-filter digestion of proteins before mass-spectrometry-based analyses (149). The two tested methods allowed the identification of no more than 200 proteins per sample for the first protocol (**Tables 4-7**) and 800 for the second (**Tables 8-9**). The identified proteins were mainly house-keeping cellular proteins that are present in large numbers in cells and are involved in various cellular processes such as cytoskeleton formation, cellular metabolism, homeostasis maintenance, etc.

During 2-DE, the low dynamic range of proteins is one of the challenging problems, because highly abundant peptides mask low abundant ones, which can make the identification of low abundant proteins difficult. One of the solutions to overcome this problem is to load more protein samples, however, this approach could result in the production of overcrowded images with non-well separated spots (148). Another explanation for the low number of identified proteins is the difficulty in separating membrane-bound hydrophobic proteins and extremely acidic or basic proteins which are not easily extracted or solubilized (150,151). Because of that, different types of proteins can always be missing. On the other hand, FASP uses filtration units with molecular weight cut-off filters of 3000 and 10,000 Da, which we used in the preparation process. However, better results can be achieved using membranes with larger pores with a cut-off of 30,000 and without any loss of proteins with low molecular weights in the range of 10,000 (149). Nano-HPLC-MS/MS analysis of protein gels done on an ORBITRAP instrument allowed the identification of a significantly higher protein number. A total number of 4735 proteins involved in a spectrum of biological functions were identified, revealing the abundance of proteins related to

neurodegenerative diseases (**Table 10**) and the overall concurrence with the previously obtained transcriptomics data (82,83).

In very few research studies comparative proteomic analyses have been used to pinpoint the differences between regenerating and non-regenerating systems, e.g. between rat peripheral sensory and motor nerves (98), after rat spinal cord transection (99) and following transection of opossum neonatal spinal cord (83,100–102). Comparative proteomic analysis has been done between rat peripheral sensory and motor nerves to pinpoint their different functions and approaches to regeneration. 2D LC-MS/MS was used to determine the protein profile of sensory and motor nerves, where a total of 1472 proteins were identified, among which 100 proteins showed differential expression between both nerves. The 56 proteins that had significantly higher expression in sensory nerves were mostly cell adhesion proteins, SNAP complex super-family of small membrane proteins, calcium-binding proteins, and enzymes such as hydrolases and transferases. The 44 proteins that had significantly higher expression in motor nerves were mainly cytoskeletal proteins, extracellular matrix proteins, and neurotrophic factors (98). The main goal of other studies was to reveal the cellular response to traumatic SCI, and thus the most prominent protein changes detected in both regenerating and non-regenerating tissues were found to be related to the inflammatory response to injury, probably overshadowing the subtler changes related to neuroregeneration. For example, a transcriptomic study was done on opossums to investigate the response to spinal cord injury (102). The aim was to identify differential gene expression in regenerating, SCI at postnatal day 7 (P7SCI) and nonregenerating, SCI at postnatal day 28 (P28SCI) cords after complete spinal transection, compared to controls, using RNA sequencing. 147 genes altered expression in both injury ages. When gene ontology overrepresentation analysis was done between the two experimental gene sets, the P7SCI gene-sets showed significant overrepresentations only in immune-associated categories, while P28SCI showed overrepresentations in the same immune categories, as well as other categories such as cell proliferation, cell adhesion, and apoptosis.

In this study, we compared the naïve mammalian spinal cord tissues with different regenerative capacities, to allow the detection of a wide spectrum of protein changes during the developmental period when regeneration stops being possible. This approach revealed the basic properties of neuronal tissue related to regeneration. The results of this study upgraded the previous data about

the genes differentially expressed in the regenerating and non-regenerating opossum spinal cord tissue (82,83). The comparison of the data obtained by the genomic and proteomic approach allowed the selection of the several most promising candidates controlling regeneration, that were tested in functional studies. In the previous studies (82,83) genes that change their expression in the opossum spinal cord during the critical period of development when regeneration stops being possible were identified, revealing molecules involved in nucleic acid management such as transcription factors and regulators, and RNA splicing factors, protein synthesis and processing, control of cell growth, structure and motility, cell signaling, and extracellular matrix molecules and their receptors. The bottleneck of the genomic approach is the difficulty to select the relevant molecules from a comprehensive list of the candidates. Thus, the previous data was upgraded with proteomic research, to facilitate the selection of several most promising candidates controlling regeneration. Until recently, there has been an implicit assumption in the proportional relationship between mRNA and protein expression measured from tissue. However, analysis of mRNA and protein expression data in multiple research studies failed to show a high correlation between the two levels (152), indicating that the relationship between mRNA and protein level varies depending on the tissue or cell type. For example, in cells that remain in stable conditions, changes observed at the protein level are mostly in line with mRNA level (153). Another explanation for the low correlation between mRNA and protein expression can be due to various factors such as different half-lives and post transcription machinery (152). Genes that are involved in cellular processes show high stability of both transcripts and protein products (154). On the other hand, genes that are associated with RNA processing have stable proteins, but unstable transcripts, while genes that are extracellular in nature, produce stable transcripts but unstable proteins (155). Many of the proteins and transcription factors are present at levels that cannot be predicted from the level of mRNA. Because of the lack of direct correlation between gene and protein, focusing on only one approach, either transcriptomic or proteomic, may result in partial explanation or misinterpretation of a particular process (153). For all of the reasons listed, a joint analysis of the transcriptomic and proteomic data can provide useful insights that may not be interpreted from individual analyses of mRNA or protein expressions (152).

Efforts were made to validate the results obtained by comparative proteomics using WB, and qRT-PCR to compare gene expression changes for the selected candidates, revealing the overall congruence of the results, both at the gene and protein level. The results coincided with the



previous studies (82,83) for the majority of the protein functional groups, but the most interesting was the finding of the myriad of the proteins known to be involved in the pathology of neurodegenerative diseases. The expression of several interesting genes and proteins related to neuroregeneration and neurodegenerative diseases was analyzed to verify the protein changes detected by MS (**Figures 12-16**). For the majority of the genes and proteins, there was a perfect correlation between the detected protein and gene changes with the results obtained by MS. For the 10 other selected molecules including MAPK10, PARK7, APBB1, BACE1, cJun, RELN, NUP43, RAB8B, PSEN1 and UCHL1, the results obtained either at the protein or gene level were not in accordance with results obtained by the MS analysis. This observation may be due to the technical limits of the techniques used (156). When performing Western blots, we extract the whole protein lysate, while in nano-HPLC-MS/MS analysis of protein gels, protein spots are cut from the gel and subjected to trypsin digestion, therefore, large losses are possible during extraction. This analysis typically requires a number of processing steps including protein lysis and extraction, denaturation, reduction of disulfide bonds, alkylation of cysteine residues, enzymatic digestion, LC separation, and analysis by a mass spectrometer. This is followed by extensive informatics processing in order to identify and quantify peptides and proteins. Also, some variations are possible in the instrument's response from run to run because of repeated injections for LC-MS/MS analysis, which is described by the instrumental variance component. Sometimes, analyses can take place over several days or even weeks. During this time, many small changes can occur in the LC-MS/MS platform: different buffer batches, delays in column and electrospray performance, calibration and adjustment shifts, and possibly low levels of detection. These changes may contribute to the observed technical error and variability in proteomic analyses and are captured by the instrumental stability component. This can be expected considering the wide range of physical properties of proteins and their peptides. Due to the complexity of these analyses, it is necessary to thoroughly understand the potential sources of variability in the technical platform and to pay close attention to protein extraction (dissection and homogenization), as this is the most critical step prior to analysis (156). Another possibility is the biological discrepancy between the gene and protein levels. In fact, unlike the genome, which is characterized by greater stability, the proteome actively changes in response to various factors, including the organism's developmental stage, as well as internal and external conditions (157). For example, a recent study done on embryonic stem cells revealed that changes in protein levels are not

accompanied by changes in corresponding mRNAs (158). It is still uncertain how closely levels of mRNAs relate to levels of their corresponding proteins. Two studies (154,159) have explored this problem in mammalian cells, and suggest only a modest correlation.

#### **5.1.1. Inhibitors of CNS axon regeneration: glial scar and myelin associated proteins**

One of the important factors that negatively affect the regeneration of neurons at the site of the lesion is the complex microenvironment. This unfavorable environment physically and chemically limits the growth and regeneration of damaged nerves, as well as the restoration of synaptic connections between neurons, which are crucial for the proper functioning of the central nervous system. A specific microenvironment arises as a result of inhibitory molecules that are released from damaged myelin, the migration of glial cells to the site of the lesion, and the formation of a scar around the site of injury. Also, in the area of injury, there is reduced production of growth factors that are very important in the self-repair of damaged neurons and neural stem cells, but also in the generation of new ones (160).

Glial cells are very important in maintaining the homeostasis of the nervous system, but they also secrete inhibitory molecules and form scar tissue, which is an element of the unfavorable microenvironment that limits the growth and regeneration ability. Oligodendrocytes are support cells that form the myelin sheath around axons. The myelin sheath, which contains 20% proteins and 80% lipids, is essential because it helps speed up the transmission of nerve stimuli. Oligodendrocytes, like other glial cells, express inhibitory molecules that initiate the development of an unfavorable microenvironment (161). It seems that the major difference between regenerative and non-regenerative vertebrates is in the composition of the glial cell population and its response to injury. The regenerative species have retained neurogenic radial glial cells characteristic of early developmental stages (20), while in non-regenerating vertebrates the radial glia differentiate into different glial populations, among which the most abundant are Glial fibrillary acidic protein (GFAP)-positive astrocytes that, upon injury, infiltrate the wound site and deposit extracellular matrix and proteoglycans resulting in the formation of a glial scar, which impedes axonal growth (23). It has been shown that GFAP is consistently upregulated with age across rodents and humans (162). Two studies showed that GFAP mRNA increases with age in rat and human brains (163) as well as in the mouse brain (164). A recent study was done on 1, 3, 6, 18 and 24 month old male Wistar rats that showed a progressive increase in astrocytic GFAP

expression in different regions of the brain with age (165). Another study was done on the hippocampi of 3 and 16 month old senescence-accelerated mice, which are a group of inbred mouse strains developed as a model for studying human aging and age-related diseases, and the results showed significant age-related increases in both protein and mRNA levels of GFAP (166). Given the fact that gliogenesis occurs during the late embryonic and postnatal period in rodents (20,167), and in the opossum cortex it was observed at P18 (168), our results for GFAP were consistent with these previous reports since it showed increased protein and mRNA levels during development (**Figure 12, Table 11A**). Other sources of regeneration inhibiting molecules are inhibitors of the axonal growth present in the CNS myelin such as myelin associated proteins. Myelin basic protein (MBP) was our second positive control when performing confirmatory tests, and it also showed increased protein and especially increased mRNA levels during development (**Figure 12, Table 11A**), which was expected since the amount of myelin in the body increases throughout development, from fetal development up until maturity (169). One study examined the expression of the MBP gene in the developing human brain and showed that the expression of MBP mRNA in the fetal and adult brain increased progressively with development (170). Besides MBP, our MS analysis detected other myelin associated proteins such as myelin associated glycoprotein, myelin oligodendrocyte glycoprotein and myelin protein zero whose expression was higher in the mature, P18 spinal cords and that was in accordance with the process of myelination in the nervous system. The molecules that influence axonogenesis have been extensively studied to identify multiple extracellular inhibitors of axonal growth, such as already mentioned myelin associated proteins, as well as tenascins, and chondroitin sulfate proteoglycans (24). On our protein lists, the MS analysis detected the higher expression of tenascin C, tenascin R, and chondroitin sulfate proteoglycan 5 in the P18 spinal cords. This was consistent with the following studies: tenascins are a family of extracellular matrix glycoproteins which are expressed in the central nervous system during embryonic and neural development and in adult tissues during processes involving wound healing and nerve regeneration (171). Chondroitin sulfate proteoglycans are widely expressed in the normal central nervous system, where they serve as guidance molecules during development and modulate synaptic connections in the adult. Increased chondroitin sulfate proteoglycan expression is commonly observed close to the lesion areas in spinal cord injury. These deposits form a barrier to regeneration causing the inability to repair damage in the brain and spinal cord (172). Although these molecules have been studied in order to identify inhibitors

of axonal growth, disrupting those inhibitory signals, either individually or in combination, have so far failed to produce robust axon regeneration.

### **5.1.2. Promoters of regeneration: proteins involved in neurodevelopment**

The potential to regenerate the nervous system is somehow lost during evolution, and a precise molecular understanding of what restricts regeneration over development and evolution is not yet clear (1). As mentioned before, the major difference among regenerative and non-regenerative vertebrates is probably in the composition of the glial cell population: the regenerative species have retained neurogenic radial glial cells characteristic of early developmental stages (20).

Brain lipid-binding protein (BLBP) is a marker for radial glia in the developing mammalian CNS. A group of scientists analyzed the expression of BLBP during embryonic CNS and postnatal cortical development in mice. They showed that BLBP expression is low during embryonic day 12 which was the earliest time point tested. After that, the expression level increased as the embryonic CNS differentiated (173). These observations were in line with our results obtained on the spinal cord where the expression of BLBP increased on the protein and mRNA level during development (**Figure 12, Table 11A**). However, this study also showed that after birth, over the 2 postnatal weeks, the BLBP expression decreased and was not detectable in the adult cortex indicating that BLBP expression correlates with early phases of cortical neural differentiation (173). The growth associated protein 43 (GAP-43) is an axonal protein and marker for neurite outgrowth which is mostly expressed in regenerating and developing nerves. A study was done on the brain and spinal cord from embryonic, postnatally developing and adult rats where they demonstrated that GAP-43 is expressed in all CNS neurons during the perinatal period, but as development proceeds its distribution is restricted to certain areas, for example, the highest level of GAP-43 expression in adult neurons is mostly limited to two regions: the hippocampus and olfactory bulb (174). Our results show increased levels of GAP-43 (**Figure 12, Table 11A**), which is in accordance with the previous studies given the fact its levels are highest in developing nerves during axonal elongation. The paired box protein Pax-2 (PAX2) is expressed during early embryonic development and has an important role in the formation of tissues and organs, especially the brain and spinal cord (175). As expected, our results showed higher expression of PAX2 during the early developmental stage, in the spinal cords of postnatal day 5 opossums, compared to older ones (**Figure 12, Table 11A**). Nuclear distribution protein nudE-like 1

(NDEL1) is a protein that participates in neurogenesis, neurite outgrowth, and neural migration (140). Our results demonstrate a modest difference at the protein level between the two developmental stages, with a slightly higher expression in the P18 spinal cords (**Figure 15**), but at the mRNA level, NDEL1 shows very high specificity for the more mature spinal cord (**Figure 16**). This observation could be due to the existence of the nuclear distribution element 1 (NDEL1) gene, which is also expressed in early neuronal development. Since the two proteins have a high sequence similarity- they share approximately 60% amino-acid sequence identity (~80% sequence similarity) (176,177), this could be the reason why we observed only a modest difference at the protein level. Flotillin 1 (FLOT1) has previously been shown to be important for the early stages of neuronal development, it is highly expressed in the nervous system and its expression is significantly associated with development (178). Reelin (RELN) is an extracellular matrix glycoprotein that has an important role during embryonic development and adulthood. Reelin mRNA expression was investigated during brain development on embryonic, postnatal and adult mice. The expression of RELN increased during early and late embryonic stages followed by significantly more widespread expression at P0 than at prenatal stages (179). For both tested proteins, our results show higher expression in the more mature spinal cord, at the protein level for FLOT1 (**Figure 15**) and mRNA level for RELN (**Figure 16**). DCC netrin 1 receptor (DCC) has a critical role in axonal regeneration and synaptic formation. Our results show increased expression of DCC mRNA level at the early developmental stage, in the P5 spinal cords (**Figure 16**). This observation is consistent with the research done on the expression patterns of guidance receptors, among which they investigated DCC, throughout mouse embryogenesis. They showed that DCC expression was present at high levels in all regions of the developing CNS that were actively undergoing neurogenesis. However, with maturation, DCC expression was downregulated throughout the CNS (180). Another protein that we tested was p44/42 MAP kinase (Erk1/Erk2) protein which showed higher expression at the protein level in the P18 spinal cords (**Figure 15**), which was expected since the ERK 1/2 cascade is important for neuron differentiation and regulation of axon regeneration, however, the phosphorylated form showed higher expression in the P5 spinal cords (**Figure 15**), which was in accordance with the previous studies since ERK 1/2 phosphorylation is required for early neuronal differentiation and survival of embryonic stem cells (138,139).

Other molecules that are active during development and have been identified as promoters of regeneration include many extracellular molecules, such as axon guidance molecules including ephrins, semaphorins, Wnt glycoproteins (25), growth factors such as NGF and BDNF (26,27) or entire intracellular molecular pathways, for example, PI3K/Akt/mammalian target of rapamycin – mTOR (28). Growth factors are molecules that have the ability to stimulate cell growth, proliferation, and differentiation. Therefore, growth factors acting in the nervous system are of fundamental importance in regulating growth and maintaining the viability of neurons and neuronal stem cells. For instance, NGF is involved in regulating the growth, maintenance, proliferation and survival of certain neurons, especially embryonic sensory neurons. NGF, like other growth factors, has a positive effect on neuronal regeneration (181). Our MS analysis detected increased expression of NGF protein in the P5 spinal cords. BDNF is a molecule that promotes survival, growth, differentiation, migration and development of a variety of CNS neurons. It is mostly expressed in the hippocampus, cortex and basal part of the forebrain. A study showed that BDNF mRNA expression increases during postnatal development and maturation of the human prefrontal cortex, being relatively low during infancy and adolescence, peak during young adulthood, and maintain at a constant level throughout adulthood and aging. This increase in BDNF mRNA levels coincides with the maturation of the frontal cortex, both structurally and functionally (182). In line with this research, on our protein lists, the MS analysis detected the higher expression of BDNF in the more mature spinal cords. Another molecule detected by our MS analysis with only a slight increase in the P18 spinal cord is the ciliary neurotrophic factor (CNTF) which has potent effects on the development and maintenance of the nervous system and is expressed during phases of neurogenesis and differentiation (183). In addition, a group of scientists showed that after SCI, the level of CNTF mRNA in the spinal cord white matter increased, suggesting CNTF may have a role in the response to SCI (184). Although approaches and strategies employed to enhance regeneration in the mammalian CNS are showing promising results, full knowledge of these molecules and the way they interact to promote or prevent regeneration is far from complete.

### 5.1.3. Proteins related to neurodegenerative diseases

All neurodegenerative diseases and traumas of the central nervous system result in progressive degeneration, loss of function and death of nerve cells. Neurodegenerative diseases are incurable disorders, and they complicate and limit the functioning and quality of life in patients. That is why this area is gaining increasing attention in research laboratories around the world in which the properties of neuroregeneration are studied, as well as the relationship between neuroregeneration and various neurodegenerative diseases (185). Common characteristics in neurodegenerative diseases are alterations in adult neurogenesis.

Amyloid proteins, especially amyloid precursor protein (APP), became interesting in research studies due to their involvement in AD. Most of the work has focused on the role of APP in the pathogenesis of AD, however, it is important to know its physiological role during development which may be important for a better understanding of AD. Recent evidence suggests that APP has a key role in development as it regulates the generation of neurons, as well as in neurite outgrowth and guidance (186). Another study investigated the developmental expression of APP in mice and showed increased expression throughout fetal and postnatal development (187). Our results obtained on the intact spinal cords show increased expression during development for two amyloid proteins: amyloid beta precursor protein binding family B member 1 (APBB1) at the protein level (**Figure 15**) and amyloid protein-binding protein 1 (APPBP1) at the mRNA level (**Figure 16**). Presenilin (PSEN1) is also associated with AD and it is thought that PSEN1 mutations cause a loss of essential presenilin functions in the brain, which in turn triggers neurodegeneration and dementia in AD (137). PSEN1 is expressed during the early stages of differentiation in neural progenitors which is important for cortical development, and in post mitotic neurons (188). A group of scientists investigated the expression of PSEN1 and PSEN2 in human and murine tissue and showed that PSEN1 and PSEN2 mRNA are expressed widely in most human and mouse tissues, including the adult brain, but with PSEN1 mRNA being expressed at significantly higher levels in developing brains (189). Our results reveal a higher expression of PSEN1 at the mRNA level in the more mature spinal cords (**Figure 16**). Rab GTPases (Rabs) like Rab8a and Rab8b are linked to Parkinson's disease through disease-associated mutations or interactions with key Parkinson's disease-related proteins (133,134). On the other hand, it is believed that over-expressing Rab7 might be beneficial in Parkinson's disease since it regulates the trafficking of late

endosomes and autophagosomes (135). Studies have shown that Rab proteins have an important role during development *in vivo* since they are broadly expressed during embryogenesis (190). Knock out of Rab7 in mice is lethal, and in such mutants, embryogenesis is dramatically affected resulting in the death of developing embryos around embryonic day seven (191). Rab8a and Rab8b proteins are also essential during embryogenesis (190). In line with these observations, our results show increased expression of Rab7 at the protein and mRNA level (**Figures 15 and 16**) and increased expression of Rab8a at the mRNA level in P5 spinal cords (**Figure 14**). Rab8b shows increased expression at the mRNA level in the more mature, P18 spinal cords (**Figure 16**). This could be due to highly dynamic Rab8 expression and localization during development (190). A recent study showed that the huntingtin protein plays an important role in repairing damaged nerve cells (146), indicating it has a central role in nerve cell regeneration in their models. They reported that huntingtin helped to keep damaged nerve cells in the embryonic state, promoting, in that way, nerve cell regeneration. In fact, in mouse models which had huntingtin deleted from the spine, recovery from spinal cord injury was reduced by 60%, suggesting that huntingtin is very important for the repair of neurons after injury. Another study reported that striatal projection neurons require HTT for motor regulation, synaptic development, cell health, and survival (192). These were interesting and important findings because much is known about the role of huntingtin protein in disease, however, there is not much information about its physiological role. We tested two proteins linked to HD: HTT and HIP1. Both of them increased significantly between P5 and P18 at the protein (**Figure 15**) and mRNA level (**Figure 14**), which marks a period of active neuronal differentiation. Our findings were in accordance with a study that investigated the expression of huntingtin on embryonic, postnatal and adult mice to determine its potential influence on brain development. The results showed that huntingtin was detected early, at all stages of embryonic and postnatal brain development, and in the adult mouse brain. The expression of huntingtin increased significantly with the maturation of neurons in the postnatal period and was regulated developmentally (193). Proteins that are involved in neurodegeneration, are also involved in plastic processes, when in physiological conditions. For these reasons, the importance and understanding of the mechanisms of neurogenesis regulation are essential for the development of new therapeutic approaches for currently incurable neurodegenerative diseases.

The results of this study suggest that proteins known to have an important role in the pathophysiology of neurodegeneration in aged CNS, could also have an important function during



CNS development. The database generated in this study provided a solid basis for further comprehensive investigation of the functional relevance of the selected proteins in spinal cord development and regeneration.

## **5.2. Functional assays**

Primary dissociated neuronal cultures are essential to study and understand CNS development and regeneration. It is important to emphasize that such cultures are mostly prepared from the hippocampus or cortex of rodents, such as mice and rats, while primary neurons deriving from other mammalian species are used less (72,167). The opossum represents a unique opportunity to study mammalian CNS that has the ability to regenerate, and several studies have demonstrated the advantages and successful regeneration after *in vitro* injury of an intact opossum spinal cord maintained in culture (68,86–88). Recently, our group established long-term primary cortical neuronal cultures from neonatal opossum *Monodelphis domestica* (120). Before that, dissociated primary neuronal cultures from opossums have not been established. In this study, we successfully established protocols for opossum spinal cord primary cultures. Before this study, no scientific literature was available on the primary dissociated spinal cultures derived from opossums. Primary cultures derived from brain tissue such as the cortex and hippocampus are most commonly used, while there are significantly fewer studies on primary spinal cord cultures.

The protocol for the spinal cord tissue dissection and cell preparation was modified according to the previously established protocols for primary cultures of neonatal rat spinal cord done by Seybold and Abrahams (194). The first modification concerned the dissection protocol. When dissecting the nerve tissue, it is important that the tissue is immersed into a solution that ensures cell survival as much as possible during isolation. We tested several different dissection solutions, and the best result was achieved with an oxygenated ice-cold Krebs solution with the addition of glucose, antibiotics and antimycotics. Next, we performed two enzymatic digestions, the first one with trypsin and the second one with collagenase type I to successfully degrade the extracellular matrix of the spinal cord, since it contains more collagen than the cortex. Finally, since the tissue from older pups (P16-18) is much more difficult to dissociate due to higher connective tissue and extracellular matrix, incubation with 5% (w/v) BSA, so-called BSA cushioning, was introduced, which largely removed the remains of dead cells and tissues after dissociation. The primary cultures derived from the opossum spinal cord, as well as the cortex, were incubated at 32°C since

opossums have a lower body temperature than other mammals (195). The good survival of these cultures at 32°C was confirmed by Puzzolo and Mallamaci (168).

Primary cultures were prepared from opossums of different ages, P5 and P18, at two different stages during culture, DIV 1 and DIV10. At DIV1, we observed cell survival and neurite outgrowth (**Figure 27, DIV1**). At DIV10 we observed neurons, with developed axons and dendrites, indicating neuronal density increased and neuronal differentiation occurred *in vitro* (**Figure 27, DIV10**). The cultures deriving from P5 had a higher yield of cells in comparison with cultures from P18. Since the spinal cords of older animals were more difficult to dissociate, we used a 5 times higher trypsin concentration along with a longer incubation time and additional trituration steps in order to dissociate the cells well. The decrease in the number of neuronal cells could be due to the presence of non-neuronal cells in the cultures, such as fibroblasts, that are more abundant in P18 cultures. This could be because of the partially removed meninges. The meninges are more adherent to the tissue during development, thus removing them during dissection is a major challenge (72). Also, since neurogenesis is followed by gliogenesis (168), in the later stages of development there is a correlation with a higher proportion of glial cells. Another explanation for the lower proportion of neurons may be their lower viability after the dissociation, as it was shown in hippocampal or cortical primary cultures from postnatal mice (72). In general, these cultures have a smaller yield of neurons, in comparison with cortical primary cell cultures (120). This may be for two reasons: firstly, the stronger enzymatic and mechanical treatment which is required for effective dissociation of the spinal cord tissue could influence the survival of the cells (196). Secondly, it is harder to remove the meninges from the spinal cord tissue, especially in older opossums when the meninges are more adherent and it is easy to lose a part of the tissue during the removal, which can also result in cultures with a smaller yield of neurons. Finally, spinal cord neurons could have a lower survival rate in culture compared to cortical neurons. We confirmed that spinal cord cultures are more challenging and more difficult to maintain than cortical, especially the spinal cultures derived from older opossum age (P16-P18), but that was in accordance with *in vivo* observations (12,79,84,85).

After the establishment of primary neuronal spinal cell cultures, we could perform neurite outgrowth tests and neuroregeneration scratch assays, in cell cultures of both ages. With these assays, we can investigate the mechanisms that inhibit neurite outgrowth and molecules that enable

the pro-regenerative state, and also investigate the regeneration of differentiated neurons of the postnatal opossum for a better understanding of the molecular mechanisms involved in CNS regeneration. Although the new scratch assay allows easy and fast measurement of neurite outgrowth after mechanical injury, the number and viability of primary spinal cord neurons were extremely small in the cultures derived from older opossum ages (**Figure 31, bottom row**). These cultures were not suitable for performing the scratch assay, compared to cultures deriving from P5, which have a higher yield of cells (**Figure 31, upper row**), and in comparison with cortical cultures, which were much more convenient to perform this type of assay and investigate the regenerative ability of primary neurons (Petrović et al., unpublished data).

### 5.2.1. PGL-137 inhibitor

As mentioned before, to test the procedure and newly established primary spinal neuronal cultures as a new *in vitro* platform to study development and regeneration and to perform functional assays, as the example, we have chosen the pharmacological polyglutamine aggregation inhibitor, PGL-137. PGL-137 is a benzothiazole compound that crosses the cell membrane and binds within the cell to secondary protein structures ( $\beta$ -folded plates), which are rich in polyglutamine. Huntington's disease is caused by dominant polyglutamine expansion within the N terminus of the huntingtin protein. Benzothiazoles were identified as potential polyglutamine aggregation inhibitors of HD. They are highly interesting molecules and very promising candidates for future drug developments (197). They have also been previously shown to be effective in treating neurodegenerative disorders such as amyotrophic lateral sclerosis (ALS) (198). For example, riluzole is a benzothiazole derivative that extends the survival of neurons in ALS patients (199,200). It was also tested for therapy of HD patients, where the treatment had positive effects on choreatic hyperkinesia (201). However, its mechanism of action is mostly unknown. A study has shown that benzothiazole derivatives are potential inhibitors of HD exon 1 aggregation *in vitro* and in cell culture model systems of HD (197). However, the mechanism of action of these molecules is unclear, especially on a molecular level. Because of that, detailed *in vitro* drug-protein binding studies are necessary and further experiments are needed to address these questions in more detail (197).

The use of the PGL-137 inhibitor on both P5 and P18 primary spinal cell cultures led to a significant decrease in the number of neurons and resulted in impaired neuronal survival,

proliferation and neurite outgrowth (**Figure 30**), which was similarly confirmed by the results obtained on the intact spinal cord tissue (**Figures 19-26**). The results obtained on the intact spinal cord and primary spinal cell culture suggest a possible role of PGL-137 inhibitor in various processes relating to neuroregeneration, including cell viability, proliferation and neuronal network formation, however, further experiments are needed to confirm these observations.

Even though the PGL-137 inhibitor is not supposed to directly inhibit HTT, we checked if it can indirectly, in any way reflect the gene expression or protein level on the intact spinal cord (**Figures 17 and 18**) and primary spinal cell cultures (**Figures 28 and 29**). Although in both preparations, the expression of HTT and HIP1 protein was decreased at the protein and mRNA level after the treatment with the inhibitor, we cannot conclude that this is because of its effect on HTT. While PGL-137 has been demonstrated to act as an inhibitor of HTT aggregation in disease, there isn't any data suggesting that it also inhibits HTT function under normal circumstances. As HTT is not known to be an enzyme, it is difficult to say in what way it can be inhibited. Therefore, we cannot conclude that our results, showing that PGL-137 affects various processes relating to neuroregeneration, are because of the effect of the inhibitor on HTT, and therefore that HTT affects neuroregeneration.

The opossum is a specific animal and nothing can be directly inferred for humans, although its genome resembles the human genome more than from mice or rats. *M. domestica* has a high degree of protein sequence homology with other mammalian species, and especially with human proteins (97), which should allow and provoke scientists for future research using opossums as a mammalian model for studying development, regeneration, and comparative evolutionary studies. There is a need to use more mammalian species in order to identify differences among mammals and to avoid making mistakes when transferring this knowledge to humans (202,203). Furthermore, all proteins that change when regeneration stops being possible are not necessarily related to regeneration and therefore further research is needed, for which we have only established a procedure and tested it with PGL-137 inhibitor, which is not specifically proven to be related to regeneration or any other process.

Future studies will be based on using opossum primary neuronal cultures for genetic manipulations of candidate molecule activity, which may have an important role in promoting or preventing regeneration. In these cultures, various drugs, including pharmacological inhibitors,

can be tested and genes can be overexpressed or silenced to better understand the molecular mechanisms of CNS regeneration. Research should definitely be expanded. In addition to pharmacological studies with specific inhibitors, genetic knockout studies should be carried out to study the influence of various interesting genes and their protein products on regeneration, implementing also techniques such as silencing or CRISPR/Cas9 technique. The latter was applied on opossums in only one study available in the literature (204) being the first report of successful demonstration of gene knockout in a marsupial. This recent study provides a fundamental discovery of the opossum, *M. domestica*, as a unique and available genetic model system for investigating comparative *in vivo* studies of gene function in mammals. These new methodologies will allow the acceleration of *in vivo* gene function studies in the marsupials that lag significantly behind those of eutherian mammals.

## 6. CONCLUSIONS

- We tested and developed protocols for mass spectrometry analysis of opossum *M. domestica* spinal cord tissue samples.
- For the first time, we identified proteins differentially present in developing, non-injured mammalian spinal cord tissue with different regenerative capacities. The database generated in this study will provide a solid basis for further comprehensive investigation of the functional relevance of the selected proteins in spinal cord development and regeneration.
- We identified a total number of 4735 proteins between the two developmental stages P5 and P18, among which 1215 proteins (25.66%) were overlapped between both biological samples, with different intensities. 918 identified proteins were unique for P5 spinal cords, while 714 were unique for P18 spinal cords. The identified proteins have a role in cellular processes such as cell growth, proliferation, differentiation, transcription, cell signaling, cytoskeleton and extracellular matrix organization, are known axon guidance molecules, neurotrophic factors or belong to particular intracellular molecular pathways like mTOR and MAPK signaling pathway.
- The most interesting result of this study is the prominent presence of the proteins related to neurodegenerative diseases (amyloid proteins and presenilin related to Alzheimer's disease, Rab GTPases linked to Parkinson's disease, huntingtin and huntingtin interacting protein 1 related to Huntington's disease) among the proteins that are differently expressed in opossum spinal cord tissues that have or do not have the neuroregenerative potential.
- We demonstrated that the results of proteomic studies are highly informative, indicative and reliable since we found large overlapping of the mass spectrometry analysis results with the other techniques that can measure or analyze the protein quantity and localization (Wester blotting, immunohistology). Moreover, the analysis of the mRNA levels of the

selected candidates were largely in accordance with the mass spectrometry studies, with some explainable exceptions.

- By confronting the results of comparative transcriptomics with proteomics, it was possible to identify molecules of interest and to substantially narrow the number of candidates for functional assays, using the PANTHER classification system.
- For the first time, we established spinal cord primary neuronal cultures from neonatal opossums of different ages and with different regenerative capacities, that represent a novel mammalian *in vitro* platform especially useful to study CNS development and regeneration.
- In the opossum primary neuronal cultures, various drugs, including pharmacological inhibitors can be tested, and genes can be overexpressed or silenced, allowing genetic manipulations of the candidate molecules, which may have an important role in promoting or preventing regeneration. It will be of great interest to further analyze the spinal cultures derived from P5 opossums and compare them with the P18 cultures or with the cortical cultures, to understand the differences in their regenerative and differentiation potentials.
- We established the procedure to test the effect of the pharmacological compounds on neuroregeneration, cell viability, proliferation and neuronal network formation on opossum primary dissected spinal neuronal cultures and on opossum intact spinal cord maintained *in vitro*.

## 7. LITERATURE

1. Tanaka EM, Ferretti P. Considering the evolution of regeneration in the central nervous system. *Nat Rev Neurosci*. 2009 Oct;10(10):713–23.
2. Bramlett HM, Dietrich WD. Progressive damage after brain and spinal cord injury: pathomechanisms and treatment strategies. *Prog Brain Res*. 2007;161:125–41.
3. Diaz Quiroz JF, Echeverri K. Spinal cord regeneration: where fish, frogs and salamanders lead the way, can we follow? *Biochem J*. 2013 May 1;451(3):353–64.
4. Brockes JP, Kumar A. Comparative aspects of animal regeneration. *Annu Rev Cell Dev Biol*. 2008;24:525–49.
5. Carlson ME, Conboy IM. Loss of stem cell regenerative capacity within aged niches. *Aging Cell*. 2007 Jun;6(3):371–82.
6. Tanaka EM, Reddien PW. The Cellular Basis for Animal Regeneration. *Developmental Cell*. 2011 Jul 19;21(1):172–85.
7. Godwin JW, Rosenthal N. Scar-free wound healing and regeneration in amphibians: immunological influences on regenerative success. *Differentiation*. 2014 Feb;87(1–2):66–75.
8. Amaya E, Kroll KL. A method for generating transgenic frog embryos. *Methods Mol Biol*. 1999;97:393–414.
9. Harland RM, Grainger RM. *Xenopus* research: metamorphosed by genetics and genomics. *Trends Genet*. 2011 Dec;27(12):507–15.
10. Yokoyama H, Maruoka T, Ochi H, Aruga A, Ohgo S, Ogino H, et al. Different requirement for Wnt/ $\beta$ -catenin signaling in limb regeneration of larval and adult *Xenopus*. *PLoS One*. 2011;6(7):e21721.
11. Becker CG, Diez Del Corral R. Neural development and regeneration: it's all in your spinal cord. *Development*. 2015 Mar 1;142(5):811–6.
12. Nicholls J, Saunders N. Regeneration of immature mammalian spinal cord after injury. *Trends Neurosci*. 1996 Jun;19(6):229–34.
13. Mladinic M, Muller KJ, Nicholls JG. Central nervous system regeneration: from leech to opossum. *The Journal of Physiology*. 2009;587(12):2775–82.
14. Kalil K, Reh T. Regrowth of severed axons in the neonatal central nervous system: establishment of normal connections. *Science*. 1979 Sep 14;205(4411):1158–61.
15. Saunders NR, Balkwill P, Knott G, Habgood MD, Møllgård K, Treherne JM, et al. Growth of axons through a lesion in the intact CNS of fetal rat maintained in long-term culture. *Proceedings of the Royal Society of London Series B: Biological Sciences*. 1992 Dec 22;250(1329):171–80.



16. Kawaguchi S, Iseda T, Nishio T. Effects of an embryonic repair graft on recovery from spinal cord injury. In: Progress in Brain Research [Internet]. Elsevier; 2004 [cited 2022 Feb 17]. p. 155–62. (Brain Mechanisms for the Integration of Posture and Movement; vol. 143). Available from: <https://www.sciencedirect.com/science/article/pii/S007961230343015X>
17. Peterson ER, Crain SM. Preferential growth of neurites from isolated fetal mouse dorsal root ganglia in relation to specific regions of co-cultured spinal cord explants. *Developmental Brain Research*. 1981 Oct 1;2(3):363–82.
18. Vanselow J, Grabczyk E, Ping J, Baetscher M, Teng S, Fishman M. GAP-43 transgenic mice: dispersed genomic sequences confer a GAP-43- like expression pattern during development and regeneration. *J Neurosci*. 1994 Feb 1;14(2):499–510.
19. Saunders NR, Kitchener P, Knott GW, Nicholls JG, Potter A, Smith TJ. Development of walking, swimming and neuronal connections after complete spinal cord transection in the neonatal opossum, *Monodelphis domestica*. *J Neurosci*. 1998 Jan 1;18(1):339–55.
20. Malatesta P, Malatesta P. Radial glia and neural stem cells. *Cell Tissue Res*. 2008;
21. Rueger MA, Schroeter M. In vivo imaging of endogenous neural stem cells in the adult brain. *World J Stem Cells*. 2015 Jan 26;7(1):75–83.
22. Mu Y, Gage FH. Adult hippocampal neurogenesis and its role in Alzheimer’s disease. *Mol Neurodegener*. 2011 Dec 22;6:85.
23. Ribotta MG, Menet V, Privat A. Glial scar and axonal regeneration in the CNS: lessons from GFAP and vimentin transgenic mice. *Acta Neurochir Suppl*. 2004;89:87–92.
24. Baldwin KT, Giger RJ. Insights into the physiological role of CNS regeneration inhibitors. *Frontiers in Molecular Neuroscience* [Internet]. 2015 [cited 2022 Feb 17];8. Available from: <https://www.frontiersin.org/article/10.3389/fnmol.2015.00023>
25. Hollis ER. Axon Guidance Molecules and Neural Circuit Remodeling After Spinal Cord Injury. *Neurotherapeutics*. 2016 Apr;13(2):360–9.
26. Xu XM, Guénard V, Kleitman N, Aebischer P, Bunge MB. A Combination of BDNF and NT-3 Promotes Supraspinal Axonal Regeneration into Schwann Cell Grafts in Adult Rat Thoracic Spinal Cord. *Experimental Neurology*. 1995 Aug 1;134(2):261–72.
27. Nakahara Y, Gage FH, Tuszynski MH. Grafts of fibroblasts genetically modified to secrete NGF, BDNF, NT-3, or basic fgf elicit differential responses in the adult spinal cord. *Cell Transplantation*. 1996 Mar 1;5(2):191–204.
28. Berry M, Ahmed Z, Morgan-Warren P, Fulton D, Logan A. Prospects for mTOR-mediated functional repair after central nervous system trauma. *Neurobiology of Disease*. 2016 Jan;85:99–110.
29. Yoon C, Tuszynski MH. Frontiers of spinal cord and spine repair: experimental approaches for repair of spinal cord injury. *Adv Exp Med Biol*. 2012;760:1–15.

30. Silva NA, Sousa N, Reis RL, Salgado AJ. From basics to clinical: a comprehensive review on spinal cord injury. *Prog Neurobiol.* 2014 Mar;114:25–57.
31. Bajwa NM, Kesavan C, Mohan S. Long-term Consequences of Traumatic Brain Injury in Bone Metabolism. *Frontiers in Neurology* [Internet]. 2018 [cited 2022 Feb 17];9. Available from: <https://www.frontiersin.org/article/10.3389/fneur.2018.00115>
32. Borgens RB, Liu-Snyder P. Understanding secondary injury. *Q Rev Biol.* 2012 Jun;87(2):89–127.
33. Liu. Role and prospects of regenerative biomaterials in the repair of spinal cord injury [Internet]. [cited 2022 Feb 17]. Available from: <https://www.nrronline.org/article.asp?issn=1673-5374;year=2019;volume=14;issue=8;spage=1352;epage=1363;aulast=Liu>
34. Dumont RJ, Okonkwo DO, Verma S, Hurlbert RJ, Boulos PT, Ellegala DB, et al. Acute spinal cord injury, part I: pathophysiologic mechanisms. *Clin Neuropharmacol.* 2001 Oct;24(5):254–64.
35. Pereira IM, Marote A, Salgado AJ, Silva NA. Filling the Gap: Neural Stem Cells as A Promising Therapy for Spinal Cord Injury. *Pharmaceuticals (Basel).* 2019 Apr 29;12(2):E65.
36. Oyibo CA. Secondary injury mechanisms in traumatic spinal cord injury: a nugget of this multiply cascade. *Acta Neurobiol Exp (Wars).* 2011;71(2):281–99.
37. Beyer F, Samper Agrelo I, Küry P. Do Neural Stem Cells Have a Choice? Heterogenic Outcome of Cell Fate Acquisition in Different Injury Models. *Int J Mol Sci.* 2019 Jan 21;20(2):E455.
38. Ahuja CS, Nori S, Tetreault L, Wilson J, Kwon B, Harrop J, et al. Traumatic Spinal Cord Injury- Repair and Regeneration. *Neurosurgery.* 2017 Mar 1;80(3S):S9–22.
39. Choong C, Rao MS. Human embryonic stem cells. *Neurosurg Clin N Am.* 2007 Jan;18(1):1–14, vii.
40. Takahashi K, Yamanaka S. Induction of pluripotent stem cells from mouse embryonic and adult fibroblast cultures by defined factors. *Cell.* 2006 Aug 25;126(4):663–76.
41. Csobonyeiova M, Polak S, Zamborsky R, Danisovic L. Recent Progress in the Regeneration of Spinal Cord Injuries by Induced Pluripotent Stem Cells. *Int J Mol Sci.* 2019 Aug 6;20(15):3838.
42. Hofer HR, Tuan RS. Secreted trophic factors of mesenchymal stem cells support neurovascular and musculoskeletal therapies. *Stem Cell Res Ther.* 2016 Sep 9;7(1):131.
43. Robinson J, Lu P. Optimization of trophic support for neural stem cell grafts in sites of spinal cord injury. *Exp Neurol.* 2017 May;291:87–97.
44. Nagata S, Fukunaga R. Granulocyte colony-stimulating factor and its receptor. *Prog Growth Factor Res.* 1991;3(2):131–41.
45. Roberts AG, Johnston EV, Shieh J-H, Sondey JP, Hendrickson RC, Moore MAS, et al. Fully Synthetic Granulocyte Colony-Stimulating Factor Enabled by Isonitrile-Mediated Coupling of Large, Side-Chain-Unprotected Peptides. *J Am Chem Soc.* 2015 Oct 14;137(40):13167–75.

46. Nishio Y, Koda M, Kamada T, Someya Y, Kadota R, Mannoji C, et al. Granulocyte colony-stimulating factor attenuates neuronal death and promotes functional recovery after spinal cord injury in mice. *J Neuropathol Exp Neurol*. 2007 Aug;66(8):724–31.
47. Song S, Kong X, Acosta S, Sava V, Borlongan C, Sanchez-Ramos J. Granulocyte-colony stimulating factor promotes brain repair following traumatic brain injury by recruitment of microglia and increasing neurotrophic factor expression. *Restor Neurol Neurosci*. 2016 Feb 24;34(3):415–31.
48. Kamiya K, Koda M, Furuya T, Kato K, Takahashi H, Sakuma T, et al. Neuroprotective therapy with granulocyte colony-stimulating factor in acute spinal cord injury: a comparison with high-dose methylprednisolone as a historical control. *Eur Spine J*. 2015 May;24(5):963–7.
49. Lima R, Monteiro S, Lopes JP, Barradas P, Vasconcelos NL, Gomes ED, et al. Systemic Interleukin-4 Administration after Spinal Cord Injury Modulates Inflammation and Promotes Neuroprotection. *Pharmaceuticals (Basel)*. 2017 Oct 24;10(4):E83.
50. Xi A, Xu Z, Liu F, Xu Y. Neuroprotective effects of monosialotetrahexosylganglioside. *Neural Regen Res*. 2015 Aug;10(8):1343–4.
51. Lingam I, Robertson NJ. Magnesium as a Neuroprotective Agent: A Review of Its Use in the Fetus, Term Infant with Neonatal Encephalopathy, and the Adult Stroke Patient. *Dev Neurosci*. 2018;40(1):1–12.
52. Alzheimer C, Werner S. Fibroblast Growth Factors and Neuroprotection. In: Alzheimer C, editor. *Molecular and Cellular Biology of Neuroprotection in the CNS* [Internet]. Boston, MA: Springer US; 2002 [cited 2022 Feb 17]. p. 335–51. (Advances in Experimental Medicine and Biology). Available from: [https://doi.org/10.1007/978-1-4615-0123-7\\_12](https://doi.org/10.1007/978-1-4615-0123-7_12)
53. Doeppner TR, Kaltwasser B, ElAli A, Zechariah A, Hermann DM, Bähr M. Acute hepatocyte growth factor treatment induces long-term neuroprotection and stroke recovery via mechanisms involving neural precursor cell proliferation and differentiation. *J Cereb Blood Flow Metab*. 2011 May;31(5):1251–62.
54. Rooney GE, Vaishya S, Ameenuddin S, Currier BL, Schiefer TK, Knight A, et al. Rigid Fixation of the Spinal Column Improves Scaffold Alignment and Prevents Scoliosis in the Transected Rat Spinal Cord. *Spine (Phila Pa 1976)*. 2008 Nov 15;33(24):E914–9.
55. Wang J, Zheng J, Zheng Q, Wu Y, Wu B, Huang S, et al. FGL-functionalized self-assembling nanofiber hydrogel as a scaffold for spinal cord-derived neural stem cells. *Mater Sci Eng C Mater Biol Appl*. 2015 Jan;46:140–7.
56. Kubinová S, Syková E. Nanotechnologies in regenerative medicine. *Minim Invasive Ther Allied Technol*. 2010 Jun;19(3):144–56.
57. Libro R, Bramanti P, Mazzon E. The combined strategy of mesenchymal stem cells and tissue-engineered scaffolds for spinal cord injury regeneration. *Exp Ther Med*. 2017 Oct;14(4):3355–68.

58. Guan S, Zhang X-L, Lin X-M, Liu T-Q, Ma X-H, Cui Z-F. Chitosan/gelatin porous scaffolds containing hyaluronic acid and heparan sulfate for neural tissue engineering. *J Biomater Sci Polym Ed*. 2013;24(8):999–1014.
59. Murphy AR, Laslett A, O'Brien CM, Cameron NR. Scaffolds for 3D in vitro culture of neural lineage cells. *Acta Biomater*. 2017 May;54:1–20.
60. Zhang G, Khan AA, Wu H, Chen L, Gu Y, Gu N. The Application of Nanomaterials in Stem Cell Therapy for Some Neurological Diseases. *Curr Drug Targets*. 2018 Feb 8;19(3):279–98.
61. Siddiqi KS, Husen A, Sohrab SS, Yassin MO. Recent Status of Nanomaterial Fabrication and Their Potential Applications in Neurological Disease Management. *Nanoscale Res Lett*. 2018 Aug 10;13:231.
62. Subramanian A, Krishnan UM, Sethuraman S. Development of biomaterial scaffold for nerve tissue engineering: Biomaterial mediated neural regeneration. *J Biomed Sci*. 2009 Nov 25;16:108.
63. Alizadeh A, Dyck SM, Karimi-Abdolrezaee S. Traumatic Spinal Cord Injury: An Overview of Pathophysiology, Models and Acute Injury Mechanisms. *Front Neurol*. 2019 Mar 22;10:282.
64. Nardone R, Florea C, Höller Y, Brigo F, Versace V, Lochner P, et al. Rodent, large animal and non-human primate models of spinal cord injury. *Zoology (Jena)*. 2017 Aug;123:101–14.
65. Kjell J, Olson L. Rat models of spinal cord injury: from pathology to potential therapies. *Dis Model Mech*. 2016 Oct 1;9(10):1125–37.
66. Kwon BK, Streijger F, Hill CE, Anderson AJ, Bacon M, Beattie MS, et al. Large animal and primate models of spinal cord injury for the testing of novel therapies. *Exp Neurol*. 2015 Jul;269:154–68.
67. Mladinic M, Nistri A, Taccola G. Acute Spinal Cord Injury In Vitro: Insight into Basic Mechanisms. In: Aldskogius H, editor. *Animal Models of Spinal Cord Repair* [Internet]. Totowa, NJ: Humana Press; 2013 [cited 2022 Feb 17]. p. 39–62. (Neuromethods). Available from: [https://doi.org/10.1007/978-1-62703-197-4\\_3](https://doi.org/10.1007/978-1-62703-197-4_3)
68. Treherne JM, Woodward SK, Varga ZM, Ritchie JM, Nicholls JG. Restoration of conduction and growth of axons through injured spinal cord of neonatal opossum in culture. *Proc Natl Acad Sci U S A*. 1992 Jan 1;89(1):431–4.
69. Varga ZM, Bandtlow CE, Erulkar SD, Schwab ME, Nicholls JG. The critical period for repair of CNS of neonatal opossum (*Monodelphis domestica*) in culture: correlation with development of glial cells, myelin and growth-inhibitory molecules. *Eur J Neurosci*. 1995 Oct 1;7(10):2119–29.
70. Varga ZM, Schwab ME, Nicholls JG. Myelin-associated neurite growth-inhibitory proteins and suppression of regeneration of immature mammalian spinal cord in culture. *Proc Natl Acad Sci U S A*. 1995 Nov 21;92(24):10959–63.
71. Mladinic M. Changes in cyclic AMP levels in the developing opossum spinal cord at the time when regeneration stops being possible. *Cell Mol Neurobiol*. 2007 Nov;27(7):883–8.

72. Beaudoin GMJ, Lee S-H, Singh D, Yuan Y, Ng Y-G, Reichardt LF, et al. Culturing pyramidal neurons from the early postnatal mouse hippocampus and cortex. *Nat Protoc.* 2012 Sep;7(9):1741–54.
73. Al-Ali H, Beckerman SR, Bixby JL, Lemmon VP. In vitro models of axon regeneration. *Exp Neurol.* 2017 Jan;287(Pt 3):423–34.
74. Humpel C. Organotypic brain slice cultures: A review. *Neuroscience.* 2015 Oct 1;305:86–98.
75. Cáceres A, Ye B, Dotti CG. Neuronal polarity: demarcation, growth and commitment. *Curr Opin Cell Biol.* 2012 Aug;24(4):547–53.
76. Kaech S, Huang C-F, Banker G. General considerations for live imaging of developing hippocampal neurons in culture. *Cold Spring Harb Protoc.* 2012 Mar 1;2012(3):312–8.
77. VandeBerg JL, Robinson ES. The Laboratory Opossum ( *Monodelphis domestica* ) in Laboratory Research. *ILAR Journal.* 1997 Jan 1;38(1):4–12.
78. Tyndale-Biscoe CH, Janssens PA. Introduction. In: Tyndale-Biscoe CH, Janssens PA, editors. *The Developing Marsupial: Models for Biomedical Research* [Internet]. Berlin, Heidelberg: Springer; 1988 [cited 2022 Feb 17]. p. 1–7. Available from: [https://doi.org/10.1007/978-3-642-88402-3\\_1](https://doi.org/10.1007/978-3-642-88402-3_1)
79. Saunders N, Adam E, Reader M, Møllgård K. *Monodelphis domestica* (grey short-tailed opossum): an accessible model for studies of early neocortical development. *AnatEmbryol(Berl).* 1989 Aug 1;180.
80. Nicholls JG, Stewart RR, Erulkar SD, Saunders NR. Reflexes, fictive respiration and cell division in the brain and spinal cord of the newborn opossum, *Monodelphis domestica*, isolated and maintained in vitro. *J Exp Biol.* 1990 Sep;152:1–15.
81. Wintzer M, Mladinic M, Lazarevic D, Casseler C, Cattaneo A, Nicholls J. Strategies for identifying genes that play a role in spinal cord regeneration. *J Anat.* 2004 Jan;204(1):3–11.
82. Mladinic M, Wintzer M, Bel ED, Casseler C, Lazarevic D, Crovella S, et al. Differential Expression of Genes at Stages When Regeneration Can and Cannot Occur after Injury to Immature Mammalian Spinal Cord. *Cell Mol Neurobiol.* 2005 Apr;25(2):407–26.
83. Mladinic M, Lefèvre C, Del Bel E, Nicholls J, Digby M. Developmental changes of gene expression after spinal cord injury in neonatal opossums. *Brain Research.* 2010 Dec;1363:20–39.
84. Saunders NR, Deal A, Knott GW, Varga ZM, Nicholls JG. Repair and Recovery Following Spinal Cord Injury in a Neonatal Marsupial (*monodelphis Domestica*). *Clinical and Experimental Pharmacology and Physiology.* 1995;22(8):518–26.
85. Wheaton BJ, Callaway JK, Ek CJ, Dziegielewska KM, Saunders NR. Spontaneous Development of Full Weight-Supported Stepping after Complete Spinal Cord Transection in the Neonatal Opossum, *Monodelphis domestica*. *PLOS ONE.* 2011 Nov 2;6(11):e26826.

86. Woodward SK, Treherne JM, Knott GW, Fernandez J, Varga ZM, Nicholls JG. Development of connections by axons growing through injured spinal cord of neonatal opossum in culture. *J Exp Biol.* 1993 Mar;176:77–88.
87. Varga ZM, Fernandez J, Blackshaw S, Martin AR, Muller KJ, Adams WB, et al. Neurite outgrowth through lesions of neonatal opossum spinal cord in culture. *J Comp Neurol.* 1996 Mar 18;366(4):600–12.
88. Lepre M, Fernández J, Nicholls JG. Re-establishment of direct synaptic connections between sensory axons and motoneurons after lesions of neonatal opossum CNS (*Monodelphis domestica*) in culture. *Eur J Neurosci.* 1998 Aug;10(8):2500–10.
89. SMITH KK. Early development of the neural plate, neural crest and facial region of marsupials. *J Anat.* 2001;199(Pt 1-2):121–31.
90. Cardoso-Moreira M, Halbert J, Valloton D, Velten B, Chen C, Shao Y, et al. Gene expression across mammalian organ development. *Nature.* 2019 Jul;571(7766):505–9.
91. Hansen VL, Miller RD. On the prenatal initiation of T cell development in the opossum *Monodelphis domestica*. *J Anat.* 2017 Apr;230(4):596–600.
92. Sakaguchi DS, Hoffelen SJ van, Theusch E, Parker E, Orasky J, Harper MM, et al. Transplantation of Neural Progenitor Cells into the Developing Retina of the Brazilian Opossum: An in vivo System for Studying Stem/Progenitor Cell Plasticity. *DNE.* 2004;26(5–6):336–45.
93. Kumar S, Hedges SB. A molecular timescale for vertebrate evolution. *Nature.* 1998 Apr;392(6679):917–20.
94. Goodstadt L, Heger A, Webber C, Ponting CP. An analysis of the gene complement of a marsupial, *Monodelphis domestica*: Evolution of lineage-specific genes and giant chromosomes. *Genome Res.* 2007 Jul;17(7):969–81.
95. Dooley JC, Franca JG, Seelke AMH, Cooke DF, Krubitzer LA. A connection to the past: *Monodelphis domestica* provides insight into the organization and connectivity of the brains of early mammals. *J Comp Neurol.* 2013 Dec 1;521(17):3877–97.
96. Carlisle A, Selwood L, Hinds LA, Saunders N, Habgood M, Mardon K, et al. Testing hypotheses of developmental constraints on mammalian brain partition evolution, using marsupials. *Sci Rep.* 2017 Jun 26;7(1):4241.
97. Mikkelsen TS, Wakefield MJ, Aken B, Amemiya CT, Chang JL, Duke S, et al. Genome of the marsupial *Monodelphis domestica* reveals innovation in non-coding sequences. *Nature.* 2007 May 10;447(7141):167–77.
98. He Q, Man L, Ji Y, Zhang S, Jiang M, Ding F, et al. Comparative proteomic analysis of differentially expressed proteins between peripheral sensory and motor nerves. *J Proteome Res.* 2012 Jun 1;11(6):3077–89.

99. Ding Q, Wu Z, Guo Y, Zhao C, Jia Y, Kong F, et al. Proteome analysis of up-regulated proteins in the rat spinal cord induced by transection injury. *Proteomics*. 2006 Jan;6(2):505–18.
100. Noor NM, Steer DL, Wheaton BJ, Ek CJ, Truettner JS, Dietrich WD, et al. Age-Dependent Changes in the Proteome Following Complete Spinal Cord Transection in a Postnatal South American Opossum (*Monodelphis domestica*). *PLOS ONE*. 2011 Nov 16;6(11):e27465.
101. Saunders NR, Noor NM, Dziegielewska KM, Wheaton BJ, Liddelow SA, Steer DL, et al. Age-Dependent Transcriptome and Proteome Following Transection of Neonatal Spinal Cord of *Monodelphis domestica* (South American Grey Short-Tailed Opossum). *PLOS ONE*. 2014 Jun 10;9(6):e99080.
102. Wheaton BJ, Sena J, Sundararajan A, Umale P, Schilkey F, Miller RD. Identification of regenerative processes in neonatal spinal cord injury in the opossum (*Monodelphis domestica*): A transcriptomic study. *J Comp Neurol*. 2021 Apr 1;529(5):969–86.
103. Zuccato C, Ciammola A, Rigamonti D, Leavitt BR, Goffredo D, Conti L, et al. Loss of huntingtin-mediated BDNF gene transcription in Huntington's disease. *Science*. 2001 Jul 20;293(5529):493–8.
104. Reiner A, Dragatsis I, Zeitlin S, Goldowitz D. Wild-type huntingtin plays a role in brain development and neuronal survival. *Mol Neurobiol*. 2003 Dec;28(3):259–76.
105. Waldbau B, Shetty AK. Behavior of neural stem cells in the Alzheimer brain. *Cell Mol Life Sci*. 2008 Aug;65(15):2372–84.
106. Bevilacqua LRM, Kerr DS, Medina JH, Izquierdo I, Cammarota M. Inhibition of hippocampal Jun N-terminal kinase enhances short-term memory but blocks long-term memory formation and retrieval of an inhibitory avoidance task. *Eur J Neurosci*. 2003 Feb;17(4):897–902.
107. Brecht S, Kirchhof R, Chromik A, Willesen M, Nicolaus T, Raivich G, et al. Specific pathophysiological functions of JNK isoforms in the brain. *Eur J Neurosci*. 2005 Jan;21(2):363–77.
108. Kuan CY, Yang DD, Samanta Roy DR, Davis RJ, Rakic P, Flavell RA. The Jnk1 and Jnk2 protein kinases are required for regional specific apoptosis during early brain development. *Neuron*. 1999 Apr;22(4):667–76.
109. Waetzig V, Zhao Y, Herdegen T. The bright side of JNKs-Multitalented mediators in neuronal sprouting, brain development and nerve fiber regeneration. *Prog Neurobiol*. 2006 Oct;80(2):84–97.
110. Eminel S, Roemer L, Waetzig V, Herdegen T. c-Jun N-terminal kinases trigger both degeneration and neurite outgrowth in primary hippocampal and cortical neurons. *J Neurochem*. 2008 Feb;104(4):957–69.
111. Yarza R, Vela S, Solas M, Ramirez MJ. c-Jun N-terminal Kinase (JNK) Signaling as a Therapeutic Target for Alzheimer's Disease. *Front Pharmacol*. 2016 Jan 12;6:321.

112. Winner B, Winkler J. Adult neurogenesis in neurodegenerative diseases. *Cold Spring Harb Perspect Biol.* 2015 Apr 1;7(4):a021287.
113. Höglinger GU, Rizk P, Muriel MP, Duyckaerts C, Oertel WH, Caille I, et al. Dopamine depletion impairs precursor cell proliferation in Parkinson disease. *Nat Neurosci.* 2004 Jul;7(7):726–35.
114. O’Keeffe GC, Tyers P, Aarsland D, Dalley JW, Barker RA, Caldwell MA. Dopamine-induced proliferation of adult neural precursor cells in the mammalian subventricular zone is mediated through EGF. *Proc Natl Acad Sci U S A.* 2009 May 26;106(21):8754–9.
115. Tiraboschi P, Hansen LA, Thal LJ, Corey-Bloom J. The importance of neuritic plaques and tangles to the development and evolution of AD. *Neurology.* 2004 Jun 8;62(11):1984–9.
116. Khairallah MI, Kassem LAA. Alzheimer’s disease: current status of etiopathogenesis and therapeutic strategies. *Pak J Biol Sci.* 2011 Feb 15;14(4):257–72.
117. Puzzo D, Privitera L, Fa’ M, Staniszewski A, Hashimoto G, Aziz F, et al. Endogenous amyloid- $\beta$  is necessary for hippocampal synaptic plasticity and memory. *Ann Neurol.* 2011 May;69(5):819–30.
118. Enciu AM, Nicolescu MI, Manole CG, Mureşanu DF, Popescu LM, Popescu BO. Neuroregeneration in neurodegenerative disorders. *BMC Neurol.* 2011 Jun 23;11(1):75.
119. Cullen DK, Gilroy M, Irons HR, LaPlaca MC. Synapse-to-neuron ratio is inversely related to neuronal density in mature neuronal cultures. *Brain Res.* 2010 Nov 4;1359:44–55.
120. Petrović A, Ban J, Tomljanović I, Pongrac M, Ivaničić M, Mikašinović S, et al. Establishment of Long-Term Primary Cortical Neuronal Cultures From Neonatal Opossum *Monodelphis domestica*. *Frontiers in Cellular Neuroscience.* 2021;15:75.
121. Barry D, McDermott K. Differentiation of radial glia from radial precursor cells and transformation into astrocytes in the developing rat spinal cord. *Glia.* 2005 May;50(3):187–97.
122. Kamizato K, Sato S, Shil SK, Umaru BA, Kagawa Y, Yamamoto Y, et al. The role of fatty acid binding protein 7 in spinal cord astrocytes in a mouse model of experimental autoimmune encephalomyelitis. *Neuroscience.* 2019 Jun;409:120–9.
123. Mladinic M, Bianchetti E, Dekanic A, Mazzone GL, Nistri A. ATF3 is a novel nuclear marker for migrating ependymal stem cells in the rat spinal cord. *Stem Cell Research.* 2014 May 1;12(3):815–27.
124. Tomljanović I, Petrović A, Ban J, Mladinic M. Proteomic analysis of opossum *Monodelphis domestica* spinal cord reveals the changes of proteins related to neurodegenerative diseases during developmental period when neuroregeneration stops being possible. *Biochemical and Biophysical Research Communications.* 2022 Jan 8;587:85–91.
125. Dineley KT, Westerman M, Bui D, Bell K, Ashe KH, Sweatt JD. Beta-amyloid activates the mitogen-activated protein kinase cascade via hippocampal  $\alpha 7$  nicotinic acetylcholine receptors: In vitro and in vivo mechanisms related to Alzheimer’s disease. *J Neurosci.* 2001 Jun 15;21(12):4125–33.



126. Madero-Pérez J, Fdez E, Fernández B, Lara Ordóñez AJ, Blanca Ramírez M, Gómez-Suaga P, et al. Parkinson disease-associated mutations in LRRK2 cause centrosomal defects via Rab8a phosphorylation. *Mol Neurodegener.* 2018 Jan 23;13(1):3.
127. O'Brien RJ, Wong PC. Amyloid Precursor Protein Processing and Alzheimer's Disease. *Annu Rev Neurosci.* 2011;34:185–204.
128. Shioda N, Han F, Fukunaga K. Role of Akt and ERK signaling in the neurogenesis following brain ischemia. *Int Rev Neurobiol.* 2009;85:375–87.
129. Flores AI, Narayanan SP, Morse EN, Shick HE, Yin X, Kidd G, et al. Constitutively Active Akt Induces Enhanced Myelination in the CNS. *J Neurosci.* 2008 Jul 9;28(28):7174–83.
130. Hu X, Hicks C, He W, Wong P, Macklin W, Trapp B, et al. BACE1 modulates myelination in the central and peripheral nervous system. *Nature neuroscience.* 2007 Jan 1;9:1520–5.
131. Yan R, Vassar R. Targeting the  $\beta$  secretase BACE1 for Alzheimer's disease therapy. *Lancet Neurol.* 2014 Mar;13(3):319–29.
132. Corrêa SAL, Eales KL. The Role of p38 MAPK and Its Substrates in Neuronal Plasticity and Neurodegenerative Disease. *J Signal Transduct.* 2012;2012:649079.
133. Shi M, Shi C, Xu Y. Rab GTPases: The Key Players in the Molecular Pathway of Parkinson's Disease. *Front Cell Neurosci.* 2017 Mar 28;11:81.
134. Bonet-Ponce L, Cookson MR. The role of Rab GTPases in the pathobiology of Parkinson' disease. *Curr Opin Cell Biol.* 2019 Aug;59:73–80.
135. Dinter E, Saridaki T, Nippold M, Plum S, Diederichs L, Komnig D, et al. Rab7 induces clearance of  $\alpha$ -synuclein aggregates. *J Neurochem.* 2016 Sep;138(5):758–74.
136. Liu Z, Meray RK, Grammatopoulos TN, Fredenburg RA, Cookson MR, Liu Y, et al. Membrane-associated farnesylated UCH-L1 promotes  $\alpha$ -synuclein neurotoxicity and is a therapeutic target for Parkinson's disease. *Proc Natl Acad Sci U S A.* 2009 Mar 24;106(12):4635–40.
137. Kelleher RJ, Shen J. Presenilin-1 mutations and Alzheimer's disease. *Proc Natl Acad Sci U S A.* 2017 Jan 24;114(4):629–31.
138. Shaul YD, Seger R. The MEK/ERK cascade: From signaling specificity to diverse functions. *Biochimica et Biophysica Acta (BBA) - Molecular Cell Research.* 2007 Aug 1;1773(8):1213–26.
139. Li Z, Theus MH, Wei L. Role of ERK 1/2 signaling in neuronal differentiation of cultured embryonic stem cells. *Dev Growth Differ.* 2006 Oct;48(8):513–23.
140. Sasaki S, Mori D, Toyo-oka K, Chen A, Garrett-Beal L, Muramatsu M, et al. Complete Loss of Ndel1 Results in Neuronal Migration Defects and Early Embryonic Lethality. *Mol Cell Biol.* 2005 Sep;25(17):7812–27.

141. Swanwick CC, Shapiro ME, Vicini S, Wenthold RJ. Flotillin-1 Promotes Formation of Glutamatergic Synapses in Hippocampal Neurons. *Dev Neurobiol*. 2010 Nov;70(13):875–83.
142. Tian Q, Sun Y, Gao T, Li J, Fang H, Zhang S. Djnedd4L Is Required for Head Regeneration by Regulating Stem Cell Maintenance in Planarians. *Int J Mol Sci*. 2021 Oct 28;22(21):11707.
143. Hirota Y, Nakajima K. Control of Neuronal Migration and Aggregation by Reelin Signaling in the Developing Cerebral Cortex. *Front Cell Dev Biol*. 2017 Apr 26;5:40.
144. Wang L, Song G, Zheng Y, Tan W, Pan J, Zhao Y, et al. Expression of Semaphorin 4A and its potential role in rheumatoid arthritis. *Arthritis Research & Therapy*. 2015 Aug 25;17(1):227.
145. Dun X-P, Parkinson DB. Role of Netrin-1 Signaling in Nerve Regeneration. *Int J Mol Sci*. 2017 Feb 24;18(3):491.
146. Poplawski GHD, Kawaguchi R, Van Niekerk E, Lu P, Mehta N, Canete P, et al. Injured adult neurons regress to an embryonic transcriptional growth state. *Nature*. 2020 May;581(7806):77–82.
147. Kee N, Sivalingam S, Boonstra R, Wojtowicz JM. The utility of Ki-67 and BrdU as proliferative markers of adult neurogenesis. *J Neurosci Methods*. 2002 Mar 30;115(1):97–105.
148. Magdeldin S, Enany S, Yoshida Y, Xu B, Zhang Y, Zureena Z, et al. Basics and recent advances of two dimensional- polyacrylamide gel electrophoresis. *Clin Proteomics*. 2014;11(1):16.
149. Wiśniewski JR. Filter Aided Sample Preparation - A tutorial. *Anal Chim Acta*. 2019 Dec 20;1090:23–30.
150. Wilkins MR, Gasteiger E, Sanchez JC, Bairoch A, Hochstrasser DF. Two-dimensional gel electrophoresis for proteome projects: the effects of protein hydrophobicity and copy number. *Electrophoresis*. 1998 Jun;19(8–9):1501–5.
151. Corthals GL, Wasinger VC, Hochstrasser DF, Sanchez JC. The dynamic range of protein expression: a challenge for proteomic research. *Electrophoresis*. 2000 Apr;21(6):1104–15.
152. Haider S, Pal R. Integrated analysis of transcriptomic and proteomic data. *Curr Genomics*. 2013 Apr;14(2):91–110.
153. Zapalska-Sozoniuk M, Chrobak L, Kowalczyk K, Kankofer M. Is it useful to use several “omics” for obtaining valuable results? *Mol Biol Rep*. 2019 Jun 1;46(3):3597–606.
154. Schwanhäusser B, Busse D, Li N, Dittmar G, Schuchhardt J, Wolf J, et al. Global quantification of mammalian gene expression control. *Nature*. 2011 May;473(7347):337–42.
155. Niekerk EA van, Tuszyński MH, Lu P, Dulin JN. Molecular and Cellular Mechanisms of Axonal Regeneration After Spinal Cord Injury \*. *Molecular & Cellular Proteomics*. 2016 Feb 1;15(2):394–408.

156. Piehowski PD, Petyuk VA, Orton DJ, Xie F, Ramirez-Restrepo M, Engel A, et al. Sources of Technical Variability in Quantitative LC-MS Proteomics: Human Brain Tissue Sample Analysis. *J Proteome Res.* 2013 May 3;12(5):2128–37.
157. Graves PR, Haystead TAJ. Molecular Biologist's Guide to Proteomics. *Microbiol Mol Biol Rev.* 2002 Mar;66(1):39–63.
158. Lu R, Markowetz F, Unwin RD, Leek JT, Airolidi EM, MacArthur BD, et al. Systems-level dynamic analyses of fate change in murine embryonic stem cells. *Nature.* 2009 Nov 19;462(7271):358–62.
159. Ghazalpour A, Bennett B, Petyuk VA, Orozco L, Hagopian R, Mungrue IN, et al. Comparative Analysis of Proteome and Transcriptome Variation in Mouse. *PLOS Genetics.* 2011 Jun 9;7(6):e1001393.
160. Xiao L, Saiki C, Ide R. Stem cell therapy for central nerve system injuries: glial cells hold the key. *Neural Regen Res.* 2014 Jul 1;9(13):1253–60.
161. Toy D, Namgung U. Role of Glial Cells in Axonal Regeneration. *Exp Neurobiol.* 2013 Jun;22(2):68–76.
162. Teter B. Rodent Aging. In: Squire LR, editor. *Encyclopedia of Neuroscience* [Internet]. Oxford: Academic Press; 2009 [cited 2022 Mar 22]. p. 397–406. Available from: <https://www.sciencedirect.com/science/article/pii/B9780080450469001200>
163. Nichols NR, Day JR, Laping NJ, Johnson SA, Finch CE. GFAP mRNA increases with age in rat and human brain. *Neurobiol Aging.* 1993 Oct;14(5):421–9.
164. Goss JR, Finch CE, Morgan DG. Age-related changes in glial fibrillary acidic protein mRNA in the mouse brain. *Neurobiol Aging.* 1991 Apr;12(2):165–70.
165. Kaur M, Sharma S, Kaur G. Age-related impairments in neuronal plasticity markers and astrocytic GFAP and their reversal by late-onset short term dietary restriction. *Biogerontology.* 2008 Dec;9(6):441–54.
166. Wu Y, Zhang A-Q, Yew DT. Age related changes of various markers of astrocytes in senescence-accelerated mice hippocampus. *Neurochem Int.* 2005 Jun;46(7):565–74.
167. Kaech S, Banker G. Culturing hippocampal neurons. *Nat Protoc.* 2006;1(5):2406–15.
168. Puzzolo E, Mallamaci A. Cortico-cerebral histogenesis in the opossum *Monodelphis domestica*: generation of a hexalaminar neocortex in the absence of a basal proliferative compartment. *Neural Dev.* 2010 Mar 19;5:8.
169. Williamson JM, Lyons DA. Myelin Dynamics Throughout Life: An Ever-Changing Landscape? *Frontiers in Cellular Neuroscience* [Internet]. 2018 [cited 2022 Mar 22];12. Available from: <https://www.frontiersin.org/article/10.3389/fncel.2018.00424>
170. Chen J, Zhao J, Xiong C, Lin J, Wang R, Li C, et al. [Expression of myelin basic protein gene in the developing human brain]. *Hua Xi Yi Ke Da Xue Xue Bao.* 1996 Sep;27(3):225–30.

171. Jones FS, Jones PL. The tenascin family of ECM glycoproteins: structure, function, and regulation during embryonic development and tissue remodeling. *Dev Dyn*. 2000 Jun;218(2):235–59.
172. Siebert JR, Conta Steencken A, Osterhout DJ. Chondroitin Sulfate Proteoglycans in the Nervous System: Inhibitors to Repair. *BioMed Research International*. 2014 Sep 18;2014:e845323.
173. Feng L, Hatten ME, Heintz N. Brain lipid-binding protein (BLBP): A novel signaling system in the developing mammalian CNS. *Neuron*. 1994 Apr 1;12(4):895–908.
174. De la Monte SM, Federoff HJ, Ng SC, Grabczyk E, Fishman MC. GAP-43 gene expression during development: persistence in a distinctive set of neurons in the mature central nervous system. *Brain Res Dev Brain Res*. 1989 Apr 1;46(2):161–8.
175. Sharma R, Sanchez-Ferraz O, Bouchard M. Pax genes in renal development, disease and regeneration. *Semin Cell Dev Biol*. 2015 Aug;44:97–106.
176. Bradshaw NJ, Hayashi MAF. NDE1 and NDEL1 from genes to (mal)functions: parallel but distinct roles impacting on neurodevelopmental disorders and psychiatric illness. *Cell Mol Life Sci*. 2017 Apr;74(7):1191–210.
177. Bradshaw NJ, Hennah W, Soares DC. NDE1 and NDEL1: twin neurodevelopmental proteins with similar ‘nature’ but different ‘nurture.’ *BioMolecular Concepts*. 2013 Oct 1;4(5):447–64.
178. Hu J, Gao Y, Huang Q, Wang Y, Mo X, Wang P, et al. Flotillin-1 Interacts With and Sustains the Surface Levels of TRPV2 Channel. *Frontiers in Cell and Developmental Biology* [Internet]. 2021 [cited 2022 Mar 23];9. Available from: <https://www.frontiersin.org/article/10.3389/fcell.2021.634160>
179. Schiffmann SN, Bernier B, Goffinet AM. Reelin mRNA expression during mouse brain development. *Eur J Neurosci*. 1997 May;9(5):1055–71.
180. Gad JM, Keeling SL, Wilks AF, Tan SS, Cooper HM. The expression patterns of guidance receptors, DCC and Neogenin, are spatially and temporally distinct throughout mouse embryogenesis. *Dev Biol*. 1997 Dec 15;192(2):258–73.
181. Aloe L, Rocco ML, Bianchi P, Manni L. Nerve growth factor: from the early discoveries to the potential clinical use. *Journal of Translational Medicine*. 2012 Nov 29;10(1):239.
182. Webster MJ, Weickert CS, Herman MM, Kleinman JE. BDNF mRNA expression during postnatal development, maturation and aging of the human prefrontal cortex. *Developmental Brain Research*. 2002 Dec 15;139(2):139–50.
183. Escartin C, Hantraye P, Déglon N. 22 - Transplants of CNTF-producing Cells for the Treatment of Huntington’s Disease. In: Halberstadt C, Emerich D, editors. *Cellular Transplantation* [Internet]. Burlington: Academic Press; 2007 [cited 2022 Mar 28]. p. 385–98. Available from: <https://www.sciencedirect.com/science/article/pii/B9780123694157500235>
184. Oyesiku NM, Wilcox JN, Wigston DJ. Changes in expression of ciliary neurotrophic factor (CNTF) and CNTF-receptor alpha after spinal cord injury. *J Neurobiol*. 1997 Mar;32(3):251–61.

185. Gitler AD, Dhillon P, Shorter J. Neurodegenerative disease: models, mechanisms, and a new hope. *Dis Model Mech*. 2017 May 1;10(5):499–502.
186. Nicolas M, Hassan BA. Amyloid precursor protein and neural development. *Development*. 2014 Jul 1;141(13):2543–8.
187. O’Hara BF, Fisher S, Oster-Granite ML, Gearhart JD, Reeves RH. Developmental expression of the amyloid precursor protein, growth-associated protein 43, and somatostatin in normal and trisomy 16 mice. *Brain Res Dev Brain Res*. 1989 Oct 1;49(2):300–4.
188. Fraser PE, Yang D-S, Yu G, Lévesque L, Nishimura M, Arawaka S, et al. Presenilin structure, function and role in Alzheimer disease. *Biochimica et Biophysica Acta (BBA) - Molecular Basis of Disease*. 2000 Jul 26;1502(1):1–15.
189. Lee MK, Slunt HH, Martin LJ, Thinakaran G, Kim G, Gandy SE, et al. Expression of Presenilin 1 and 2 (PS1 and PS2) in Human and Murine Tissues. *J Neurosci*. 1996 Dec 1;16(23):7513–25.
190. Nassari S, Del Olmo T, Jean S. Rabs in Signaling and Embryonic Development. *Int J Mol Sci*. 2020 Feb 5;21(3):1064.
191. Kawamura N, Sun-Wada G-H, Aoyama M, Harada A, Takasuga S, Sasaki T, et al. Delivery of endosomes to lysosomes via microautophagy in the visceral endoderm of mouse embryos. *Nat Commun*. 2012;3:1071.
192. Burrus CJ, McKinstry SU, Kim N, Ozlu MI, Santoki AV, Fang FY, et al. Striatal Projection Neurons Require Huntingtin for Synaptic Connectivity and Survival. *Cell Rep*. 2020 Jan 21;30(3):642–657.e6.
193. Bhide PG, Day M, Sapp E, Schwarz C, Sheth A, Kim J, et al. Expression of Normal and Mutant Huntingtin in the Developing Brain. *J Neurosci*. 1996 Sep 1;16(17):5523–35.
194. Seybold VS, Abrahams LG. Primary cultures of neonatal rat spinal cord. *Methods Mol Med*. 2004;99:203–13.
195. Harder JD, Hsu MJ, Garton DW. Metabolic Rates and Body Temperature of the Gray Short-Tailed Opossum (*Monodelphis domestica*) during Gestation and Lactation. *Physiological Zoology*. 1996 Mar;69(2):317–39.
196. Malon JT, Cao L. Preparation of Primary Mixed Glial Cultures from Adult Mouse Spinal Cord Tissue. *J Vis Exp*. 2016 Nov 19;(117).
197. Heiser V, Engemann S, Bröcker W, Dunkel I, Boeddrich A, Waelter S, et al. Identification of benzothiazoles as potential polyglutamine aggregation inhibitors of Huntington’s disease by using an automated filter retardation assay. *Proc Natl Acad Sci U S A*. 2002 Dec 10;99(Suppl 4):16400–6.
198. Jimonet P, Audiau F, Barreau M, Blanchard JC, Boireau A, Bour Y, et al. Riluzole series. Synthesis and in vivo “antiglutamate” activity of 6-substituted-2-benzothiazolamines and 3-substituted-2-imino-benzothiazolines. *J Med Chem*. 1999 Jul 29;42(15):2828–43.

199. Bensimon G, Lacomblez L, Meininger V. A controlled trial of riluzole in amyotrophic lateral sclerosis. ALS/Riluzole Study Group. *N Engl J Med*. 1994 Mar 3;330(9):585–91.
200. Lacomblez L, Bensimon G, Leigh PN, Guillet P, Meininger V. Dose-ranging study of riluzole in amyotrophic lateral sclerosis. Amyotrophic Lateral Sclerosis/Riluzole Study Group II. *Lancet*. 1996 May 25;347(9013):1425–31.
201. Rosas HD, Koroshetz WJ, Jenkins BG, Chen YI, Hayden DL, Beal MF, et al. Riluzole therapy in Huntington's disease (HD). *Mov Disord*. 1999 Mar;14(2):326–30.
202. Bonfanti L, Peretto P. Adult neurogenesis in mammals—a theme with many variations. *Eur J Neurosci*. 2011 Sep;34(6):930–50.
203. Rodemer W, Gallo G, Selzer ME. Mechanisms of Axon Elongation Following CNS Injury: What Is Happening at the Axon Tip? *Front Cell Neurosci*. 2020 Jul 3;14:177.
204. Kiyonari H, Kaneko M, Abe T, Shiraishi A, Yoshimi R, Inoue K, et al. Targeted gene disruption in a marsupial, *Monodelphis domestica*, by CRISPR/Cas9 genome editing. *Current Biology*. 2021 Sep 13;31(17):3956–3963.e4.

## 8. LIST OF ABBREVIATIONS

2-DE; two-dimensional gel electrophoresis  
A $\beta$ ;  $\beta$ -amyloid  
AD; Alzheimer's disease  
APBB1; amyloid beta precursor protein binding family B member 1  
APP; amyloid-precursor protein  
APPBP1; amyloid protein-binding protein 1  
AU; arbitrary units  
BDNF; brain-derived neurotrophic factor  
bFGF; basic fibroblast growth factor  
BLBP; brain lipid-binding protein  
CNS; central nervous system  
CNTF; ciliary neurotrophic factor  
Ct; cycle threshold  
DAPI; 4',6-diamidino-2-phenylindole  
DCC; DCC netrin 1 receptor  
DG; dentate gyrus  
DIV; days *in vitro*  
E; embryonic day  
EGF; epithelial growth factor  
EGFR; epidermal growth factor receptor  
eNSC; endogenous neural stem cells  
ESC; embryonic stem cells  
FASP; filter aided sample preparation  
FGF2; fibroblast growth factor 2  
FLOT1; flotillin 1  
GAP43; growth associated protein 43  
GAPDH; Glyceraldehyde-3-phosphate dehydrogenase  
G-CSF; glycoprotein granulocyte colony-stimulating factor

GFAP; glial fibrillary acidic protein  
GOI; genes of interest  
HD; Huntington's disease  
HIP1; huntingtin interacting protein 1  
HTT; huntingtin  
IL-4; interleukin-4  
iPSC; induced pluripotent stem cells  
JNK; c-Jun N-terminal kinase  
Ki67; marker of proliferation Ki67  
LC-MS/MS; liquid chromatography tandem mass spectrometry  
MAP2; microtubule-associated protein 2  
MBP; myelin basic protein  
MS; mass spectrometry  
MSC; mesenchymal stem cells  
mTOR; mammalian target of rapamycin  
NDD; neurodegenerative diseases  
NDE1; nuclear distribution element 1  
NDEL1; nuclear distribution protein nudeE-like 1  
NeuN; neuronal nuclear protein  
NGF; nerve growth factor  
NPC; neural progenitor cells  
NSC; neural stem cells  
OPC; oligodendrocyte progenitor cells  
P; postnatal day  
PAX2; paired box protein Pax-2  
PD; Parkinson's disease  
PNS; peripheral nervous system  
PSEN1; presenilin 1  
qRT-PCR; quantitative reverse transcription polymerase chain reaction  
Rabs; Rab GTPases



RELN; reelin

ROI; region of interest

RT; room temperature

SCI; spinal cord injury

SGZ; subgranular zone

SMI32; selective neurofilament

SVZ; subventricular zone

Syn1; Synapsin 1

TBI; traumatic brain injury

TGF- $\beta$ ; transforming growth factor

VEGF; vascular endothelial growth factor

WB; western blot

## 9. LIST OF FIGURES

Figure 1. Pathological and physiological changes during acute and chronic phases after spinal cord injury.....	5
Figure 2. Human embryonic stem cells (hESC), induced pluripotent stem cells (iPSC) and ependymal stem/progenitor cells (epSPC) as promising tools in the therapy of SCI.....	8
Figure 3. Neural stem cell (NSCs) sources and their therapeutic applicability after cell transplantation.....	10
Figure 4. Opossum <i>Monodelphis domestica</i> .....	16
Figure 5. The age, body weight and size of opossums.....	17
Figure 6. Stage correspondences across species throughout the entire development.....	18
Figure 7. Schematic representation of the equipment needed for maintaining the spinal cord preparation in culture.....	40
Figure 8. Differential protein expression pattern of opossum spinal cord tissue represented in the 2D gel.....	47
Figure 9. Differential protein expression pattern of opossum spinal cord tissue represented in 2D gel.....	50
Figure 10. Functional classification of the proteins identified by MS as differentially distributed in the opossum P5 and P18 spinal cords.....	61
Figure 11. Functional classification of the proteins identified by MS as differentially distributed in the opossum P5 and P18 spinal cords.....	62
Figure 12. The MS analysis of the proteins differently distributed in the P5 and P18 opossum spinal cords and the validation of the results by WB and qRT-PCR.....	66
Figure 13. Immuno-staining for PAX2 and BLBP, differentially expressed in P5 and P18 opossum spinal cords.....	67
Figure 14. qRT-PCR analysis of the selected proteins related to neurodegenerative diseases in P5 and P18 opossum spinal cord tissue.....	68
Figure 15. WB analysis of proteins related to regeneration and neurodegenerative diseases in P5 and P18 opossum spinal cord tissue.....	72
Figure 16. qRT-PCR analysis of proteins related to regeneration and neurodegenerative diseases in P5 and P18 opossum spinal cord tissue.....	73

Figure 17. WB analysis of HTT and HIP1 protein in P5 and P18 opossum spinal cord tissue after treatment with PGL-137 inhibitor.....	78
Figure 18. qRT-PCR analysis of HTT and HIP1 protein in P5 and P18 opossum spinal cord tissue after treatment with PGL-137 inhibitor.....	79
Figure 19. Immuno-staining for HTT after treatment with PGL-137 inhibitor in the P5 spinal cord tissue.....	80
Figure 20. Immuno-staining for HTT in P18 after treatment with PGL-137 inhibitor in the P18 spinal cord tissue.....	81
Figure 21. Immuno-staining for MAP2 and Ki67 after treatment with PGL-137 inhibitor in the P5 spinal cord tissue.....	82
Figure 22. Immuno-staining for MAP2 and Ki67 after treatment with PGL-137 inhibitor in the P18 spinal cord tissue.....	83
Figure 23. Immuno-staining for NeuN after treatment with PGL-137 inhibitor in the P5 spinal cord tissue.....	84
Figure 24. Immuno-staining for NeuN after treatment with PGL-137 inhibitor in the P18 spinal cord tissue.....	85
Figure 25. Immuno-staining for SYN1 and SMI32 after treatment with PGL-137 inhibitor in the P5 spinal cord tissue.....	86
Figure 26. Immuno-staining for SYN1 and SMI32 after treatment with PGL-137 inhibitor in the P18 spinal cord tissue.....	87
Figure 27. Brightfield images of spinal cord primary cell cultures from P5 and P18 opossums at two different stages during culture, DIV1 and DIV10.....	90
Figure 28. WB analysis of HTT and HIP1 protein in P5 and P18 primary spinal cell cultures after treatment with PGL-137 inhibitor.....	91
Figure 29. qRT-PCR analysis of HTT and HIP1 protein in P5 and P18 primary spinal cell cultures after treatment with PGL-137 inhibitor.....	92
Figure 30. Primary neuronal cultures.....	93
Figure 31. Brightfield images of the scratch test performed on primary spinal neuronal cultures from P5 and P18 opossums at different stages during culture, DIV10, DIV14 and DIV21.....	94

## 10. LIST OF TABLES

Table 1. List of primary antibodies.....	27-28
Table 2. List of secondary antibodies.....	28
Table 3. Primers used for qRT-PCR analysis.....	28-29
Table 4. List of proteins identified from opossum spinal cord tissue P5 using 2D electrophoresis in combination with MALDI-TOF/MS.....	48
Table 5. List of proteins identified from opossum spinal cord tissue P18 using 2D electrophoresis in combination with MALDI-TOF/MS.....	49
Table 6. List of proteins identified from opossum spinal cord tissue P5 using 2D electrophoresis in combination with MALDI-TOF/MS.....	51
Table 7. List of proteins identified from opossum spinal cord tissue P18 using 2D electrophoresis in combination with MALDI-TOF/MS.....	52
Table 8. List of proteins specific for rat spinal cord tissue using FASP method in combination with ACQUITY UPLC M-Class system coupled on-line to a Synapt G2-Si.....	53-54
Table 9. List of proteins specific for rat spinal cord tissue kept in culture for 24 h using FASP method in combination with ACQUITY UPLC M-Class system coupled on-line to a Synapt G2-Si.....	54-55
Table 10. Classification of the proteins identified by MS as differentially distributed in the opossum P5 and P18 spinal cords in divergent molecular pathways with emphasis on functional groups related to neurodegenerative disease.....	63-65
Table 11. Selected proteins detected by mass spectrometry as differentially distributed in P5 and P18 opossum spinal cords.....	69
Table 12. Proteins important for regeneration and neurodegenerative diseases detected by mass spectrometry in P5 and P18 opossum spinal cords.....	70-71

# Ivana Tomljanović

Date of birth: 25/10/1991 | **Nationality:** Croatian | **Gender:** Female | (+385) 977257074 | [ivana.tomljanovic00@gmail.com](mailto:ivana.tomljanovic00@gmail.com) |

Marina Držića 11, 47000, Karlovac, Croatia

## WORK EXPERIENCE

09/2017 – CURRENT – Rijeka, Croatia

**RESEARCH ASSISTANT** – UNIVERSITY OF RIJEKA, DEPARTMENT OF BIOTECHNOLOGY

Working on the research project of Croatian Science Foundation IP-06-2016 "Exploring the borderline between neurodegeneration and neuroregeneration: identification of key molecules with proteomics and functional assays in the mammalian spinal cord". Supervisor: prof. Miranda Mladinić Pejatović

Assistant on the following research projects:

- 2019 – 2021: University of Rijeka research grant #18-258-6427 "Identification of key molecules controlling HSP mediated neuroprotection and neuroregeneration after *in vitro* opossum spinal cord injury", PI prof. Miranda Mladinić Pejatović
- 2019 – 2021: University of Rijeka research grant #18-290-1463 "Development of the new method for quantification and identification of neural stem cells of the mammalian central nervous system", PI associate prof. Jelena Ban

## EDUCATION AND TRAINING

06/2016 – CURRENT

**PHD STUDENT** – University of Rijeka, Department of Biotechnology

10/2013 – 07/2015

**MASTER OF SCIENCE (M.SC.) IN DRUG RESEARCH AND DEVELOPMENT** – University of Rijeka, Department of Biotechnology

10/2010 – 07/2013

**BACHELOR OF SCIENCE (B.SC.) IN BIOTECHNOLOGY AND DRUG RESEARCH** – University of Rijeka, Department of Biotechnology

## SCIENTIFIC TRAINING

23.07.2018.-today

Assistant, Laboratory for molecular neurobiology

prof. Miranda Mladinić Pejatović

Department of Biotechnology, Rijeka

- Working on the research project of Croatian Science Foundation "Exploring the borderline between neurodegeneration and neuroregeneration: identification of key molecules with proteomics and functional assays in the mammalian spinal cord".

October and december 2017.

International School for Advanced Studies (SISSA), Trieste, Italy

Laboratory for Neurobiology, prof. Andrea Nistri

- Working with intact spinal cord preparation, dissecting and maintaining tissue *in vitro* and experience in experimental immunofluorescence techniques.

## PUBLICATIONS

---

Petrović, A.; Ban, J.; Ivaničić, M.; **Tomljanović, I.**; Mladinic, M. The Role of ATF3 in Neuronal Differentiation and Development of Neuronal Networks in Opossum Postnatal Cortical Cultures. *Int. J. Mol. Sci.* 2022, 23, 4964. <https://doi.org/10.3390/ijms23094964>

**Ivana Tomljanović**, Antonela Petrović, Jelena Ban, Miranda Mladinic. Proteomic analysis of opossum *Monodelphis domestica* spinal cord reveals the changes of proteins related to neurodegenerative diseases during developmental period when neuroregeneration stops being possible. *Biochemical and Biophysical Research Communications*, 2022, 587; 85-91; <https://doi.org/10.1016/j.bbrc.2021.11.078>

Petrović A, Ban J, **Tomljanović I**, Pongrac M, Ivaničić M, Mikašinović S and Mladinic M (2021) Establishment of Long-Term Primary Cortical Neuronal Cultures From Neonatal Opossum *Monodelphis domestica*. *Front. Cell. Neurosci.* 15:661492. doi: 10.3389/fncel.2021.661492

Petrovic A, Kaur J, **Tomljanovic I**, Nistri A, Mladinic M. Pharmacological induction of Heat Shock Protein 70 by celastrol protects motoneurons from excitotoxicity in the rat spinal cord *in vitro*. *European Journal of Neuroscience* - 2018.

Grbčić, Petra; **Tomljanović, Ivana**; Klobučar, Marko; Pavelić, Sandra Kraljević; Lučin, Ksenija; Sedić, Mirela. Dual sphingosine kinase inhibitor SKI-II enhances sensitivity to 5-fluorouracil in hepatocellular carcinoma cells via suppression of osteopontin and FAK/IGF-1R signalling. *Biochemical and Biophysical Research Communications* 487 782-788 -2017.

## CONFERENCES, SUMMER SCHOOLS AND PRESENTATIONS

---

3D cell culture and organoids conference, May 18th, 2021 (online meeting)

3rd Rijeka Forum on Neurodegenerative Diseases- diagnosis and treatment in early stage of disease, 17-18th October, 2019, Rijeka

23rd Young Neuroscientist Meeting, June 13th, 2016, Trieste

NeuRi student congress, June 2019, poster presentation: "Identification of key molecules involved in neuroprotection and neuroregeneration using new *in vitro* preparations of opossum *Monodelphis domestica* central nervous system"

VI. Croatian Congress of Neuroscience in Osijek, September 16-18, 2017, poster presentation: "Identification of key molecules underlying neuronal regeneration in the opossum spinal cord"

Summer School of Mass Spectrometry "3rd International Mass Spectrometry School" (IMSS), July 2-8, 2017 in Dubrovnik, poster presentation: "Identification of key molecules underlying neuronal regeneration in the opossum spinal cord"

21st Young Neuroscientist Meeting in Zagreb, June 29, 2017, poster presentation: "Identification of key molecules underlying neuronal regeneration in the opossum spinal cord"

Summer school "From Electrophysiology to Imaging and BioNanotechnology" in Trieste from June 20 to July 1, 2016

---

## LABORATORY AND RESEARCH SKILLS

Work with cell cultures, *in vitro* assays for monitoring cell proliferation, proteomics methods (WB and 2DE) for isolation, separation and validation of proteins, PCR and qRT-PCR, preparation of samples for analysis on mass spectrometer, MALDI TOF MS analysis, dissection and work with opossum primary cell cultures from the spinal cord and cortex, intact spinal cord *in vitro* tissue culture, immunohistochemistry, light and fluorescence microscopy.

Computer programs: ImageJ; QuantityOne; Image Master 2D Platinum; GraphPad Prism; MS Office.

---

## TEACHING ACTIVITY

Molecular Neurobiology EBIL124

Undergraduate university study "Biotechnology and drug research" Department of Biotechnology

University of Rijeka

Assistant

Pharmacology BIL203

Undergraduate university study "Biotechnology and drug research" Department of Biotechnology

University of Rijeka

Assistant

---

## ORGANISATIONAL SKILLS

Supervised and guided three master students from 2019 - 2021 at the Department of Biotechnology, University of Rijeka

Head of a student project " Spinal Cord Regeneration" funded by University of Rijeka Student Association, May- December 2017

Participation in the organization of the Open Day Festival at the Department of Biotechnology

## DRIVING LICENCE

---

B category

## LANGUAGE SKILLS

---

Mother tongue(s): **CROATIAN**

Other language(s):

	UNDERSTANDING		SPEAKING		WRITING
	Listening	Reading	Spoken production	Spoken interaction	
<b>ENGLISH</b>	C2	C1	C1	C1	C1
<b>GERMAN</b>	A2	A2	A2	A2	A2

*Levels: A1 and A2: Basic user; B1 and B2: Independent user; C1 and C2: Proficient user*